Source assessment of fine carbonaceous aerosols in urban Sydney

Chuanping Meng

B.Eng.   M.Sc.Eng.

May 2018

MACQUARIE
University
SYDNEY·AUSTRALIA

Department of Environmental Sciences

Faculty of Science and Engineering

Macquarie University

This thesis is presented for the degree of Doctor of Philosophy.

Cover photos:

Comparison photos of Sydney haze days and Sydney clean blue days near Opera House and Harbour Bridge.

TABLE OF CONTENTS

ABSTRACT

Australia is a world famous livable country, with major large Australian cities such as Sydney, Melbourne, Perth and Adelaide all featuring in the top 10 World's most livable cities in recent years. Sydney, because of its benign environment and mild climate, attracts thousands of tourists and immigrants every year. Although in most of cases Sydney has above averaged air quality, occasional bush fires/prescribed burns and domestic heating during cold periods can still bring deleterious impacts on air quality and potentially then on human health. Moreover, in summer stronger solar radiation in Sydney is also one of the factors for an increase in $PM_{2.5}$ levels. Source apportionment research on carbonaceous aerosols, the most substantial component of $PM_{2.5}$, is still very limited in Sydney.

This thesis mainly contains three parts. Chapter 2 and Chapter 3 focus on chemical characterization of non-polar (PAHs and n-alkanes) and typical polar molecular organic tracers in cold period $PM_{2.5}$ aerosols at an urban Sydney site. Chapter 4 comprehensively assesses the various contributions of fossil/non-fossil and primary/secondary sources to $PM_{2.5}$ using radiocarbon analyses under different cases. A refined EC tracer method was used to estimate the secondary organic carbon by estimating hourly primary OC/EC ratio ((OC/EC)pri).

The findings in Chapter 2 and Chapter 3 indicate that during urban Sydney cold seasons biomass burning, traffic, biogenic activities, secondary sources were distinguished and identified via source indices analysis. Specially, for non-polar organic compounds, 3-4 ring PAHs were mainly from vehicular emissions and 5-6 ring PAHs were derived from biomass burning, while, fossil fuel combustion, notably traffic exhaust made a distinct contribution to n-alkanes concentrations, particularly in winter. Three distinct sources of n-alkanes were identified, and their contributions were estimated using a PCA-MLR model; these sources were, fossil fuel combustion (74%), biomass burning + road dust (20%) and biogenic sources (6%). The chemical analysis of polar organic compounds suggests that the site was significantly influenced by the emissions from wintertime domestic wood combustion and autumn time controlled bushfire prevention burns. In autumn, hardwood was found as a predominant source combined with some softwood burning, whereas in winter hardwood and grass combustion are the main type of biomass burnt. It is apparent that during the cold seasons the primary sources of the polar fraction of the organic component of PM are biomass combustion.

For the eight limited selected radiocarbon analysis $PM_{2.5}$ samples, the average abundances of SOA and PCA were 2.3 $\mu g \cdot m^{-3}$ and 8.9 $\mu g \cdot m^{-3}$, respectively for the Rozelle and Macquarie University (MQ) sites, accounting for 11% and 42% of the $PM_{2.5}$ mass. Higher proportions of POC_{nf} (POC_{nf}: non-fossil sources in primary organic carbon (POC)) and $EC_{biomass}$ ($EC_{biomass}$: biomass burning sources in EC) were determined in winter samples, amounting to 60% and 11% compared with 50% and 4% in the summer samples. This suggests that biofuel combustion mainly wood burning for household heating in the cold season would be a major contributor to total carbon in the collected particulates.

DECLARATION

I certify that the work in this thesis has not previously been submitted for a degree or diploma nor has it been submitted as part of requirements for a degree at any other university or institution other than Macquarie University.

I also certify that the thesis is an original piece of research and it has been written by me. Any help and assistance that I have received in my research work and the preparation of the thesis itself has been appropriately acknowledged.

In addition, I certify that all information sources and literature used are indicated in the thesis.

Chuanping Meng

May 2018

ACKNOWLEDGEMENTS

Last but not least, I specially thank my University, Macquarie University, who accepted me, gave me the chance to study in Australia, a research budget, a conference budget and understanding, trust and support. I love my University and Australia! Having joys and tears; having frustrations and accomplishments, they are all very precious treasures and memories in my life. I learned many things, not only academic knowledge but also knowledge about life and culture. This learning experience opened my eyes and broadened my horizons, which makes me become more strong and mature. I thank all the people helped me and I will never forget their kindness in my whole life. Much Appreciated and Grateful!

Notes regarding thesis format and author contributions to publications

Chapters within this thesis are written as manuscripts suitable for publication. The first chapter illustrates a broad introduction to the scientific background, current research progress and development on carbonaceous aerosols and the aims of the study. These objectives are addressed in the Chapters 2 to 4. Chapter 5 presents a brief discussion, the details of the thesis conclusions, which examines the overall findings, and some recommendations for future work.

CHAPTER 2

Polycyclic aromatic hydrocarbons and n-alkanes in $PM_{2.5}$ aerosols at a highly biogenic source dominated urban site (Sydney) in Australia

Meng, C. (85%), Nelson, P.F. (15%). Polycyclic aromatic hydrocarbons and n-alkanes in $PM_{2.5}$ aerosols at a highly biogenic source dominated urban site (Sydney) in Australia. To be submitted to *Atmospheric Environment*.

The concept of this paper was developed by myself in consultation with my supervisor. I collected all the fine particulate samples and carried out all laboratory analyses. Prof. Nelson provided a brand new gas chromatography/mass spectrometry for chemical analysis and financial support for series cost of sampling, standards and gas chromatography/mass spectrometry training. Prof. Nelson edited and reviewed the paper.

CHAPTER 3

Chemical characterization of polar organic compounds in $PM_{2.5}$ aerosols at an urban site in Sydney

Meng, C. (85%), Nelson, P.F. (15%). Chemical characterization of polar organic compounds in $PM_{2.5}$ aerosols at an urban site in Sydney. To be submitted to *Atmospheric Environment*.

This paper was developed by myself in consultation with my supervisor. I conducted all the field work, laboratory analyses, and data interpretation. All experimental materials and instruments are under the support of Prof. Nelson, including HiVol samplers, a brand new gas chromatography/mass spectrometry, chemical standards and training cost of gas chromatography/mass spectrometry. Prof. Nelson reviewed and edited the chapter.

CHAPTER 4

Application of radiocarbon analysis to source apportionment of carbonaceous $PM_{2.5}$ in urban Sydney: Insights from different seasonal biomass burning triggered haze events

Meng, C. (85%), Nelson, P.F. (15%). Application of radiocarbon analysis to source apportionment of carbonaceous $PM_{2.5}$ in urban Sydney: Insights from different seasonal biomass burning triggered haze events. To be submitted to *Environmental Science and Technology*.

I developed the concept for this paper in consultation with my supervisor, performed all the field work and the laboratory analyses. Radiocarbon analysis conducted in this study benefit from AINSE research funds awarded to Prof. Nelson. The text was edited and reviewed by Prof. Nelson.

Acronyms and Abbreviations

ACL	Average chain length
Ace	Acenaphthene
Acy	Acenaphthylene
AMS	Accelerator mass spectrometry
Ant	Anthracene
BaA	Benzo[a]anthracene
BaP	Benzo[a]pyrene
BbF	Benzo[b]fluoranthene
BgP	Benzo[g,h,i]perylene
BkF	Benzo[k]fluoranthene
Chry	Chrysene
CM	Carbonaceous matter
CPI	Carbon preference index
CPI_{total}	Whole range of n-alkanes (C_{17}-C_{30})
$CPI_{petrogenic}$	Petrogenic n-alkanes (C_{17}-C_{24})
$CPI_{biogenic}$	Biogenic n-alkanes (C_{25}-C_{30})
CuO	Copper Oxide
DbA	Dibenzo[a,h]anthracene
EC	Elemental carbon
EC_{bio}	$EC_{biomass}$: biomass burning sources in EC
EC_f	EC_{fossil}: fossil fuel sources in wEC
EC_{nf}	$EC_{non-fossil}$: non-fossil fuel sources in wEC
Flo	Fluorene
Flu	Fluoranthene
GC/MS	Gas chromatography-mass spectrometry
InP	Indeno[1,2,3-c,d]pyrene
MLR	Multivariate linear regression
Nap	Naphthalene
NCM	Non-carbonaceous matter
NSW EPA	New South Wales Environment Protection Authority
OA	Organic aerosols
OC	Organic carbon
OM	Organic matter
PAHs	Polycyclic aromatic hydrocarbons
PCA	Principal Component Analysis
Phe	Phenanthrene
$PM_{2.5}$	Particulate matter consisting of particles with an aerodynamic diameter less than 2.5 μm
pMC	Percent modern carbon
POA	Primary organic aerosols
POC	Primary organic carbon
POC_{nf}	$POC_{non-fossil}$: non-fossil fuel sources (biomass burning and biogenic sources) in POC
Pyr	Pyrene
SOA	Secondary organic aerosol
SOC	Secondary organic carbon
SOC_f	SOC_{fossil}: fossil fuel sources in SOC
SOC_{nf}	$SOC_{non-fossil}$: non-fossil fuel sources (biomass burning and biogenic sources) in SOC

TAL	Total n-alkanes
TAR	Terrigenous to aquatic ratio
TC	Total carbon
TC_f	TC_{fossil}: fossil fuel sources in TC
$\mu g/m^3$	Microgram per cubic meter
VOC	Volatile organic compound
wEC	After water wash EC
WHO	World Health Organization
WINSOC	Water-insoluble organic carbon
$WINSOC_f$	$WINSOC_{fossil}$: fossil fuel sources in WINSOC
WINTC	water-insoluble total carbon
$WINTC_f$	$WINTC_{fossil}$: fossil fuel sources in WINTC
WNA%	Plant wax n-alkanes ratio
WSOC	Water-soluble organic carbon
$WSOC_f$	$WSOC_{fossil}$: fossil fuel sources in WSOC

CHAPTER 1: INTRODUCTION

Carbonaceous aerosols

Carbonaceous aerosols are one of the most abundant and controversial components (20–80%) of atmospheric fine particulates ($PM_{2.5}$) and substantially affect both climate and human health (Anenberg et al., 2012; Lelieveld et al., 2015). Other fine atmospheric particulates include ammonium sulphate, ammonium nitrate and metals; in much lower concentrations, sodium nitrate, calcium sulfate, sea salt and mineral dust (Behera and Sharma, 2010; Chow et al., 2015; Gugamsetty et al., 2012). Many natural events, such as Himalayan glacier melting, drought and flood are strongly associated with carbonaceous aerosols (Trenberth, 2011; Zhao et al., 2013).

Compositions and carbon fractions of carbonaceous aerosols

The carbonaceous fraction of ambient particulate matter consists of elemental carbon (EC) and a variety of organic compounds (organic carbon, EC). EC also called black carbon (BC) or graphitic carbon, has a chemical structure similar to impure graphite and is emitted directly into the atmosphere predominantly during combustion (Koch and Del Genio, 2010; Pio et al., 2011). Carbonaceous particles mainly consist of weakly refractory and light polycyclic or polyacidic hydrocarbons (organic carbon, OC) and strongly refractory and highly polymerized EC (Herich et al., 2014).

OC is either emitted directly by sources (primary OC, POC), or can be formed in situ by condensation of low-volatility products of the photo-oxidation of hydrocarbons (secondary OC, SOC) (Lu et al., 2011). In terms of different water solubility, OC can be divided into water soluble OC (WSOC) and water insoluble OC (WINSOC). WSOC is normally comprised of SOC, part of biomass burning based POC and primary biogenic carbon (Hoyle et al., 2011; Pathak et al., 2011). Thus, OC is categorized not only with respect to primary/secondary sources, but also in the aspect of water solubility. Despite the fact that these two classification methods appear to overlap with the definition of OC, measurement of WSOC is an effective way to estimate SOC and POC, which assists further source apportionment of carbonaceous aerosols directly (Ram and Sarin, 2011; Ram et al., 2010; Zhang et al., 2012b).

With respect to EC, char and soot carbon fractions are further classified under the IMPROVE-A protocol, which isolates char and soot using different combustion temperatures. Char and

soot have distinct chemical and optical properties (Cao et al., 2012; Han et al., 2010; Kim et al., 2011b).

Table 1 compares the difference between the above carbon fractions (OC, EC, WSOC, WINSOC, SOC, POC, char and soot) under the aspects of their profiles, chemical constituents, and emission sources to explicitly illustrate the subdivisions of carbonaceous aerosols.

Table 1.1. Comparison of characterization of different carbon fractions.

	Carbonaceous aerosols			
	OC		EC	
	WSOC	WINSOC	Char	Soot
profiles	volatile; colourless/light colour	volatile; colourless/light colour	less volatile; coloured	less volatile; coloured
chemicals	low molecular mass hydrocarbons; humic-like substances	polycyclic aromatic hydrocarbons; biopolymers	graphene layers	thermally refractory black carbon
sources	SOA+POA[1]	POA	primary	primary

[1]POA contain primary biogenic aerosols as well as primary biomass burning aerosols

Climate and health effects of carbonaceous aerosols

Carbonaceous aerosols impact the climate of Earth directly via absorbing and scattering radiation and, indirectly, by acting as cloud condensation and ice nuclei for cloud and precipitation formation (Chung et al., 2012). OC can influence the absorption of EC through the lensing effect; and can cool the atmosphere by increasing the reflectivity of the Earth. EC is the most well-known light absorbing aerosol component (McNeill, 2017; Zaveri et al., 2012). WSOC exhibits light absorbing properties as well, contributing to both a direct positive climate forcing and a semi-direct climate effect, by heating and evaporation of clouds. Overall, OC/EC ratio determines the net climate forcing of carbonaceous aerosols (Safai et al., 2014).

Much attention is paid to the climate influence of carbonaceous aerosols. However, there is still a large uncertainty about detailed apportionment and quantification of sources of carbonaceous aerosols because the organic component may comprise hundreds or thousands of individual organic species, most of which are individually present at ultra-trace concentrations (Herckes et al., 2013; Li et al., 2016; Zhang et al., 2011). What is more, some toxic compounds, such as PAHs, have been proven to be able to dramatically harm human

2

health. $PM_{2.5}$ can enter the human lung and can even reach the bloodstream, affecting both lungs and heart (Weidemann et al., 2016). The possible health consequences range from simple irritation of the airways (such as coughing or difficulties in breathing) to premature death in people with heart or lung disease (Zhang et al., 2017b). Furthermore, airborne particulate matter results not only from direct emissions of particles but also from emissions of certain gases that either condense as particles directly or undergo chemical transformation to a species that condenses as a particle (Kim et al., 2017).

Moreover, these aerosols can cause respiratory and cardiovascular diseases (Liu et al., 2013). The International Agency for Research on Cancer (IARC) announced that outdoor air pollution and $PM_{2.5}$ are carcinogenic to humans (Ikemori et al., 2015). Therefore, insight into the sources and quantitatively apportioned sources of carbonaceous aerosol is crucial for policies to mitigate the impact of carbonaceous aerosols on human health and climate change.

Specific sources of carbonaceous aerosols

Organic aerosols originate mainly from three sources: combustion of fossil fuels, biomass burning and biogenic sources (Calvo et al., 2013; McDonald et al., 2018). All these sources can contribute to both primary and secondary organic aerosols (POAs and SOAs) (Belis et al., 2013b; Li et al., 2016).

Biogenic POAs consist of pollen, plant debris, fungal spores and microorganisms (Gilardoni et al., 2011; Pavuluri et al., 2013). Biogenic SOAs originate from volatile organic compounds (VOCs) emitted by plants, e.g. isoprene, monoterpenes (α-pinene and β-pinene) (Carlton et al., 2010; Genberg et al., 2011; Russell et al., 2011; Updyke et al., 2012) and cineole (Keywood et al., 2015). The emission of biogenic VOCs is related to the growing season and temperature, and is significantly greater during the warmer months of the year (Carslaw et al., 2010), at least for deciduous trees.

Primary fossil-fuel-based emissions from traffic and industry contribute to organic aerosols, as do secondary particles arising from the emission of fossil-fuel derived VOCs (Cao et al., 2013; Herich et al., 2011; Huang et al., 2014). These are examples of anthropogenic influences on the formation of particulate matter.

Biomass burning, e.g. forest fires or bush fires, is common during dry periods and is a large contributor to aerosol particles globally. These emissions can occur both in anthropogenic and

natural ways. The burning of biomass for domestic heating and risk reduction purposes (anthropogenic contribution), is also a major source of particles, especially in South Asia (Cong et al., 2015b), Australia (Keywood et al., 2013; Reisen et al., 2011) and China (Desyaterik et al., 2013; Tao et al., 2013a, b). There are also problems in some European cities near Alpine areas e.g. Zurich, where approximately 65% of the winter carbonaceous aerosol has been found to originate from biomass burning (Herich et al., 2011). During winter biomass burning is also a large contributor to aerosol mass in European countries (Reche et al., 2012; Viana et al., 2013) and Australia (Clarke et al., 2011; Johnston et al., 2013; Zhang et al., 2013b). As with primary fossil fuel based aerosols, primary biomass based aerosols can transform to secondary biomass derived aerosols as well (Cheng et al., 2013; Fu et al., 2012a; Saleh et al., 2014). It should be noted that approximately 90% of biomass burning is caused by human-induced fires and only a minor fraction arise from natural sources such as lightning strikes (Chen et al., 2017; Lamarque et al., 2010).
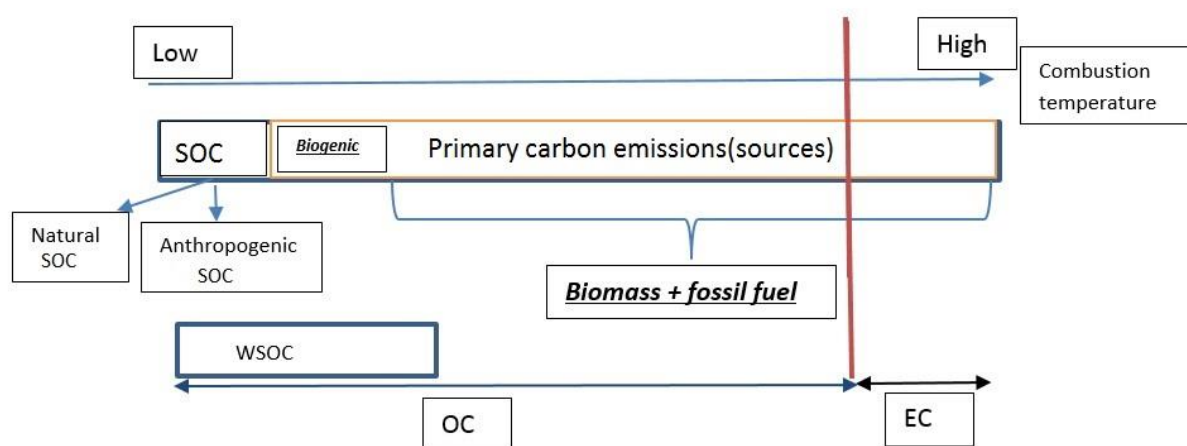
Natural SOC: secondary product from forest (*secondary biogenic*)
Anthropogenic SOC: secondary product from biomass and fossil emissions (*secondary biomass + fossil fuel*)
Figure 1.1. Carbon fractions and their corresponding emission sources.

Unlike Table 1.1, Figure 1.1 describes various carbon fractions and their respective sources according to their combustion temperature during separation processes, measured by gas chromatography/mass spectrometry (GC/MS) techniques and OC/EC thermal separation.

In comparison with the organic content of particulate matter, EC has less complex emission sources, which only originate from primary emissions, namely, incomplete fossil fuel combustion and biomass burning (Cao et al., 2013; Evangeliou et al., 2017). What is more, domestic wood combustion and diesel automotive sources are effective sources of EC per unit of fuel burned (Cong et al., 2015a; Liu et al., 2015).

Quantifying the contributions of primary and secondary particles from key sources is central to the development of control strategies for the reduction of population exposure and the incidence of particle-related mortality and morbidity (Cope et al., 2014).

Techniques and methods to evaluate carbonaceous aerosols sources

At present, three techniques and methods are utilized to identify and quantify the sources of carbonaceous aerosols, including chemical techniques, mathematical modelling methods and meteorological data analyses.

Chemical techniques refer to applied chemical analyses, for example, biomarker analysis (Dubois and Jacob, 2016; Gantt and Meskhidze, 2013), online organic aerosol analysis, using aerosol mass spectrometry (Szidat, 2017a; Zhang et al., 2011) and isotopic analysis (radiocarbon ^{14}C, stable carbon ^{13}C and nitrogen isotope ^{15}N) (Bird and Ascough, 2012; Szidat, 2017b; Szidat et al., 2018; Zhang et al., 2018). These analyses measure certain individual or bulk carbon fractions, which can explain carbonaceous aerosol sources from the perspective of chemistry microscopically and macroscopically.

A number of mathematical models, based on various algorithms, have been used to develop our understanding of source-receptor relationships for nonreactive species in an air-shed. These methods include: top-down studies–chemical mass balance (CMB) used for source apportionment (Chow et al., 2010; Fu et al., 2012b; Johnson et al., 2011); bottom-up studies– receptor modelling (Belis et al., 2013a; Bove et al., 2014; Pirovano et al., 2015; Squizzato et al., 2018), such as principal component analysis (PCA); Positive matrix factorization (PMF) used for source identification/apportionment (Belis et al., 2013b; Hwang and Hopke, 2011); and the empirical orthogonal function (EOF) method, used for identification of the location and strengths of emission sources. PCA is applied to many samples from the same site taken over a number of sampling periods, and EOF operates on many samples from many sites taken over the same period (Argyropoulos et al., 2017; Choudhary and Babu, 2011; Hopke, 2009; Seinfeld and Pandis, 2016).

Meteorological transport methods include some dispersion models such as open-air (urban sites) (Ancelet et al., 2014; Mazaheri et al., 2016) and back trajectories of Hybrid Single Particle Lagrangian Integrated Trajectory-HYSPLIT (long range transport) (Khan et al., 2016). Remote-sensing datasets (satellite data) from NASA's Moderate Resolution Imaging Spectrometer (MODIS) Active Fire Product algorithm can also be used to analyse the

variability of carbonaceous aerosols sources (Kaskaoutis et al., 2014). As this study mainly focuses on ground-based observations of carbonaceous aerosol properties to interpret carbonaceous aerosol sources, only chemical analysis methods (organic marker and radiocarbon analysis) are discussed specifically below.

Organic biomarkers

Organic biomarkers, as a widely recognized approach to trace sources in the organic geochemistry field (Nebbioso and Piccolo, 2013), have also been used extensively to distinguish sources for carbonaceous aerosols as well ; some unique biomarkers, such as hydro-PAHs, which can indicate and demonstrate the sole source from coal combustion (Zhu et al., 2018) have also been used.

Certain organic biomarkers can not only identify emission sources, but also assist apportioning sources quantitatively (Zhang et al., 2011). Additionally, organic biomarker concentrations, as input data of chemical transport models, can assist in identifying the origin of pollutants and the formation of particulate matter spatially and temporally (Jiang et al., 2012; Zhang et al., 2012a).

Tables 1.2 and 1.3 list some common organic tracers, classified according to polarity and their respective potential source contributors. Non-polar organic tracers all derive from primary sources (Lin et al., 2015; Mirante et al., 2013; Qadir et al., 2013). Polar organic biomarkers can originate from both primary sources and secondary sources (Engel and Macko, 2013; Kim et al., 2011a). Unique organic tracers are illustrated in bold. Although several important organic markers have varieties of source contributors, elevated concentrations of these organic compounds have attracted the attention of researchers world-wide (Gantt and Meskhidze, 2013; Mancilla et al., 2016; Menon, 2016).

Specifically, n-alkanes include C_{10}-C_{34} carbon alkanes, among them lower molecular weight alkanes, such as C_{10}-C_{17} normally derived from marine sources (Stone et al., 2010; Wang et al., 2015); C_{23}-C_{25} alkanes were reported to originate from traffic emission (Chen et al., 2014; Gentner et al., 2017; Guo et al., 2013), while biogenic activities can emit higher molecular weight alkanes (Després et al., 2012; Xing et al., 2011). PAHs (polycyclic aromatic hydrocarbons) contain 16 types of World Health Organization (WHO) designated PAHs (Nap: naphthalene, Acy: acenaphthylene, Ace: acenaphthene, Flo: fluorene, Phe: phenanthrene, Ant: anthracene, Flu: fluoranthene, Pyr: pyrene, BaA: bbenzo[a]anthracene, Chry: chrysene, BbF: benzo[b]fluoranthene, BkF: benzo[k]fluoranthene, BaP: benzo[a]pyrene, InP: indeno[1,2,3-

6

c,d]pyrene, DbA: dibenzo[a,h]anthracene, BgP: benzo[g,h,i]perylene) and some derived PAH groups (hydro-PAHs and nitro-PAHs, etc), which are emitted from multiple primary sources or incomplete combustion (Hasheminassab et al., 2013; Pant and Harrison, 2013). Hopanes consist of $17\alpha(H),21\beta(H)$-norhopane, $17\alpha(H),21\beta(H)$-hopane, $22S$-$17\alpha(H),21\beta(H)$-homohopane and $22R$-$17\alpha(H),21\beta(H)$-homohopane, while steranes are $20(R+S)$, $\alpha\beta\beta$-cholestane, $20(R+S)$, $\alpha\beta\beta$-ergostane, $20(R+S)$, $\alpha\beta\beta$-sitostane (Daher et al., 2012; Li et al., 2013). Resin acids and methoxyphenols are particular softwood and hardwood combustion biomarkers, which include dehydroabietic acid, β-sitosterol and 4-hydroxybenzoic acid; as well as syringic acid, syringol, vanillin and vanillic acid, respectively (Mikuška et al., 2017).

Higher concentrations of alkanoic acids and alkenoic acids are usually observed appearing from C_{16} and C_{18} (Shannigrahi et al., 2014). The principal saccharide biomarkers are galactose, glucose, mannitol and arabitol (Jia and Fraser, 2011). C_2-C_4 dicarboxylic acids are oxalic acid, malonic acid and succinic acid, which are markers for either primary sources (biomass burning/road dust) or secondary natural/anthropogenic sources (Abdullahi et al., 2013).

Except for the above discussed primary organic compounds, some of the relatively unstable VOCs emerging from primary emission sources can undergo a series of atmospheric photo-chemical reactions which convert them into other VOCs (SOA) (Zhang et al., 2015a). Selected typical natural/anthropogenic secondary organic biomarkers are introduced below.

Isoprene, as a precursor, engaging in photo-chemical oxidation can produce several secondary organic compounds, mainly including DL-Threitol, 2-methyltetrols, 2-methylglyceric acid, *cis*-2-methyl-1,3,4-trihydroxy-1-butene, 3-methyl-2,3,4-trihydroxy-1-butene, trans-2-methyl-1,3, 4-trihydroxy-1-butene, 3-methyltetrahydrofuran-3, 4-diols and C_5-alkene-triols (Shiraiwa et al., 2017; Xu et al., 2015).

Also α-Pinene (monoterpenes) can be transformed into *cis*-pinonic acid, pinic acid, 3-methyl-1,2,3- butanetricarboxylic acid, 1,2,3- butanetricarboxylic acid (MBTCA), 3-hydroxyglutaric acid, 3/2-hydroxy-4,4-dimethylglutaric acid, 2-hydroxy-4-isopropyladipic acid, 3-(2-hydroxyethyl)-2,2-dimothylcyclobutane carboxylic acid, 3-acetylglutaric acid, 3-acethladipic acid, 3-isopropylglutaric acid and 3-acetyl hexanedioic acid via atmospheric oxidation peocesses (Epstein et al., 2014; Zhang et al., 2017a; Zhang et al., 2015b). β-caryophyllenic acid, β-caryophyllinic acid and 2,3-dihydroxyisopentanol (DHIP) are generated from β-caryophyllene and 2-methyl-3-buten-2-ol (MBO), respectively (Ding et al., 2012; Khan et al.,

2017). Diaterebic acid acetate and diaterpenylic acid acetate are atmospheric tracers for secondary organic aerosol formation from cineole (a VOC emitted from eucalypt) oxidation (Iinuma et al., 2016; Keywood et al., 2015).

The compound 2, 3-dihydroxy-4-oxopentanoic acid was detected to be formed from toluene and xylenes, which are common primary emissions from anthropogenic biomass burning and fossil fuel combustion (Ervens et al., 2011; Gentner et al., 2017; Zhu et al., 2017). Heo et al. observed that naphthalene can be converted into phthalic acid and methyl phthalic acid in the Los Angeles Basin under active photo-oxidation conditions (Heo et al., 2015).

C_2-C_4 dicarboxylic acids have various sources (Kawamura and Bikkina, 2016). They can either derive from biomass burning and road dust, and therefore are regarded as primary organic biomarkers, or can be generated from primary low molecular weight VOC, and then classified as secondary organic biomarkers (Bikkina et al., 2017; Mochizuki et al., 2017). C_7-C_9 dicarboxylic acids, predominantly azelaic acid (C_9), are found as secondary organic biomarkers in several urban sites worldwide, formed from high molecular weight VOC (García Álvarez et al., 2017; Mesquita et al., 2017).

Table 1.2. Non-polar organic tracers and their corresponding source contributors.

Non-polar primary organic biomarkers	
Compound name	Potential source contributors
N-alkanes	biomass burning + fossil fuel(traffic + coal) + biogenic emissions + meat cooking
PAHs	biomass burning + fossil fuel(traffic + coal)
Retene	**biomass burning**
Cholestane	**cooking**
Hopanes and steranes	**fossil fuel (petroleum biomarker-traffic)**

Table 1.3. Polar organic tracers and their corresponding source contributors.

Polar primary organic biomarkers	
Compound name	Potential source contributors
Alkanoic acids	biomass burning + fossil fuel
Alkenoic acids	biomass burning + fossil fuel + meat cooking
Monosaccharide anhydrides (levoglucosan, mannosan, galactosan)	**biomass burning**
Resin acids	**softwood burning**

Methoxyphenols	**hardwood burning**
Saccharides	biomass burning/primary biogenic emissions/road dust
Dicarboxylic acids(C_2-C_4)	biomass burning + road dust

Polar secondary organic biomarkers

Compound name	Potential source contributors
Isoprene derived compounds	**secondary biogenic sources**
Monoterpenes derived compounds	**secondary biogenic sources**
Cineole derived compounds	**secondary biogenic sources from eucalyptus**
Aromatic derived compounds	secondary anthropogenic sources derived from primary biomass burning and fossil fuel precursors (toluene, xylenes and naphthalene)
Dicarboxylic acids(C_2-C_4)	secondary natural/anthropogenic sources derived from low molecular weighted precursors emitted from forest fire/(fossil fuel and biomass burning) sources
Dicarboxylic acids(C_7-C_9)	secondary natural/anthropogenic sources derived from high molecular weighted precursors emitted from forest fire/(biomass burning and fossil fuel) sources

Despite the fact that specific airborne ambient molecular organic biomarkers can help identify sources, a single approach is not enough to provide comprehensive information for characterization and source apportionment of carbonaceous aerosols. In addition, the molecular organic biomarker technique still has some limitations. The organic component comprises thousands of individual organic species, most of which are individually present at ultra-trace levels. Quantified priority organic biomarker compounds account for less than one hundredth of organic fractions in $PM_{2.5}$ (Heal et al., 2011).

In contrast to organic biomarkers, determination of the radiocarbon (^{14}C) proportion of bulk carbon offers a unique possibility for apportioning sources of carbonaceous aerosol particles, which can unambiguously discriminate fossil and non-fossil emissions (Martinsson et al., 2017).

Radiocarbon analysis

The radioisotope of carbon (^{14}C) is an ideal tracer for distinguishing between fossil and contemporary carbon (Gilardoni et al., 2011). Living material is in equilibrium with CO_2 in the atmosphere containing a known abundance of ^{14}C. The ^{14}C isotope decays with a half-life of 5,370 years, which is negligible in comparison with the age of fossil carbon sources (Ceburnis et al., 2011). Thus, in principle, determination of the ratio of ^{14}C abundance in a sample to its abundance in contemporary carbon directly yields the proportion of contemporary to fossil carbon in the sample (Glasius et al., 2011). However, it should be

noted that ^{14}C of total carbon (TC) from aerosols will not provide complete or comprehensive information on the emission sources or the formation process, since OC and EC do not originate from the same processes (Sun et al., 2012). Therefore, using ^{14}C content in EC and OC, the contribution of biogenic and fossil OC for summer conditions as well as the fraction of EC from residential wood burning during winter was directly quantified for several areas in the world (Bernardoni et al., 2013; Zhang et al., 2014b; Zhang et al., 2015d; Zotter et al., 2014).

Szidat et al. (Szidat et al., 2008) studied carbonaceous aerosols by separate analysis of ^{14}C in EC and OC. EC_{wood} (wood burning, the only major origin of non-fossil EC), EC_{fossil} (fossil fuel sources in EC), OC_{fossil} (fossil fuel sources in OC) and $OC_{non\text{-}fossil}$ (non-fossil sources in OC) fractions were quantified. The last fraction comprised OC from wood burning as well as primary biogenic OC ($OC_{biogenic}$) and biogenic SOA ($SOA_{biogenic}$). In order to assess their contributions to $OC_{non\text{-}fossil}$, OC_{wood} (wood burning sources in OC) was estimated from EC_{wood} using an average EC/OC emission ratio and $OC_{biogenic}$ was calculated by subtraction.

Using a ^{14}C source apportionment approach, Sheesley at al. found that a majority (or at least a large proportion) of EC is from biomass combustion in the Maldives and India, respectively (Bikkina et al., 2016; Sheesley et al., 2011). Recently, Chen et al. used top down ^{14}C measurements in urban sites to determine that fossil combustion was responsible for the EC fraction in East China (Chen et al., 2013). Minguillón et al. combined ^{14}C data, aerosol mass spectrometry data and correlations between fossil OC and fossil EC to obtain the result that fossil OC at Barcelona is ~47% primary whereas at MSY (a mountain rural site) fossil OC is mainly secondary (~85%) (Minguillón et al., 2011).

One thing that should be mentioned is since Australia is trying to shift the energy structure to more non-fossil fuel constituents, 9–10% ethanol is added in regular unleaded petrol, which is called fuel E10. As ethanol belongs to non-fossil fuel, minor traffic emissions contribute to new carbon fraction in aerosols. Additionally, usage of E10 fuel would result in the elevated level of non-fossil derived secondary particles particularly during high solar radiation days (Schulz and Clark, 2011).

Current research on carbonaceous aerosols

Overview

10

Currently, assessment of the origin of air pollutants may be based on either emission inventories, with detailed information on emission factors and activities combined with dispersion modelling (Herich et al., 2014), or by source apportionment estimates based on chemical analysis of the source-diagnostic composition of ambient aerosols (Wang et al., 2016).

Bottom-up studies, namely, adopting emission inventories associated with chemical-transport models have some limitations, such as the large variations in fuel types and burning combustion conditions. This variability leads to emission factors and activities being inherently more complex and uncertain (Andersson et al., 2011).

Top-down studies normally apply receptor modellings, such as Positive Matrix Factorization (PMF), Multilinear Engine-2 (ME-2) and Principal Components Analysis (PCA), to apportion certain carbon fractions using molecular organic tracers and/or coupling with radiocarbon data (Piletic et al., 2013; Sheesley et al., 2017).

What is more, in addition to the above offline quantitative methods for source assessment of carbonaceous aerosols, online aerosol mass spectrometry is also commonly used for quantifying organic aerosols. Factor analysis of aerosol mass spectra from an aerosol mass spectrometer enables the deconvolution of organic matter into different factors based on their mass spectral fingerprints (Ulevicius et al., 2016). The combination of measurements and source apportionment techniques allows a better characterization of the carbonaceous aerosol sources.

Current studies on radiocarbon based source apportionment of carbonaceous aerosols

At present, radiocarbon analysis of OC and EC still does not have a uniform performance standard. There are several reasons for this. One is that this technique has continued to develop over the last 20 years with many improvements and a new recognition of its scope by scientists in the research field.

Several top international research laboratories, mainly in Europe, have attempted to explore an optimal approach to isolate OC and EC for radiocarbon analysis unambiguously. The major problem is that there is still no confirmed standard for separation of OC and EC. Demarcation between OC and EC is methodologically defined. Popular OC/EC protocols

include the NIOSH (The National Institute for Occupational Safety and Health) protocol, IMPROVE (U.S. Interagency Monitoring of PROtected Visual Environments) protocol, IMPROVE_A protocol and EUSAAR (European Supersites for Atmospheric Aerosol Research) protocol, which were all proposed at different times and in different areas. The principal difference between various protocols is the different combustion temperatures for determining the contribution of OC.

The exact value of the OC heating temperature should be decided according to the sampling site. Specifically, different sampling sites may have different OC/EC ratios. Higher OC heating temperatures can result in overestimation of EC concentrations, which have been reported to have large discrepancies (up to a factor of 7) (Han et al., 2016). Thus, different OC/EC samples may need to use different optimum thermal/optical protocols for analysis. For example, the EUSAAR protocol is modified for rural sampling sites (Cavalli et al., 2010), whereas IMPROVE and IMPROVE_A may be more suitable for urban site samples (Han et al., 2016). In addition, there are protocols for bushfire filter samples (Iinuma et al., 2016).

In summary, samples from different sampling site require the use of different OC/EC protocols which, in turn, lead to different OC/EC separation methods for radiocarbon analysis. To date, Szidat's group (University of Bern) have developed a comprehensive strategy for isolation of OC and EC for radiocarbon analysis. They set up a device to couple the OC/EC analyzer to the cryogenic traps, which solved the problem of specific OC/EC separation temperatures. In addition, they modified their EUSAAR protocol by changing the carrier gas heating temperature in Step 1, and adding one more flash heating to reduce the artifacts and separate OC/EC completely (Zhang et al., 2012c). This Swiss_4S protocol has been validated by a US research group, which confirmed it to be the premium one currently available (Mouteva et al., 2015). The next development was an online coupling instrument, by means of an elemental analyser with a MICADAS Accelerated Mass Spectrometry (AMS), for fast and automatic radiocarbon measurement of aerosol samples in 2015 (Salazar et al., 2015).

Before the Swiss_4S protocol, the CTO-375 method proposed by Gustafsson (Zencak et al., 2007) and THEODORE (two-step heating system for the OC/EC determination of radiocarbon in the environment) developed by Szidat's group (Zhang et al., 2010) were popularly used for radiocarbon measurements in Europe (Andersson et al., 2011; Dusek et al., 2014; Ulevicius et al., 2016), China (Zhang et al., 2015d) (Liu et al., 2014; Liu et al., 2016; Zhang et al., 2014a, 2015c; Zhang et al., 2013a) and South Asia (Bosch et al., 2014; Budhavant et al., 2015; Kirillova et al., 2013; Kirillova et al., 2014). Nevertheless, all the

12

above research is still based on NIOSH and EUSAAR protocols for OC/EC separation. In our study, IMPROVE_A protocol was used for OC/EC analyses under a thermal/optical reflectance (TOR) method for charring adjustment.

Since there is no standard way to conduct carbon species separation for radiocarbon analysis, and no efficient method to validate various separation methods, the only way to confirm and assess the method used in this thesis is to refer to the previous experiments from other labs. According to previous empirical research, the following separation methods have been proposed for this research.

1. ^{14}C data in TC and WINTC:

   Radiocarbon data is obtained directly via radiocarbon analysis in total carbon (TC) and water-insoluble total carbon (WINTC), which is water-washed to remove water soluble organic carbon based on the method used in Yttri et al (Yttri et al., 2009).

2. ^{14}C data in EC:

   Remove less refractory OC: to avoid the overestimation of EC because of charring, water treatment is first applied to wash these components; then dried samples are heated at 375 ℃ for 1h with high purity oxygen to remove less refractory OC fractions; water treatment or acid treatment plus high purity oxygen combustion at low temperature are confirmed as an efficient method to reduce pyrolysis of thermally less refractory OC. However, different labs adopt different temperatures to remove OC from 340-475 ℃ centigrade (Bench, 2012; Szidat et al., 2013).

Thus, to be consistent with OC/EC analyses under IMPROVE_A protocol, 580 ℃ under pure Helium for 10 minutes was conducted to totally remove OC compared with 650 ℃ in the EUSAAR protocol.

Aims

Wood materials due to their cheaper prices and convenient usage are widely used for small scale domestic heating and cooking fuel in developing countries (Ezzati and Baumgartner, 2017; Villalobos et al., 2017) and even in some developed countries, such as North America, Australia, and some wealthy European countries for residential heating purposes (Hong et al., 2017; López-Aparicio et al., 2017; Rokoff et al., 2017). Utilization of residential wood appliances, for example, wood heaters and wood stoves can produce toxic substances that impact human health and, in addition, wood burning is one of the dominant contributors to carbonaceous aerosols (Herich et al., 2014). Figure 1.2 demonstrates a photo taken at Eastwood, one of Sydney's densely populated suburban areas. Here residential wood

appliances are very popular and frequently used by Australian families. Furthermore, at night the strong wood smoke can be smelt almost every day during cold periods in this and other suburban areas.

Owing to extreme weather caused by climate change in recent years, Sydney has suffered elevated $PM_{2.5}$ levels, arising from wood combustion. However, studies about carbonaceous aerosols in Sydney are rare and information on source apportionment and chemical compositions of carbonaceous aerosols in Australia is still very limited.

Most importantly, scientists have basically focused on studies in northern Australia and South Australia. Meyer et al (Meyer et al., 2008) applied a model to study biomass burning emissions over northern Australia constrained by aerosol measurements. O'brien et al (O'brien and Mitchell, 2003) investigated atmospheric heating caused by carbonaceous aerosols. Frequent forest fires and biomass burning throughout the year, plus residential heating in winter make a great contribution to PM levels in Sydney. This project will provide basic scientific data for future monitoring and policy development.

Figure 1.2. Small scale individual domestic heating using a residential wood stove, at Eastwood in the Sydney metropolitan area taken in June 2017.

The overall aims of this thesis are to:

a. Measure and quantify organic species (polar and non-polar organic molecular marker compounds) in $PM_{2.5}$ in a residential urban area in Sydney during prescribed burns and domestic heating periods.

b. Identify sources of organic aerosols via the typical organic tracers and evaluate relative

14

contributions of each source to certain organic species by means of correlation analysis and Principle Component Analysis (PCA).

Justify selection of statistical tool: Although PMF V5 is reputed by large potentials and more advanced functions, owing to limited aerosol samples in this study (20 samples), PMF V5 conducting two constrains cannot demonstrate more advantages than PCA-MLR, whereas PCA using orthogonal method is more suitable for small size samples (Viana et al., 2008). On the other hand, research performed in Los Angeles indicates that PMF V5 is not suitable for SOA dominated aerosol samples (Heo et al., 2015). Consequently, after considering various factors and weighting cons and pros, PCA-MLR was selected to apportion sources of fine carbonaceous aerosols.

c. Introduce a radiocarbon technique to analyse ^{14}C in each carbon fraction in order to achieve relatively complete source assessment of fine carbonaceous aerosols collected in different seasons at two urban sites in Sydney

d. Discuss and evaluate the current OC/EC protocol and isolation method for radiocarbon analysis in OC and EC. Propose a preliminary idea to establish more standardized guidelines for OCEC analysis.

Fulfilling these aims will contribute to a better understanding of the organic compositions of fine carbonaceous aerosols during cold periods and of the differences of source contributions of fine carbonaceous aerosols collected during various sampling events. This information will provide further scientific evidence on which to base air quality management strategies.

Structure of the Thesis

The three studies presented in this thesis are: (a) characterization of polar organic tracers in urban Sydney carbonaceous aerosols; (b) characterization of non-polar organic compounds in urban Sydney fine carbonaceous aerosols; and (c) source assessment of fine urban Sydney carbonaceous aerosols based on radiocarbon analysis.

Chapter 1 introduces background information on carbonaceous aerosols, including their compositions and impacts as well as research methods and analysis. Previous studies are described with respect to using top-down and bottom-up approaches to quantify carbonaceous aerosols sources.

Chapter 2 characterizes two categories of non-polar organic chemicals, PAHs and alkanes, using diagnostic ratios and related indexes, and fingerprints potential sources of PAHs and alkanes, applying correlation analysis and PCA-MLR modelling.

Chapter 3 goes on to use similar methods to ascertain the crucial polar organic tracers in fine carbonaceous aerosols of urban Sydney.

Having assessed the diversity of aerosol components, Chapter 4 utilizes these data to evaluate the source contributions to different carbonaceous aerosol samples collected in haze, sunny or on stable meteorological condition days, respectively, based on ^{14}C data in each carbon fraction. The variation of absolute concentrations and relative contributions to carbonaceous aerosols dominated by wood burning are elucidated.

The final Chapter 5 synthesizes all thesis findings. Implications of the research are discussed and some recommendations proposed. Limitations and priorities for future research are briefly outlined.

References

Abdullahi, K.L., Delgado-Saborit, J.M., Harrison, R.M., 2013. Emissions and indoor concentrations of particulate matter and its specific chemical components from cooking: A review. Atmospheric Environment 71, 260-294.

Ancelet, T., Davy, P.K., Trompetter, W.J., Markwitz, A., Weatherburn, D.C., 2014. Sources and transport of particulate matter on an hourly time-scale during the winter in a New Zealand urban valley. Urban Climate 10, 644-655.

Andersson, A., Sheesley, R.J., Kruså, M., Johansson, C., Gustafsson, Ö., 2011. 14 C-Based source assessment of soot aerosols in Stockholm and the Swedish EMEP-Aspvreten regional background site. Atmospheric environment 45, 215-222.

Anenberg, S.C., Schwartz, J., Shindell, D., Amann, M., Faluvegi, G., Klimont, Z., Janssens-Maenhout, G., Pozzoli, L., Van Dingenen, R., Vignati, E., 2012. Global air quality and health co-benefits of mitigating near-term climate change through methane and black carbon emission controls. Environmental Health Perspectives 120, 831.

Argyropoulos, G., Samara, C., Diapouli, E., Eleftheriadis, K., Papaoikonomou, K., Kungolos, A., 2017. Source apportionment of PM 10 and PM 2.5 in major urban Greek agglomerations using a hybrid source-receptor modeling process. Science of The Total Environment 601, 906-917.

Behera, S.N., Sharma, M., 2010. Reconstructing primary and secondary components of PM2. 5 composition for an urban atmosphere. Aerosol Science and Technology 44, 983-992.

Belis, C., Karagulian, F., Larsen, B., Hopke, P., 2013a. Critical review and meta-analysis of ambient particulate matter source apportionment using receptor models in Europe. Atmospheric Environment 69, 94-108.

Belis, C., Karagulian, F., Larsen, B.R., Hopke, P., 2013b. Critical review and meta-analysis of ambient particulate matter source apportionment using receptor models in Europe. Atmospheric Environment 69, 94-108.

Bench, G., 2012. INTERCOMPARISON OF 14C ANALYSIS OF CARBONACEOUS AEROSOLS: EXERCISE 2009. Lawrence Livermore National Laboratory (LLNL), Livermore, CA.

Bernardoni, V., Calzolai, G., Chiari, M., Fedi, M., Lucarelli, F., Nava, S., Piazzalunga, A., Riccobono, F., Taccetti, F., Valli, G., 2013. Radiocarbon analysis on organic and elemental carbon in aerosol samples and source apportionment at an urban site in Northern Italy. Journal of Aerosol Science 56, 88-99.

Bikkina, S., Andersson, A., Sarin, M., Sheesley, R., Kirillova, E., Rengarajan, R., Sudheer, A., Ram, K., Gustafsson, Ö., 2016. Dual carbon isotope characterization of total organic carbon in wintertime carbonaceous aerosols from northern India. Journal of Geophysical Research: Atmospheres 121, 4797-4809.

Bikkina, S., Kawamura, K., Sarin, M., 2017. Secondary Organic Aerosol Formation over Coastal Ocean: Inferences from Atmospheric Water-Soluble Low Molecular Weight Organic Compounds. Environmental Science & Technology 51, 4347-4357.

Bird, M.I., Ascough, P.L., 2012. Isotopes in pyrogenic carbon: a review. Organic Geochemistry 42, 1529-1539.

Bosch, C., Andersson, A., Kirillova, E.N., Budhavant, K., Tiwari, S., Praveen, P., Russell, L.M., Beres, N.D., Ramanathan, V., Gustafsson, Ö., 2014. Source-diagnostic dual-isotope composition and optical properties of water-soluble organic carbon and elemental carbon in the South Asian outflow intercepted over the Indian Ocean. Journal of Geophysical Research: Atmospheres 119.

Bove, M., Brotto, P., Cassola, F., Cuccia, E., Massabò, D., Mazzino, A., Piazzalunga, A., Prati, P., 2014. An integrated PM 2.5 source apportionment study: positive matrix factorisation vs. the chemical transport model CAMx. Atmospheric environment 94, 274-286.

Budhavant, K., Andersson, A., Bosch, C., Kruså, M., Kirillova, E., Sheesley, R., Safai, P., Rao, P., Gustafsson, Ö., 2015. Radiocarbon-based source apportionment of elemental carbon aerosols at two South Asian receptor observatories over a full annual cycle. Environmental Research Letters 10, 064004.

Calvo, A., Alves, C., Castro, A., Pont, V., Vicente, A., Fraile, R., 2013. Research on aerosol sources and chemical composition: past, current and emerging issues. Atmospheric Research 120, 1-28.

Cao, J.-j., Wang, Q.-y., Chow, J.C., Watson, J.G., Tie, X.-x., Shen, Z.-x., Wang, P., An, Z.-s., 2012. Impacts of aerosol compositions on visibility impairment in Xi'an, China. Atmospheric Environment 59, 559-566.

Cao, J.-J., Zhu, C.-S., Tie, X.-X., Geng, F.-H., Xu, H.-M., Ho, S., Wang, G.-H., Han, Y.-M., Ho, K.-F., 2013. Characteristics and sources of carbonaceous aerosols from Shanghai, China. Atmospheric Chemistry and Physics 13, 803-817.

Carlton, A.G., Pinder, R.W., Bhave, P.V., Pouliot, G.A., 2010. To what extent can biogenic SOA be controlled? Environmental science & technology 44, 3376-3380.

Carslaw, K., Boucher, O., Spracklen, D., Mann, G., Rae, J., Woodward, S., Kulmala, M., 2010. A review of natural aerosol interactions and feedbacks within the Earth system. Atmospheric Chemistry and Physics 10, 1701-1737.

Cavalli, F., Viana, M., Yttri, K.E., Genberg, J., Putaud, J.-P., 2010. Toward a standardised thermal-optical protocol for measuring atmospheric organic and elemental carbon: the EUSAAR protocol. Atmospheric Measurement Techniques 3, 79-89.

Ceburnis, D., Garbaras, A., Szidat, S., Rinaldi, M., Fahrni, S., Perron, N., Wacker, L., Leinert, S., Remeikis, V., Facchini, M., 2011. Quantification of the carbonaceous matter origin in submicron marine aerosol by 13 C and 14 C isotope analysis. Atmospheric Chemistry and Physics 11, 8593-8606.

Chen, B., Andersson, A., Lee, M., Kirillova, E.N., Xiao, Q., Kruså, M., Shi, M., Hu, K., Lu, Z., Streets, D.G., 2013. Source forensics of black carbon aerosols from China. Environmental science & technology 47, 9102-9108.

Chen, J., Li, C., Ristovski, Z., Milic, A., Gu, Y., Islam, M.S., Wang, S., Hao, J., Zhang, H., He, C., 2017. A review of biomass burning: Emissions and impacts on air quality, health and climate in China. Science of the Total Environment 579, 1000-1034.

Chen, Y., Cao, J., Zhao, J., Xu, H., Arimoto, R., Wang, G., Han, Y., Shen, Z., Li, G., 2014. n-Alkanes and polycyclic aromatic hydrocarbons in total suspended particulates from the southeastern Tibetan Plateau: concentrations, seasonal variations, and sources. Science of the total environment 470, 9-18.

Cheng, Y., Engling, G., He, K.-B., Duan, F.-K., Ma, Y.-L., Du, Z.-Y., Liu, J.-M., Zheng, M., Weber, R.J., 2013. Biomass burning contribution to Beijing aerosol. Atmospheric Chemistry and Physics 13, 7765-7781.

Choudhary, A., Babu, K., 2011. Source apportionment of aerosol in delhi using unmix receptor model.

Chow, J.C., Lowenthal, D.H., Chen, L.-W.A., Wang, X., Watson, J.G., 2015. Mass reconstruction methods for PM2. 5: a review. Air Quality, Atmosphere & Health 8, 243-263.

Chow, J.C., Watson, J.G., Lowenthal, D.H., Chen, L.-W.A., Motallebi, N., 2010. Black and organic carbon emission inventories: review and application to California. Journal of the Air & Waste Management Association 60, 497-507.

Chung, C.E., Ramanathan, V., Decremer, D., 2012. Observationally constrained estimates of carbonaceous aerosol radiative forcing. Proceedings of the National Academy of Sciences 109, 11624-11629.

Clarke, H.G., Smith, P.L., Pitman, A.J., 2011. Regional signatures of future fire weather over eastern Australia from global climate models. International Journal of Wildland Fire 20, 550-562.

Cong, Z., Kang, S., Kawamura, K., Liu, B., Wan, X., Wang, Z., Gao, S., Fu, P., 2015a. Carbonaceous aerosols on the south edge of the Tibetan Plateau: concentrations, seasonality and sources. Atmospheric chemistry and physics 15, 1573-1584.

Cong, Z., Kawamura, K., Kang, S., Fu, P., 2015b. Penetration of biomass-burning emissions from South Asia through the Himalayas: new insights from atmospheric organic acids. Scientific reports 5, 9580.

18

Cope, M., Keywood, M., Emmerson, K., Galbally, I., Boast, K., Chambers, S., Cheng, M., Crumeyrolle, S., Dunne, E., Fedele, R., 2014. Sydney Particle Study-Stage-II. Sydney Particle Study Final Report, CAWCR Publication.

Daher, N., Ruprecht, A., Invernizzi, G., De Marco, C., Miller-Schulze, J., Heo, J.B., Shafer, M.M., Shelton, B.R., Schauer, J.J., Sioutas, C., 2012. Characterization, sources and redox activity of fine and coarse particulate matter in Milan, Italy. Atmospheric Environment 49, 130-141.

Després, V., Huffman, J.A., Burrows, S.M., Hoose, C., Safatov, A., Buryak, G., Fröhlich-Nowoisky, J., Elbert, W., Andreae, M., Poeschl, U., 2012. Primary biological aerosol particles in the atmosphere: a review. Tellus B: Chemical and Physical Meteorology 64, 15598.

Desyaterik, Y., Sun, Y., Shen, X., Lee, T., Wang, X., Wang, T., Collett, J.L., 2013. Speciation of "brown" carbon in cloud water impacted by agricultural biomass burning in eastern China. Journal of Geophysical Research: Atmospheres 118, 7389-7399.

Ding, X., Wang, X.M., Gao, B., Fu, X.X., He, Q.F., Zhao, X.Y., Yu, J.Z., Zheng, M., 2012. Tracer-based estimation of secondary organic carbon in the Pearl River Delta, south China. Journal of Geophysical Research: Atmospheres 117.

Dubois, N., Jacob, J., 2016. Molecular biomarkers of Anthropic impacts in natural archives: A review. Frontiers in Ecology and Evolution 4, 92.

Dusek, U., Monaco, M., Prokopiou, M., Gongriep, F., Hitzenberger, R., Meijer, H., Röckmann, T., 2014. Evaluation of a two-step thermal method for separating organic and elemental carbon for radiocarbon analysis. Atmospheric Measurement Techniques 7, 1943-1955.

Engel, M., Macko, S.A., 2013. Organic geochemistry: principles and applications. Springer Science & Business Media.

Epstein, S.A., Blair, S.L., Nizkorodov, S.A., 2014. Direct photolysis of α-pinene ozonolysis secondary organic aerosol: effect on particle mass and peroxide content. Environmental science & technology 48, 11251-11258.

Ervens, B., Turpin, B., Weber, R., 2011. Secondary organic aerosol formation in cloud droplets and aqueous particles (aqSOA): a review of laboratory, field and model studies. Atmospheric Chemistry and Physics 11, 11069-11102.

Evangeliou, N., Shevchenko, V., Espen Yttri, K., Eckhardt, S., Sollum, E., Pokrovsky, O.S., Kobelev, V.O., Korobov, V.B., Lobanov, A.A., Starodymova, D.P., 2017. Elemental carbon in snow from Western Siberia and Northwestern European Russia during spring 2014, 2015 and 2016, EGU General Assembly Conference Abstracts, p. 7764.

Ezzati, M., Baumgartner, J.C., 2017. Household energy and health: where next for research and practice? The Lancet 389, 130-132.

Fu, P., Kawamura, K., Chen, J., Li, J., Sun, Y., Liu, Y., Tachibana, E., Aggarwal, S., Okuzawa, K., Tanimoto, H., 2012a. Diurnal variations of organic molecular tracers and stable carbon isotopic composition in atmospheric aerosols over Mt. Tai in the North China Plain: an influence of biomass burning. Atmospheric Chemistry and Physics 12, 8359-8375.

Fu, T.-M., Cao, J., Zhang, X., Lee, S., Zhang, Q., Han, Y., Qu, W., Han, Z., Zhang, R., Wang, Y., 2012b. Carbonaceous aerosols in China: top-down constraints on primary sources and estimation of secondary contribution. Atmospheric chemistry and physics 12, 2725-2746.

Gantt, B., Meskhidze, N., 2013. The physical and chemical characteristics of marine primary organic aerosol: a review. Atmospheric Chemistry and Physics 13, 3979-3996.

García Álvarez, M.I., Van Drooge, B.L., Rodríguez González, S., Alastuey, A., 2017. Speciation of organic aerosols in the Saharan Air Layer and in the free troposphere westerlies [Discussion paper].

Genberg, J., Hyder, M., Stenström, K., Bergström, R., Simpson, D., Fors, E., Jönsson, J.Å., Swietlicki, E., 2011. Source apportionment of carbonaceous aerosol in southern Sweden. Atmospheric Chemistry and Physics 11, 11387-11400.

Gentner, D.R., Jathar, S.H., Gordon, T.D., Bahreini, R., Day, D.A., El Haddad, I., Hayes, P.L., Pieber, S.M., Platt, S.M., de Gouw, J., 2017. Review of urban secondary organic aerosol

formation from gasoline and diesel motor vehicle emissions. Environmental science & technology 51, 1074-1093.

Gilardoni, S., Vignati, E., Cavalli, F., Putaud, J., Larsen, B., Karl, M., Stenström, K., Genberg, J., Henne, S., Dentener, F., 2011. Better constraints on sources of carbonaceous aerosols using a combined 14 C–macro tracer analysis in a European rural background site. Atmospheric Chemistry and Physics 11, 5685-5700.

Glasius, M., La Cour, A., Lohse, C., 2011. Fossil and nonfossil carbon in fine particulate matter: A study of five European cities. Journal of Geophysical Research: Atmospheres 116.

Gugamsetty, B., Wei, H., Liu, C.-N., Awasthi, A., Hsu, S.-C., Tsai, C.-J., Roam, G.-D., Wu, Y.-C., Chen, C.-F., 2012. Source characterization and apportionment of PM10, PM2. 5 and PM0. 1 by using positive matrix factorization. Aerosol Air Qual. Res 12, 476-491.

Guo, S., Hu, M., Guo, Q., Zhang, X., Schauer, J., Zhang, R., 2013. Quantitative evaluation of emission controls on primary and secondary organic aerosol sources during Beijing 2008 Olympics. Atmospheric Chemistry and Physics 13, 8303-8314.

Han, Y., Cao, J., Lee, S., Ho, K., An, Z., 2010. Different characteristics of char and soot in the atmosphere and their ratio as an indicator for source identification in Xi'an, China. Atmospheric Chemistry and Physics 10, 595-607.

Han, Y., Chen, L.-W., Huang, R.-J., Chow, J., Watson, J., Ni, H., Liu, S., Fung, K., Shen, Z., Wei, C., 2016. Carbonaceous aerosols in megacity Xi'an, China: Implications of thermal/optical protocols comparison. Atmospheric Environment 132, 58-68.

Hasheminassab, S., Daher, N., Schauer, J.J., Sioutas, C., 2013. Source apportionment and organic compound characterization of ambient ultrafine particulate matter (PM) in the Los Angeles Basin. Atmospheric environment 79, 529-539.

Heal, M.R., Naysmith, P., Cook, G.T., Xu, S., Duran, T.R., Harrison, R.M., 2011. Application of 14 C analyses to source apportionment of carbonaceous PM 2.5 in the UK. Atmospheric Environment 45, 2341-2348.

Heo, J., de Foy, B., Olson, M.R., Pakbin, P., Sioutas, C., Schauer, J.J., 2015. Impact of regional transport on the anthropogenic and biogenic secondary organic aerosols in the Los Angeles Basin. Atmospheric Environment 103, 171-179.

Herckes, P., Valsaraj, K.T., Collett Jr, J.L., 2013. A review of observations of organic matter in fogs and clouds: Origin, processing and fate. Atmospheric research 132, 434-449.

Herich, H., Gianini, M., Piot, C., Močnik, G., Jaffrezo, J.-L., Besombes, J.-L., Prévôt, A., Hueglin, C., 2014. Overview of the impact of wood burning emissions on carbonaceous aerosols and PM in large parts of the Alpine region. Atmospheric environment 89, 64-75.

Herich, H., Hueglin, C., Buchmann, B., 2011. A 2.5 year's source apportionment study of black carbon from wood burning and fossil fuel combustion at urban and rural sites in Switzerland. Atmospheric Measurement Techniques 4, 1409-1420.

Hong, K.Y., Weichenthal, S., Saraswat, A., King, G.H., Henderson, S.B., Brauer, M., 2017. Systematic identification and prioritization of communities impacted by residential woodsmoke in British Columbia, Canada. Environmental Pollution 220, 797-806.

Hopke, P.K., 2009. Theory and application of atmospheric source apportionment. Developments in environmental science 9, 1-33.

Hoyle, C., Boy, M., Donahue, N., Fry, J., Glasius, M., Guenther, A., Hallar, A., Huff Hartz, K., Petters, M., Petäjä, T., 2011. A review of the anthropogenic influence on biogenic secondary organic aerosol. Atmospheric Chemistry and Physics 11, 321-343.

Huang, R.-J., Zhang, Y., Bozzetti, C., Ho, K.-F., Cao, J.-J., Han, Y., Daellenbach, K.R., Slowik, J.G., Platt, S.M., Canonaco, F., 2014. High secondary aerosol contribution to particulate pollution during haze events in China. Nature 514, 218.

Hwang, I.-J., Hopke, P.K., 2011. Comparison of Source Apportionment of PM 2.5 Using PMF2 and EPA PMF Version 2. Asian Journal of Atmospheric Environment 5, 86-96.

Iinuma, Y., Keywood, M., Herrmann, H., 2016. Characterization of primary and secondary organic aerosols in Melbourne airshed: The influence of biogenic emissions, wood smoke and bushfires. Atmospheric environment 130, 54-63.

Ikemori, F., Honjyo, K., Yamagami, M., Nakamura, T., 2015. Influence of contemporary carbon originating from the 2003 Siberian forest fire on organic carbon in PM 2.5 in Nagoya, Japan. Science of the Total Environment 530, 403-410.

Jia, Y., Fraser, M., 2011. Characterization of saccharides in size-fractionated ambient particulate matter and aerosol sources: the contribution of primary biological aerosol particles (PBAPs) and soil to ambient particulate matter. Environmental science & technology 45, 930-936.

Jiang, F., Liu, Q., Huang, X., Wang, T., Zhuang, B., Xie, M., 2012. Regional modeling of secondary organic aerosol over China using WRF/Chem. Journal of aerosol science 43, 57-73.

Johnson, T.M., Guttikunda, S., Wells, G.J., Artaxo, P., Bond, T.C., Russell, A.G., Watson, J.G., West, J., 2011. Tools for improving air quality management: A review of top-down source apportionment techniques and their application in developing countries.

Johnston, F.H., Hanigan, I.C., Henderson, S.B., Morgan, G.G., 2013. Evaluation of interventions to reduce air pollution from biomass smoke on mortality in Launceston, Australia: retrospective analysis of daily mortality, 1994-2007. Bmj 346, e8446.

Kaskaoutis, D., Kumar, S., Sharma, D., Singh, R.P., Kharol, S., Sharma, M., Singh, A., Singh, S., Singh, A., Singh, D., 2014. Effects of crop residue burning on aerosol properties, plume characteristics, and long-range transport over northern India. Journal of Geophysical Research: Atmospheres 119, 5424-5444.

Kawamura, K., Bikkina, S., 2016. A review of dicarboxylic acids and related compounds in atmospheric aerosols: Molecular distributions, sources and transformation. Atmospheric research 170, 140-160.

Keywood, M., Cope, M., Meyer, C.M., Iinuma, Y., Emmerson, K., 2015. When smoke comes to town: The impact of biomass burning smoke on air quality. Atmospheric Environment 121, 13-21.

Keywood, M., Kanakidou, M., Stohl, A., Dentener, F., Grassi, G., Meyer, C., Torseth, K., Edwards, D., Thompson, A.M., Lohmann, U., 2013. Fire in the air: Biomass burning impacts in a changing climate. Critical Reviews in Environmental Science and Technology 43, 40-83.

Khan, M., Jenkin, M., Foulds, A., Derwent, R., Percival, C., Shallcross, D., 2017. A modeling study of secondary organic aerosol formation from sesquiterpenes using the STOCHEM global chemistry and transport model. Journal of Geophysical Research: Atmospheres 122, 4426-4439.

Khan, M.B., Masiol, M., Formenton, G., Di Gilio, A., de Gennaro, G., Agostinelli, C., Pavoni, B., 2016. Carbonaceous PM 2.5 and secondary organic aerosol across the Veneto region (NE Italy). Science of the Total Environment 542, 172-181.

Kim, K.-H., Jahan, S.A., Kabir, E., 2011a. A review of diseases associated with household air pollution due to the use of biomass fuels. Journal of hazardous materials 192, 425-431.

Kim, K.-H., Kumar, P., Szulejko, J.E., Adelodun, A.A., Junaid, M.F., Uchimiya, M., Chambers, S., 2017. Toward a better understanding of the impact of mass transit air pollutants on human health. Chemosphere.

Kim, K.H., Sekiguchi, K., Kudo, S., Sakamoto, K., 2011b. Characteristics of Atmospheric Elemental Carbon(Char and Soot) in Ultrafine and Fine Particles in a Roadside Environment, Japan. Aerosol and Air Quality Resarch 11, 1-12.

Kirillova, E.N., Andersson, A., Sheesley, R.J., Kruså, M., Praveen, P., Budhavant, K., Safai, P., Rao, P., Gustafsson, Ö., 2013. 13C-and 14C-based study of sources and atmospheric processing of water-soluble organic carbon (WSOC) in South Asian aerosols. Journal of Geophysical Research: Atmospheres 118, 614-626.

Kirillova, E.N., Andersson, A., Tiwari, S., Srivastava, A.K., Bisht, D.S., Gustafsson, Ö., 2014. Water-soluble organic carbon aerosols during a full New Delhi winter: Isotope-based source apportionment and optical properties. Journal of Geophysical Research: Atmospheres 119, 3476-3485.

Koch, D., Del Genio, A., 2010. Black carbon semi-direct effects on cloud cover: review and synthesis. Atmospheric Chemistry and Physics 10, 7685-7696.

Lamarque, J.-F., Bond, T.C., Eyring, V., Granier, C., Heil, A., Klimont, Z., Lee, D., Liousse, C., Mieville, A., Owen, B., 2010. Historical (1850–2000) gridded anthropogenic and biomass burning emissions of reactive gases and aerosols: methodology and application. Atmospheric Chemistry and Physics 10, 7017-7039.

Lelieveld, J., Evans, J.S., Fnais, M., Giannadaki, D., Pozzer, A., 2015. The contribution of outdoor air pollution sources to premature mortality on a global scale. Nature 525, 367.

Li, W., Shao, L., Zhang, D., Ro, C.-U., Hu, M., Bi, X., Geng, H., Matsuki, A., Niu, H., Chen, J., 2016. A review of single aerosol particle studies in the atmosphere of East Asia: morphology, mixing state, source, and heterogeneous reactions. Journal of Cleaner Production 112, 1330-1349.

Li, X., Wang, Y., Guo, X., Wang, Y., 2013. Seasonal variation and source apportionment of organic and inorganic compounds in PM2. 5 and PM10 particulates in Beijing, China. Journal of Environmental Sciences 25, 741-750.

Lin, Y., Ma, Y., Qiu, X., Li, R., Fang, Y., Wang, J., Zhu, Y., Hu, D., 2015. Sources, transformation, and health implications of PAHs and their nitrated, hydroxylated, and oxygenated derivatives in PM2. 5 in Beijing. Journal of Geophysical Research: Atmospheres 120, 7219-7228.

Liu, D., Li, J., Zhang, Y., Xu, Y., Liu, X., Ding, P., Shen, C., Chen, Y., Tian, C., Zhang, G., 2013. The use of levoglucosan and radiocarbon for source apportionment of PM2. 5 carbonaceous aerosols at a background site in East China. Environmental science & technology 47, 10454-10461.

Liu, J., Li, J., Zhang, Y., Liu, D., Ding, P., Shen, C., Shen, K., He, Q., Ding, X., Wang, X., 2014. Source apportionment using radiocarbon and organic tracers for PM2. 5 carbonaceous aerosols in Guangzhou, South China: Contrasting local-and regional-scale haze events. Environmental science & technology 48, 12002-12011.

Liu, J., Mo, Y., Li, J., Liu, D., Shen, C., Ding, P., Jiang, H., Cheng, Z., Zhang, X., Tian, C., 2016. Radiocarbon-derived source apportionment of fine carbonaceous aerosols before, during, and after the 2014 Asia-Pacific Economic Cooperation (APEC) summit in Beijing, China. Journal of Geophysical Research: Atmospheres 121, 4177-4187.

Liu, S., Aiken, A.C., Gorkowski, K., Dubey, M.K., Cappa, C.D., Williams, L.R., Herndon, S.C., Massoli, P., Fortner, E.C., Chhabra, P.S., 2015. Enhanced light absorption by mixed source black and brown carbon particles in UK winter. Nature communications 6, 8435.

López-Aparicio, S., Vogt, M., Schneider, P., Kahila-Tani, M., Broberg, A., 2017. Public participation GIS for improving wood burning emissions from residential heating and urban environmental management. Journal of environmental management 191, 179-188.

Lu, Z., Zhang, Q., Streets, D.G., 2011. Sulfur dioxide and primary carbonaceous aerosol emissions in China and India, 1996–2010. Atmospheric Chemistry and Physics 11, 9839-9864.

Mancilla, Y., Mendoza, A., Fraser, M., Herckes, P., 2016. Organic composition and source apportionment of fine aerosol at Monterrey, Mexico, based on organic markers. Atmospheric Chemistry and Physics 16, 953-970.

Martinsson, J., Abdul Azeem, H., Sporre, M.K., Bergström, R., Ahlberg, E., Öström, E., Kristensson, A., Swietlicki, E., Eriksson Stenström, K., 2017. Carbonaceous aerosol source apportionment using the Aethalometer model–evaluation by radiocarbon and levoglucosan analysis at a rural background site in southern Sweden. Atmospheric Chemistry and Physics 17, 4265-4281.

Mazaheri, M., Reche, C., Rivas, I., Crilley, L.R., Álvarez-Pedrerol, M., Viana, M., Tobias, A., Alastuey, A., Sunyer, J., Querol, X., 2016. Variability in exposure to ambient ultrafine particles in urban schools: Comparative assessment between Australia and Spain. Environment international 88, 142-149.

McDonald, B.C., de Gouw, J.A., Gilman, J.B., Jathar, S.H., Akherati, A., Cappa, C.D., Jimenez, J.L., Lee-Taylor, J., Hayes, P.L., McKeen, S.A., 2018. Volatile chemical products emerging as largest petrochemical source of urban organic emissions. Science 359, 760-764.

McNeill, V.F., 2017. Atmospheric Aerosols: Clouds, Chemistry, and Climate. Annual Review of Chemical and Biomolecular Engineering.

22

Menon, D.D., 2016. An Evaluation of exposures to respirable particulates, environmental PM2. 5, PAHs and metal compounds in Western Australia.

Mesquita, S.R., van Drooge, B.L., Dall'Osto, M., Grimalt, J.O., Barata, C., Vieira, N., Guimarães, L., Piña, B., 2017. Toxic potential of organic constituents of submicron particulate matter (PM1) in an urban road site (Barcelona). Environmental Science and Pollution Research, 1-10.

Meyer, C.M., Luhar, A.K., Mitchell, R.M., 2008. Biomass burning emissions over northern Australia constrained by aerosol measurements: I—Modelling the distribution of hourly emissions. Atmospheric Environment 42, 1629-1646.

Mikuška, P., Kubátková, N., Křůmal, K., Večeřa, Z., 2017. Seasonal variability of monosaccharide anhydrides, resin acids, methoxyphenols and saccharides in PM2. 5 in Brno, the Czech Republic. Atmospheric Pollution Research 8, 576-586.

Minguillón, M.C., Perron, N., Querol, X., Szidat, S., Fahrni, S., Alastuey, A., Jimenez, J., Mohr, C., Ortega, A., Day, D., 2011. Fossil versus contemporary sources of fine elemental and organic carbonaceous particulate matter during the DAURE campaign in Northeast Spain. Atmospheric chemistry and physics 11, 12067-12084.

Mirante, F., Alves, C., Pio, C., Pindado, O., Perez, R., Revuelta, M.A., Artiñano, B., 2013. Organic composition of size segregated atmospheric particulate matter, during summer and winter sampling campaigns at representative sites in Madrid, Spain. Atmospheric research 132, 345-361.

Mochizuki, T., Kawamura, K., Miyazaki, Y., Wada, R., Takahashi, Y., Saigusa, N., Tani, A., 2017. Secondary formation of oxalic acid and related organic species from biogenic sources in a larch forest at the northern slope of Mt. Fuji. Atmospheric Environment.

Mouteva, G., Fahrni, S., Santos, G., Randerson, J., Zhang, Y., Szidat, S., Czimczik, C., 2015. Accuracy and precision of 14 C-based source apportionment of organic and elemental carbon in aerosols using the Swiss_4S protocol. Atmospheric Measurement Techniques Discussions 8.

Nebbioso, A., Piccolo, A., 2013. Molecular characterization of dissolved organic matter (DOM): a critical review. Analytical and bioanalytical chemistry 405, 109-124.

O'brien, D., Mitchell, R., 2003. Atmospheric heating due to carbonaceous aerosol in northern Australia—confidence limits based on TOMS aerosol index and sun-photometer data. Atmospheric Research 66, 21-41.

Pant, P., Harrison, R.M., 2013. Estimation of the contribution of road traffic emissions to particulate matter concentrations from field measurements: a review. Atmospheric environment 77, 78-97.

Pathak, R.K., Wang, T., Ho, K., Lee, S., 2011. Characteristics of summertime PM 2.5 organic and elemental carbon in four major Chinese cities: implications of high acidity for water-soluble organic carbon (WSOC). Atmospheric Environment 45, 318-325.

Pavuluri, C.M., Kawamura, K., Uchida, M., Kondo, M., Fu, P., 2013. Enhanced modern carbon and biogenic organic tracers in Northeast Asian aerosols during spring/summer. Journal of Geophysical Research: Atmospheres 118, 2362-2371.

Piletic, I.R., Offenberg, J.H., Olson, D.A., Jaoui, M., Krug, J., Lewandowski, M., Turlington, J.M., Kleindienst, T.E., 2013. Constraining carbonaceous aerosol sources in a receptor model by including 14 C data with redox species, organic tracers, and elemental/organic carbon measurements. Atmospheric environment 80, 216-225.

Pio, C., Cerqueira, M., Harrison, R.M., Nunes, T., Mirante, F., Alves, C., Oliveira, C., de la Campa, A.S., Artiñano, B., Matos, M., 2011. OC/EC ratio observations in Europe: Re-thinking the approach for apportionment between primary and secondary organic carbon. Atmospheric Environment 45, 6121-6132.

Pirovano, G., Colombi, C., Balzarini, A., Riva, G., Gianelle, V., Lonati, G., 2015. PM2. 5 source apportionment in Lombardy (Italy): comparison of receptor and chemistry-transport modelling results. Atmospheric Environment 106, 56-70.

Qadir, R., Abbaszade, G., Schnelle-Kreis, J., Chow, J., Zimmermann, R., 2013. Concentrations and source contributions of particulate organic matter before and after implementation of a low emission zone in Munich, Germany. Environmental pollution 175, 158-167.

Ram, K., Sarin, M., 2011. Day–night variability of EC, OC, WSOC and inorganic ions in urban environment of Indo-Gangetic Plain: implications to secondary aerosol formation. Atmospheric Environment 45, 460-468.

Ram, K., Sarin, M., Tripathi, S., 2010. A 1 year record of carbonaceous aerosols from an urban site in the Indo-Gangetic Plain: Characterization, sources, and temporal variability. Journal of Geophysical Research: Atmospheres 115.

Reche, C., Viana, M., Amato, F., Alastuey, A., Moreno, T., Hillamo, R., Teinilä, K., Saarnio, K., Seco, R., Peñuelas, J., 2012. Biomass burning contributions to urban aerosols in a coastal Mediterranean City. Science of the Total Environment 427, 175-190.

Reisen, F., Meyer, C.M., McCaw, L., Powell, J.C., Tolhurst, K., Keywood, M.D., Gras, J.L., 2011. Impact of smoke from biomass burning on air quality in rural communities in southern Australia. Atmospheric Environment 45, 3944-3953.

Rokoff, L.B., Koutrakis, P., Garshick, E., Karagas, M.R., Oken, E., Gold, D.R., Fleisch, A.F., 2017. Wood Stove Pollution in the Developed World: A Case to Raise Awareness Among Pediatricians. Current Problems in Pediatric and Adolescent Health Care.

Russell, L.M., Bahadur, R., Ziemann, P.J., 2011. Identifying organic aerosol sources by comparing functional group composition in chamber and atmospheric particles. Proceedings of the National Academy of Sciences 108, 3516-3521.

Safai, P., Raju, M., Rao, P., Pandithurai, G., 2014. Characterization of carbonaceous aerosols over the urban tropical location and a new approach to evaluate their climatic importance. Atmospheric environment 92, 493-500.

Salazar, G., Zhang, Y., Agrios, K., Szidat, S., 2015. Development of a method for fast and automatic radiocarbon measurement of aerosol samples by online coupling of an elemental analyzer with a MICADAS AMS. Nuclear Instruments and Methods in Physics Research Section B: Beam Interactions with Materials and Atoms 361, 163-167.

Saleh, R., Robinson, E.S., Tkacik, D.S., Ahern, A.T., Liu, S., Aiken, A.C., Sullivan, R.C., Presto, A.A., Dubey, M.K., Yokelson, R.J., 2014. Brownness of organics in aerosols from biomass burning linked to their black carbon content. Nature Geoscience 7, 647.

Schulz, M., Clark, S., 2011. Vehicle emissions and fuel economy effects of 16% butanol and various ethanol blended fuels (E10, E20, and E85). Journal of ASTM International 8, 1-19.

Seinfeld, J.H., Pandis, S.N., 2016. Atmospheric chemistry and physics: from air pollution to climate change. John Wiley & Sons.

Shannigrahi, A.S., Pettersson, J.B., Langer, S., Arrhenius, K., Hagström, M., Janhäll, S., Hallquist, M., Pathak, R.K., 2014. n-Alkanoic monocarboxylic acid concentrations in urban and rural aerosols: Seasonal dependence and major sources. Atmospheric research 143, 228-237.

Sheesley, R.J., Andersson, A., Gustafsson, Ö., 2011. Source characterization of organic aerosols using Monte Carlo source apportionment of PAHs at two South Asian receptor sites. Atmospheric environment 45, 3874-3881.

Sheesley, R.J., Nallathamby, P.D., Surratt, J.D., Lee, A., Lewandowski, M., Offenberg, J.H., Jaoui, M., Kleindienst, T.E., 2017. Constraints on primary and secondary particulate carbon sources using chemical tracer and 14 C methods during CalNex-Bakersfield. Atmospheric Environment.

Shiraiwa, M., Li, Y., Tsimpidi, A.P., Karydis, V.A., Berkemeier, T., Pandis, S.N., Lelieveld, J., Koop, T., Pöschl, U., 2017. Global distribution of particle phase state in atmospheric secondary organic aerosols. Nature communications 8.

Squizzato, S., Masiol, M., Rich, D.Q., Hopke, P.K., 2018. A long-term source apportionment of PM2. 5 in New York State during 2005–2016. Atmospheric Environment 192, 35-47.

Stone, E., Schauer, J., Quraishi, T.A., Mahmood, A., 2010. Chemical characterization and source apportionment of fine and coarse particulate matter in Lahore, Pakistan. Atmospheric Environment 44, 1062-1070.

Sun, X., Hu, M., Guo, S., Liu, K., Zhou, L., 2012. 14C-Based source assessment of carbonaceous aerosols at a rural site. Atmospheric Environment 50, 36-40.

Szidat, S., 2017a. Radiocarbon analysis with accelerator mass spectrometry: recent developments and applications.

Szidat, S., 2017b. Source apportionment of atmospheric aerosols using radiocarbon.

Szidat, S., Bench, G., Bernardoni, V., Calzolai, G., Czimczik, C.I., Derendorp, L., Dusek, U., Elder, K., Fedi, M., Genberg, J., 2013. Intercomparison of 14 C analysis of carbonaceous aerosols: exercise 2009. Radiocarbon 55, 1496-1509.

Szidat, S., Ruff, M., Wacker, L., Synal, H., Hallquist, M., Shannigrahi, A.S., Yttri, K.E., Dye, C., Simpson, D., 2008. Fossil and non-fossil sources of organic carbon (OC) and elemental carbon (EC) in Goteborg, Sweden. Atmospheric Chemistry and Physics Discussions 8, 16255-16289.

Szidat, S., Vonwiller, M., Salazar Quintero, G.A., Hu, W., Jimenez, J., Edgerton, E., Shaw, S., Prevot, A., 2018. Quantification of Fossil and Non-Fossil SOA from Combined 14C/AMS-PMF Analysis for the SOAS Field Campaign.

Tao, J., Zhang, L., Engling, G., Zhang, R., Yang, Y., Cao, J., Zhu, C., Wang, Q., Luo, L., 2013a. Chemical composition of PM2. 5 in an urban environment in Chengdu, China: Importance of springtime dust storms and biomass burning. Atmospheric Research 122, 270-283.

Tao, J., Zhang, L., Engling, G., Zhang, R., Yang, Y., Cao, J., Zhu, C., Wang, Q., Luo, L., 2013b. Chemical composition of PM 2.5 in an urban environment in Chengdu, China: importance of springtime dust storms and biomass burning. Atmospheric Research 122, 270-283.

Trenberth, K.E., 2011. Changes in precipitation with climate change. Climate Research 47, 123-138.

Ulevicius, V., Byčenkienė, S., Bozzetti, C., Vlachou, A., Plauškaitė, K., Mordas, G., Dudoitis, V., Abbaszade, G., Remeikis, V., Garbaras, A., 2016. Fossil and non-fossil source contributions to atmospheric carbonaceous aerosols during extreme spring grassland fires in Eastern Europe. Atmospheric chemistry and physics 16, 5513-5529.

Updyke, K.M., Nguyen, T.B., Nizkorodov, S.A., 2012. Formation of brown carbon via reactions of ammonia with secondary organic aerosols from biogenic and anthropogenic precursors. Atmospheric environment 63, 22-31.

Viana, M., Kuhlbusch, T., Querol, X., Alastuey, A., Harrison, R., Hopke, P., Winiwarter, W., Vallius, M., Szidat, S., Prévôt, A., 2008. Source apportionment of particulate matter in Europe: a review of methods and results. Journal of aerosol science 39, 827-849.

Viana, M., Reche, C., Amato, F., Alastuey, A., Querol, X., Moreno, T., Lucarelli, F., Nava, S., Calzolai, G., Chiari, M., 2013. Evidence of biomass burning aerosols in the Barcelona urban environment during winter time. Atmospheric environment 72, 81-88.

Villalobos, A.M., Barraza, F., Jorquera, H., Schauer, J.J., 2017. Wood burning pollution in southern Chile: PM 2.5 source apportionment using CMB and molecular markers. Environmental Pollution 225, 514-523.

Wang, J., Ho, S.S.H., Cao, J., Huang, R., Zhou, J., Zhao, Y., Xu, H., Liu, S., Wang, G., Shen, Z., 2015. Characteristics and major sources of carbonaceous aerosols in PM2. 5 from Sanya, China. Science of the Total Environment 530, 110-119.

Wang, L., Zhou, X., Ma, Y., Cao, Z., Wu, R., Wang, W., 2016. Carbonaceous aerosols over China—review of observations, emissions, and climate forcing. Environmental Science and Pollution Research 23, 1671-1680.

Weidemann, E., Andersson, P.L., Bidleman, T., Boman, C., Carlin, D.J., Collina, E., Cormier, S.A., Gouveia-Figueira, S.C., Gullett, B.K., Johansson, C., 2016. 14th congress of combustion by-products and their health effects—origin, fate, and health effects of combustion-related air

pollutants in the coming era of bio-based energy sources. Environmental Science and Pollution Research 23, 8141-8159.

Xing, L., Zhang, H., Yuan, Z., Sun, Y., Zhao, M., 2011. Terrestrial and marine biomarker estimates of organic matter sources and distributions in surface sediments from the East China Sea shelf. Continental Shelf Research 31, 1106-1115.

Xu, L., Guo, H., Boyd, C.M., Klein, M., Bougiatioti, A., Cerully, K.M., Hite, J.R., Isaacman-VanWertz, G., Kreisberg, N.M., Knote, C., 2015. Effects of anthropogenic emissions on aerosol formation from isoprene and monoterpenes in the southeastern United States. Proceedings of the National Academy of Sciences 112, 37-42.

Yttri, K.E., Dye, C., Braathen, O.-A., Simpson, D., Steinnes, E., 2009. Carbonaceous aerosols in Norwegian urban areas. Atmospheric Chemistry and Physics 9, 2007-2020.

Zaveri, R.A., Shaw, W.J., Cziczo, D.J., Schmid, B., Ferrare, R., Alexander, M.L., Alvarez, R., Arnott, W.P., Atkinson, D.B., Baidar, S., 2012. Overview of the 2010 carbonaceous aerosols and radiative effects study (CARES). Atmospheric Chemistry and Physics.

Zencak, Z., Elmquist, M., Gustafsson, Ö., 2007. Quantification and radiocarbon source apportionment of black carbon in atmospheric aerosols using the CTO-375 method. Atmospheric Environment 41, 7895-7906.

Zhang, H., Li, J., Ying, Q., Yu, J.Z., Wu, D., Cheng, Y., He, K., Jiang, J., 2012a. Source apportionment of PM2. 5 nitrate and sulfate in China using a source-oriented chemical transport model. Atmospheric environment 62, 228-242.

Zhang, Q., Jimenez, J.L., Canagaratna, M.R., Ulbrich, I.M., Ng, N.L., Worsnop, D.R., Sun, Y., 2011. Understanding atmospheric organic aerosols via factor analysis of aerosol mass spectrometry: a review. Analytical and bioanalytical chemistry 401, 3045-3067.

Zhang, R., Wang, G., Guo, S., Zamora, M.L., Ying, Q., Lin, Y., Wang, W., Hu, M., Wang, Y., 2015a. Formation of urban fine particulate matter. Chemical Reviews 115, 3803-3855.

Zhang, X., Lambe, A.T., Upshur, M.A., Brooks, W.A., Gray Bé, A., Thomson, R.J., Geiger, F.M., Surratt, J.D., Zhang, Z., Gold, A., 2017a. Highly Oxygenated Multifunctional Compounds in α-Pinene Secondary Organic Aerosol. Environmental Science & Technology 51, 5932-5940.

Zhang, X., Liu, Z., Hecobian, A., Zheng, M., Frank, N., Edgerton, E., Weber, R., 2012b. Spatial and seasonal variations of fine particle water-soluble organic carbon (WSOC) over the southeastern United States: implications for secondary organic aerosol formation. Atmospheric Chemistry and Physics 12, 6593-6607.

Zhang, X., McVay, R.C., Huang, D.D., Dalleska, N.F., Aumont, B., Flagan, R.C., Seinfeld, J.H., 2015b. Formation and evolution of molecular products in α-pinene secondary organic aerosol. Proceedings of the National Academy of Sciences 112, 14168-14173.

Zhang, Y.-L., El-Haddad, I., Huang, R.-J., Ho, K.-F., Cao, J.-J., Han, Y., Zotter, P., Bozzetti, C., Daellenbach, K.R., Slowik, J.G., 2018. Large contribution of fossil fuel derived secondary organic carbon to water soluble organic aerosols in winter haze in China. Atmospheric chemistry and physics 18, 4005-4017.

Zhang, Y.-L., Huang, R.-J., El Haddad, I., Ho, K.-F., Cao, J.-J., Han, Y., Zotter, P., Bozzetti, C., Daellenbach, K., Canonaco, F., 2014a. Fossil vs. non-fossil sources of fine carbonaceous aerosols in four Chinese cities during the extreme winter haze episode in 2013. Atmospheric Chemistry & Physics Discussions 14, 26257-26296.

Zhang, Y.-L., Huang, R.-J., El Haddad, I., Ho, K.-F., Cao, J.-J., Han, Y., Zotter, P., Bozzetti, C., Daellenbach, K., Canonaco, F., 2015c. Fossil vs. non-fossil sources of fine carbonaceous aerosols in four Chinese cities during the extreme winter haze episode of 2013. Atmospheric chemistry and physics 15, 1299-1312.

Zhang, Y.-L., Li, J., Zhang, G., Zotter, P., Huang, R.-J., Tang, J.-H., Wacker, L., Prévôt, A.S., Szidat, S.n., 2014b. Radiocarbon-based source apportionment of carbonaceous aerosols at a regional background site on Hainan Island, South China. Environmental science & technology 48, 2651-2659.

Zhang, Y.-L., Schnelle-Kreis, J.r., Abbaszade, G.l., Zimmermann, R., Zotter, P., Shen, R.-r., Schäfer, K., Shao, L., Prévôt, A.S., Szidat, S.n., 2015d. Source apportionment of elemental

carbon in Beijing, China: insights from radiocarbon and organic marker measurements. Environmental science & technology 49, 8408-8415.

Zhang, Y., Li, J., Zhang, G., Prévôt, A., Szidat, S., 2013a. Radiocarbon-based source apportionment of elemental carbon and organic carbon at a regional background site on Hainan Island, South China.

Zhang, Y., Liu, D., Shen, C., Ding, P., Zhang, G., 2010. Development of a preparation system for the radiocarbon analysis of organic carbon in carbonaceous aerosols in China. Nuclear Instruments and Methods in Physics Research Section B: Beam Interactions with Materials and Atoms 268, 2831-2834.

Zhang, Y., Obrist, D., Zielinska, B., Gertler, A., 2013b. Particulate emissions from different types of biomass burning. Atmospheric Environment 72, 27-35.

Zhang, Y., Perron, N., Ciobanu, V., Zotter, P., Minguillón, M., Wacker, L., Prévôt, A., Baltensperger, U., Szidat, S., 2012c. On the isolation of OC and EC and the optimal strategy of radiocarbon-based source apportionment of carbonaceous aerosols. Atmospheric Chemistry and Physics 12, 10841-10856.

Zhang, Z.-H., Khlystov, A., Norford, L.K., Tan, Z.-K., Balasubramanian, R., 2017b. Characterization of traffic-related ambient fine particulate matter (PM 2.5) in an Asian city: Environmental and health implications. Atmospheric Environment 161, 132-143.

Zhao, S., Ming, J., Sun, J., Xiao, C., 2013. Observation of carbonaceous aerosols during 2006–2009 in Nyainqêntanglha Mountains and the implications for glaciers. Environmental Science and Pollution Research 20, 5827-5838.

Zhu, T., Rao, Z., Guo, F., Zhan, N., Wang, Y., Arandiyan, H., Li, X.-j., 2018. Simultaneous Determination of 32 Polycyclic Aromatic Hydrocarbon Derivatives and Parent PAHs Using Gas Chromatography–Mass Spectrometry: Application in Groundwater Screening. Bulletin of environmental contamination and toxicology 101, 664-671.

Zhu, Y., Yang, L., Kawamura, K., Chen, J., Ono, K., Wang, X., Xue, L., Wang, W., 2017. Contributions and source identification of biogenic and anthropogenic hydrocarbons to secondary organic aerosols at Mt. Tai in 2014. Environmental Pollution 220, 863-872.

Zotter, P., Ciobanu, V., Zhang, Y., El-Haddad, I., Macchia, M., Daellenbach, K., Salazar, G., Huang, R.-J., Wacker, L., Hueglin, C., 2014. Radiocarbon analysis of elemental and organic carbon in Switzerland during winter-smog episodes from 2008 to 2012–Part 1: Source apportionment and spatial variability. Atmospheric chemistry and physics 14, 13551-13570.

CHAPTER 2

Paper One

Polycyclic aromatic hydrocarbons and n-alkanes in PM$_{2.5}$ aerosols at a highly biogenic source dominated urban site (Sydney) in Australia

Meng, C., Nelson, P.F.

The paper measures, characterizes, identifies and sources of typical non-polar organic compounds (PAHs and n-alkanes) in urban Sydney ambient fine particulate. Diagnostic ratios, correlation analysis and principal component analysis (PCA) techniques are used to distinguish and assess the contribution of diverse sources. The results suggest that PAHs mainly originate from wood burning during cold seasons for the samples collected in this study. More sources contribute to PM$_{2.5}$ associated n-alkanes, containing traffic exhaust, plant wax, biomass burning and road dust resuspension.

Polycyclic aromatic hydrocarbons and n-alkanes in PM$_{2.5}$ aerosols at a highly biogenic source dominated urban site (Sydney) in Australia

Chuanping Meng [a,*], Peter F. Nelson [a, b]

[a] Department of Environmental Sciences, Faculty of Science and Engineering, Macquarie University, North Ryde, Sydney, New South Wales, 2109, Australia
[b] Macquarie University Centre for Energy and Environmental Contaminants, Macquarie University, North Ryde, Sydney, New South Wales, Australia

[*] Corresponding author e-mail: Chuanping.meng@students.mq.edu.au

ABSTRACT

Multiple (nineteen) 48h PM$_{2.5}$ samples were collected using a high volume sampler at an urban site in north western Sydney during autumn and winter in 2014. For these samples the mean ($\pm$ standard deviation) mass concentrations of PM$_{2.5}$ were 9.4 $\pm$ 2.6 µg·m^{-3} and 7.1 $\pm$ 2.4 µg·m^{-3}, respectively. Hazard reduction burns during from the 22nd May to 30th May 2014 may be a reason for the slight elevation of PM$_{2.5}$ concentrations in autumn. Organic constituents account for 40–61% and 12–78% of PM$_{2.5}$ mass during autumn and winter, with an average value of 46 $\pm$ 7% and 38 $\pm$ 20%, respectively. N-alkanes (C$_{17}$-C$_{30}$) and 16 PAHs bound to PM$_{2.5}$ were detected and quantified by gas chromatography coupled with mass spectrometry.

Comprehensive source indices analysis, including diagnostic ratios and correlation analysis were applied to the n-alkanes and PAH results to provide some insight into the source profile. The results suggest that 3-4 ring PAHs were mainly from vehicular emissions and 5-6 ring PAHs were derived from biomass burning, while, fossil fuel combustion, notably traffic exhaust made a distinct contribution to n-alkanes concentrations, particularly in winter. Contributions from biogenic materials were slightly higher in autumn. Three distinct sources of n-alkanes were identified, and their contributions were estimated using a PCA-MLR model; these sources were, fossil fuel combustion (74%), biomass burning + road dust (20%) and biogenic sources (6%).

Keywords: N-alkanes, PAHs, biomass burning, fossil fuel, biogenic sources.

Introduction

PM$_{2.5}$ aerosols (particulate matter with an aerodynamic diameter less than 2.5 μm) are of worldwide concern owing to severe impacts on climate forcing, human health, and visibility degradation. PM$_{2.5}$ chemical components mainly include sulphate, nitrate, sea salt, mineral dust and organic fractions (Philip et al., 2014). The organic fractions are a series of complex, variable and highly diverse chemical compounds, and may account for 20–90% of the mass of PM$_{2.5}$ particles, although with significant variation both spatially and temporally (Kanakidou et al., 2005). These organic aerosols (OA) originate from primary and secondary sources, and both anthropogenic activities and biogenic activities are involved in their creation (Gelencsér et al., 2007). Primary organic aerosols (POA) are directly emitted from combustion and other primary sources, including biomass burning, vehicular traffic emissions and primary biogenic processes. Secondary organic aerosols (SOA) are produced in the atmosphere by photo oxidation of volatile or semi volatile organic precursors derived from both anthropogenic activities and biogenic sources (Heo et al., 2013). Organic aerosols are normally categorised into polar and non-polar compounds. Non-polar compounds mainly contain alkanes, PAHs. Both n-alkanes and PAHs are well known to have detrimental effects on human beings and ecosystems (Lu et al., 2015), while, n-alkanes with numbers of carbon atoms greater than 16 have been shown to have a detrimental influence on skin and engender skin cancer in humans.

Sydney is the most populous city in Australia and Oceania. Although the air quality of Sydney is less seriously polluted than that in some developing countries, such as India, China and Mexico, PM concentrations are comparable to those in European countries (Fiore et al., 2012). However, due to population growth and urbanisation, Sydney's air quality has deteriorated markedly from 30 years ago (Cohen et al., 2011b). The National Environment Protection Council (NEPC) in Australia established strict ambient air quality standards (National Environment Protection Measures, NEPMs) more stringent than those in the EU and the US. The Australian NEPM fine particle advisory reporting standards are a maximum daily average PM$_{2.5}$ of 25 μg/m^3, and a maximum annual average of 8 μg/m^3 [1]. On 23 Dec 2014, The National Environment Protection Council (NEPC) published submissions on theNEPMs for Ambient Air Quality (AAQ) variation based on the latest scientific

---

[1] National standards for criteria air pollutants in Australia, available at http://www.environment.gov.au/protection/publications/factsheet-national-standards-criteria-air-pollutants-australia, 2005.

understanding of the health risks arising from airborne particle pollution, which recommended a reversion of the standards to take into account new evidence that a 6 µg/m^3 PM$_{2.5}$ standard would avoid 700 premature deaths per year. In winter and autumn, the inhabitants are frequently exposed to emissions generated from biomass burning both from residential heating and also episodically controllable bushfires, and the latter occasionally cause episodes of severe high levels of air pollution (Johnston et al., 2011). Sydney is often characterised by high solar radiation and abundant biogenic volatile organic compounds (VOCs) emissions (including isoprene, α-pinene and other terpenes) particularly during periods of summer and spring time that favour photochemical reactions and formation of SOAs (Goldstein and Galbally, 2007; Maleknia et al., 2009). Insight into the sources, fate, composition and transformation of OAs can aid the development of emission inventories and establishment of effective abatement plans. Important information on sources, transport and organic composition characterization of PM$_{2.5}$ has been acquired in many countries (Heo et al., 2015; van Drooge and Grimalt, 2015; Wang et al., 2015a) using organic molecular markers. However, limited literature is available on the organic constituents of PM$_{2.5}$ in Sydney urban areas (Cohen et al., 2011a; Cope et al., 2013; Knibbs et al., 2009) and knowledge about source apportionment of organic aerosols is not as well understood as it is in some other countries (Mikuška et al., 2015; Wang et al., 2015c).

The sampling campaign was conducted during the colder seasons as there was an expectation that enhanced concentrations of organic aerosols may be apparent, caused by residential heating using wood fired heaters at the lower temperatures (EPA, 2017). N-alkanes (C$_{17}$-C$_{30}$) and 16 priority PAHs were detected and quantified. To better interpret the dataset obtained, several diagnostic ratios were introduced to reveal the sources of a homologous series of two compound classes (n-alkanes and PAHs). Furthermore, correlation analysis and PCA-MLR analysis were performed to characterise and quantify source contributions. Finally, the carcinogenic potential of the PAH mixture and the contributions of the previously identified n-alkanes were estimated.

Materials and Methods

Sample collection sites

From 17 May to 29 June 2014 (autumn and winter), PM$_{2.5}$ samples were collected for 48h on quartz filters (Tissuquartz^{TM} 8 x 10 inch, Pallflex, Pall Corporation) at an urban site from north western Sydney (n = 19 filters). The site is shown on a satellite image in Figure 1. The

32

study was carried out at an area co-located with an Automated Weather Station operated by the Department of Environmental Sciences of Macquarie University, situated in a residential area northwest of the city of Sydney (33 °45' 55.1" South, 151 °7' 3.2" East and 66.8 m above mean sea level). The Automated Weather Station is located to the north of the university on the northern side of the M2 Hills motorway, within the sports grounds of Macquarie University at North Ryde, NSW, Australia, and adjacent to a vegetated and wooded area of Lane Cove River State Park. The atmospheric samples are therefore likely to be influenced by vehicle emissions, residential emissions and biogenic activities.

A high volume sampler equipped with a $PM_{2.5}$ size selective inlet (Ecotech 3000, Ecotech Pty Ltd) was used to sample the ambient air at a flow rate of 67.8 m^3/h. Sample collection followed Method AS 3580.9.6-1990, as well as guidance from Approved Methods for the Sampling and Analysis of Air Pollutants in New South Wales (NSW EPA). Prior to sampling, quartz filters were pre-treated in a muffle furnace at 550 °C for 24h to eliminate organic components, weighted to a resolution of 0.1 mg (Sartorius, BP 221S), individually wrapped in a prebaked aluminium foil packed into air-tight plastic bags. After sample collection, the filters were again sealed in pre-baked aluminium foil and stored in a -4 °C refrigerator before chemical analyses. A field blank was obtained by placing the filter on the filter cartridge of the sampler for a few seconds without activating the air pump.
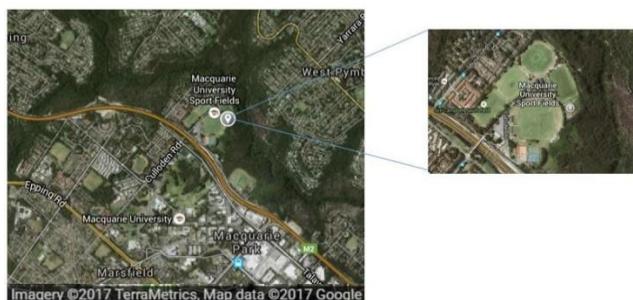
Figure 1. Map of the site location-automatic weather station in Macquarie University sports field (Map data: Google, DigitalGlobe)

Analytical methods

The soluble organic content of the filters were extracted using a Dionex Accelerated Solvent Extractor using the following program: preheat = 5 min; heat = 5 min; static = 5 min; pressure = 1500 psi; flush = 70%, purge = 300 sec; cycles=3; solvent = dichloromethane/methanol mixture (Honeywell, Australia, 9:1, v/v). Extracts were reduced by rotary evaporator and

then blown down to dryness by a gentle stream of ultrapure nitrogen on a heating block at 60 °C and gravimetrically quantified. Extracts were resuspended in dichloromethane-hexane (Honeywell, Australia, 1:1, v/v) to 1 ml. Insoluble particles observed in the extracts were removed by glass wool filled Pasteur pipettes. Extraction recoveries are > 75%.

A 0.5 ml aliquot of the extracts were analysed for non-polar compounds content, including C_{17}-C_{30} alkanes, 16 PAHs (Naphthalene: Nap, Acenaphthylene: Acy, Acenaphthene: Ace, Fluorene: Flo, Phenanthrene: Phe, Anthracene: Ant, Fluoranthene: Flu, Pyrene: Pyr,Bbenzo[a]anthracene: BaA, Chrysene: Chry, Benzo[b]fluoranthene: BbF, Benzo[k]fluoranthene: BkF, Benzo[a]pyrene: BaP, Indeno[1,2,3-c,d]pyrene: InP, Dibenzo[a,h]anthracene: DbA, Benzo[g,h,i]perylene: BgP). Prior to running GC/MS, $C_{24}D_{50}$ (N-Tetracosane-D_{50}) was added as an internal standard to each of the vials.

N-alkanes and PAHs were determined by Gas chromatography/Mass selective detection (GC/MSD, Agilent, 7890A, 5977B) operated in electron ionization (EI) mode. The GC was equipped with a capillary column HP5-MS, 0.25 mm film thickness, 0.25 mm inside diameter and length 30 m. A splitless injection with pressure pulse of 30 psi and pulse hold time of 0.70 min was used to minimize flashback and molecular weight discrimination. Auto-injections of 1.0 μL were conducted at an inlet temperature of 280 °C and purge time of 0.50 min using an Agilent single-taper, deactivated inlet liner with glass wool. The MS transfer line temperature was maintained at 320 °C. The MSD was optimised for maximum mass-ion signal response operated at source and quadrupole temperatures of 300 °C and 200 °C, respectively. Ultra-high-purity He (99.99%) at a constant flow rate at 1 mL/min was used as the carrier gas. The oven temperature was: initially 45 °C for 2 min; to 180 °C at 10 °C/min then hold for 2 min; to 280 °C at 2 °C/min then hold for 2 min; and finally to 320 °C at 2 °C/min and hold for 10 min.

Qualitative identification was based on the retention time of the authentic target analyte standard's quantitation ion and on the relative abundance of the quantitation and qualifier ions. Quantification analysis was performed using external standard calibration curves and internal standard in MS quantitative analysis software MassHunter. No organic compounds were detected on field blanks.

Statistical Analysis

T test, Non-parametric Kruskal-Wallis H test and Mann-Whitney U test in SPSS (v23.0) were applied to distinguish differences among $PM_{2.5}$, PAHs and n-alkanes profiles during weekdays and weekend in autumn and winter. A correlation analysis was conducted using a univariate Pearson correlation coefficient to determine relationships among each species, including $PM_{2.5}$, PAHs, n-alkanes and meteorological parameters (daily averages). This approach could be used to evaluate whether each individual species ($PM_{2.5}$, PAHs and n-alkanes) arise from the same sources (Singare, 2015). Principal Component Analysis (PCA) and Multivariate linear regression (MLR) can be utilized to determine potential sources and quantify source contributions to samples. PCA refers to the use of normalized Varimax rotation method to reduce the number of variables and maintain the original information at the same time in order to categorize the similar variable into the same group (factor). MLR is used to calculate linear relations of each factor to obtain specific source contributions (Jamhari et al., 2014).

Results and Discussion

Meteorology and Abundance of pollutants ($PM_{2.5}$, PAHs and n-alkanes)

Meteorological data (temperature, wind speed and solar radiation) averaged to 15 minute intervals are determined by the Automated Weather Station. A summary of temperature, wind speed, solar radiation data, $PM_{2.5}$ concentrations, organic extract weights, total PAHs and n-alkanes are reported in Table 1 (Detailed daily data are shown in Appendix A, Supplementary Tables S1-S2). For meteorological data only temperature showed significant differences ($p = 0.01 < 0.05$) between autumn and winter. Compared to autumn, winter had lower temperatures ranging from 3.6 ℃ to 21.4 ℃, while, the values in autumn were 8.1 ℃ to 25.9 ℃. However, for the remaining indices (wind speed, solar radiation data, $PM_{2.5}$ concentrations, organic extract weights, totals PAHs and n-alkanes), the differences were not statistically significant ($p > 0.05$).

Table 1. Meteorological conditions (daily averages), concentrations of $PM_{2.5}$, organic fraction, PAHs, n- alkanes and associated indices during the sampling period

	Autumn (n=7)				Winter (n=12)			
	Mean	Median	Minimum	Maximum	Mean	Median	Minimum	Maximum
Temperature (°C)	16.5	16.2	8.1	25.9	12.7	13.0	3.6	21.4
Wind speed (m/s)	1.0	0.8	0.0	4.1	1.2	0.9	0.0	5.9
Solar radiation (w/m^2)	40.0	40.8	31.2	51.8	29.8	30.0	10.4	47.2
$PM_{2.5}$ ($\mu g \cdot m^{-3}$)	9.4	10.0	6.5	13.8	7.1	6.6	4.0	12.0
Organic compounds ($\mu g \cdot m^{-3}$)	4.3	4.0	3.1	6.2	2.9	2.5	0.6	7.4
PAHs ($ng\ m^{-3}$)	2.9	2.3	2.0	4.8	3.3	2.8	1.6	10.0
N-alkanes ($ng\ m^{-3}$)	29.3	22.2	14.7	66.4	23.1	26.2	17.4	33.1
PAHs/organic compounds ($x10^4$)	7.0	6.0	4.0	10.0	14.0	13.0	5.0	27.0
N-alkanes/organic compounds ($x10^4$)	99.0	55.0	42.0	154.0	149.0	121.2	32.0	419.0

Sydney is a highly urbanised coastal city, thus $PM_{2.5}$ pollution levels are influenced by weather variability especially temperature and wind conditions and location and intensity of local emission sources, such as domestic heating and transport. In winter, even if colder temperatures increased the usage of wood heaters which is an important contributor for $PM_{2.5}$ concentration levels, higher wind speed can result in reductions in $PM_{2.5}$ concentration levels (Gupta et al., 2007; Hine et al., 2007; Hinwood et al., 2007). During 38 sampling days, $PM_{2.5}$ concentrations were on average 9.43 µg/m³ and 7.09 µg/m³ in autumn and winter, respectively, which were much lower than the NEPC 24h standard of 25 µg/m³, whereas as Figure 2 shows, for 6 days $PM_{2.5}$ levels exceeded the NEPC annual $PM_{2.5}$ advisory reporting standard (ARS) of 8 µg/m³, accounting for 32% of the sampling period. During these exceeding days, the organic fraction accounted for 34–61% of $PM_{2.5}$ mass.
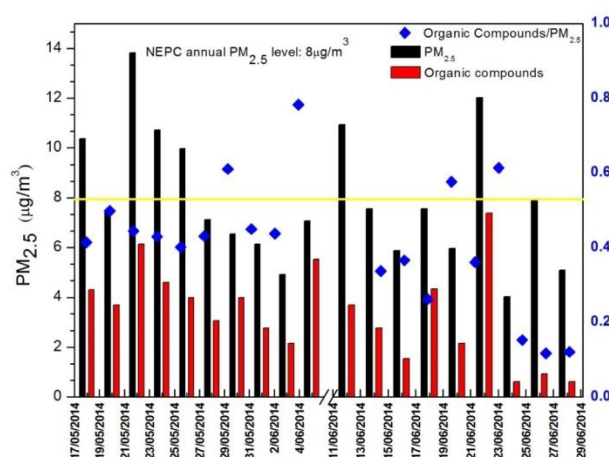
Figure 2. $PM_{2.5}$ and organic compounds concentrations and organic compound/$PM_{2.5}$ concentration ratios during the sampling period (18/05/2014–28/06/2014).

36

PAHs concentrations between on weekdays and weekends during autumn and winter

PM$_{2.5}$ concentrations, individual PAHs concentrations (ng $\cdot$m^{-3}) and values for meteorological variables are depicted in Table 2 (Appendix A, Supplementary Table S3-Table S4) list 16 PAHs concentrations on each sampling day). PAHs are emitted to the atmosphere as consequences of incomplete combustion of fossil fuel or biomass and are frequently used as primary organic tracers (Ravindra et al., 2008). Due to the lower temperatures in winter and autumn it is believed that this results in more biomass burning resulting from domestic heating, compared to the warmer periods of the year (Kingham and Dorset, 2011). This is likely to be particularly obvious on weekends when residents are domiciled rather than absent at work for most of the day. This hypothesis is confirmed as the concentrations of PAHs compounds observed were higher in winter than in autumn. In addition, according to statistical analysis, unlike meteorological parameters (wind speed and solar radiation) and PM indices (PM$_{2.5}$ and organic fractions) during autumn weekdays and weekends, which were not significantly different ($p > 0.05$) from those during winter weekdays and weekends, some PAHs especially naphthalene and phenanthrene showed significant differences among these four episodes ($p < 0.05$). Naphthalene and phenanthrene presented lower levels in winter. However, in fact, the lower ambient temperature in winter should favor the partition to particle surface since the gas phase PAH will condense onto atmospheric particles due to lower temperature (Ho et al., 2009). Thus, this may indicate the different source contributions in autumn and winter. Similarly with other 3-4 ring PAHs (anthracene, fluoranthene and pyrene), phenanthrene, an important indicator of traffic emissions especially diesel combustion (Yadav et al., 2013; Zhu et al., 2015; Zhu et al., 2014), decreased in winter.

The highest PAHs levels were observed during winter weekend sampling with an average concentration of 4.62 ng$\cdot$m^{-3}, and these comprised 0.06% of the mass (7.71 μg$\cdot$m^{-3}) of PM$_{2.5}$, even though higher wind speeds were encountered during these periods. PAHs concentrations during the autumn weekend campaign were slightly lower with an average concentration of 4.55 ng$\cdot$m^{-3} although these are very similar to those during winter weekends. PAHs concentrations during autumn and winter weekday were both lower than those during the weekend which were about double the weekday values, even though winter weekdays had lower temperature and higher wind speed, with a mean concentration of 2.22 ng$\cdot$m^{-3} and 2.67 ng$\cdot$m^{-3}, respectively.

Table 2. $PM_{2.5}$ concentrations, PAHs concentrations (ng·m^{-3}) and values for meteorological variables (daily averages)

	Autumn (n=7)		Winter (n=12)	
	Weekday n = 5	Weekend n = 2	Weekday n = 8	Weekend n = 4
Temperature(℃)	16.4	16.4	12.8	12.9
Wind Speed (m/s)	0.9	0.8	1.2	1.4
Solar radiation (w/m^2)	41.6	39.3	28.3	30.5
$PM_{2.5}$ (µg·m^{-3})	9.0 ±3.0	10.6 ±0.2	6.8 ±2.1	7.7 ±3.0
Naphthalene	0.02 ±0.00	0.03 ±0.00	0.01 ±0.00	0.01 ±0.01
Acenaphthylene	0.03 ±0.00	0.04 ±0.00	0.03 ±0.00	0.04 ±0.01
Acenaphthene	0.02 ±0.01	0.03 ±0.02	0.03 ±0.01	0.03 ±0.01
Fluorene	0.0 3±0.00	0.03 ±0.00	0.03 ±0.00	0.03 ±0.00
Phenanthrene	0.06 ±0.01	0.08 ±0.01	0.05 ±0.01	0.05 ±0.01
Anthracene	0.08 ±0.01	0.08 ±0.01	0.07 ±0.00	0.08 ±0.01
Fluoranthene	0.06 ±0.01	0.09 ±0.01	0.06 ±0.01	0.07 ±0.03
Pyrene	0.06 ±0.01	0.10 ±0.01	0.06 ±0.01	0.08 ±0.03
Benzo[a]anthracene	0.16 ±0.01	0.20 ±0.01	0.17 ±0.02	0.20 ±0.04
Chrysene	0.15 ±0.04	0.18 ±0.00	0.15 ±0.02	0.17 ±0.04
Benzo[b]fluoranthene	0.32 ±0.03	0.46 ±0.01	0.34 ±0.08	0.50 ±0.30
Benzo[k]fluoranthene	0.30 ±0.03	0.42 ±0.01	0.33 ±0.08	0.46 ±0.30
Benzo[a]pyrene	0.14 ±0.20	0.40 ±0.01	0.25 ±0.22	0.25 ±0.50
Indeno[1,2,3-c,d]pyrene	0.49 ±0.11	1.54 ±0.20	0.61 ±0.48	1.61 ±1.63
Dibenzo[a,h]anthracene	n.d	n.d	0.03 ±0.09	0.23 ±0.30
Benzo[g,h,i]perylene	0.27 ±0.15	0.88 ±0.04	0.44 ±0.19	0.81 ±0.63
Sum	2.22 ±0.31	4.55 ±0.30	2.67 ±1.06	4.62 ±3.70
PAHs/$PM_{2.5}$($x10^4$)	2.40	4.30	3.90	6.00

n.d.: not detected.

Sixteen PAHs were identified during the sampling campaign, except dibenzo[a,h]anthracene, which was not detected during the autumn sampling campaign. Figure 3 shows the distribution of individual PAHs compounds during the four sampling campaigns. Among them, 5-6 ring PAHs were found as the dominant compounds, these are mainly benzo[b]fluoranthene, benzo[k]fluoranthene, benzo[a]pyrene, indeno[1,2,3-c,d]pyrene and benzo[g,h,i]perylene, followed by 4 ring PAHs including fluoranthene, pyrene, benzo[a]anthracene and chrysene. Indeno[1,2,3-c,d]pyrene was the most abundant PAH species, contributing 22.1–34.8% to the total PAH concentrations during four sampling campaign, followed by benzo[g,h,i]perylene (12.7–19.3%). However, lower molecular weight PAHs (especially for 2-3 ring PAHs) had very low concentrations compared to higher molecular weight PAHs. This is due to the higher volatility of the lower molecular weight PAHs and results in them being more prone to exist in the gas phase (Xie et al., 2014a). As for 4 ring PAHs, measurements made during autumn weekends had the highest average

concentrations, followed by winter weekends. 5-6 ring PAHs had similar trends except for benzo[a]pyrene, which indicates that benzo[a]pyrene probably had a different source or contribution between other species.
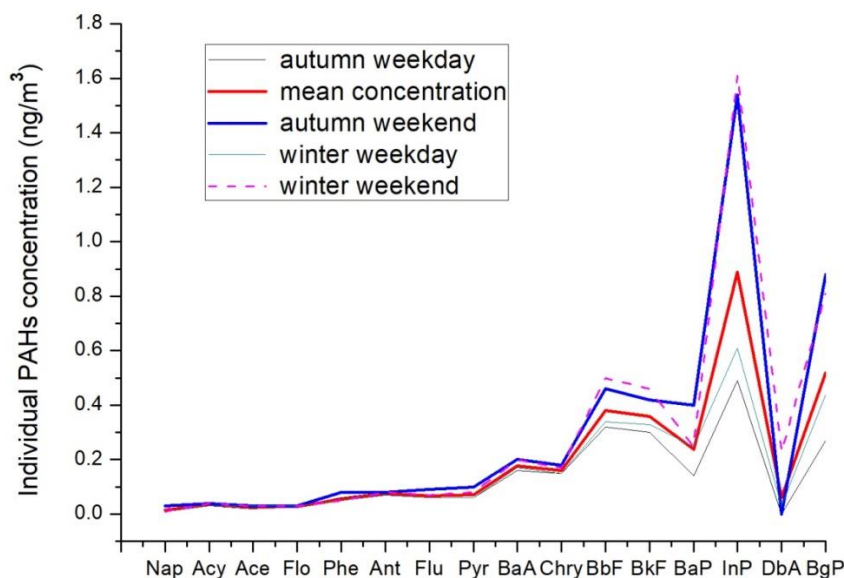
Figure 3. Distribution of Individual PAHs compounds during four sampling campaigns

Diagnostic ratios analysis

In many studies, PAHs diagnostic ratios are used for source identification, including BaA/BaP, BbF/BkF, BaA/(BaA + Chry) and InP/(InP + BgP) (Akyüz and Çabuk, 2008; Bulejko et al., 2016; Kirso et al., 2006; Křůmal et al., 2013; Pies et al., 2008). However, according to this previous research, adoption of specific value of PAH ratios to identify sources should be used cautiously, due to comfounding issues such as PAH atmospheric degradation, partitioning of lower molecular weight PAHs to the gas phase, the complexity and variety of possible PAHs sources (Křůmal et al., 2013; van Drooge and Grimalt, 2015). In addition, the presence of gas-phase PAHs was not evaluated and measured and no information on gas-particle partitioning of semi-volatile PAHs compounds is available. Thus, in this study, limited species, basically 4-6 ring PAHs (fluoranthene, pyrene, anthracene, phenanthrene, benzo[a]anthracene, chrysene, benzo[a]pyrene, dibenzo[a,h]anthracene and benzo[g,h,i]perylene) were selected to avoid ambiguous discussions and conclusions.

Table 3. Computed diagnostic ratios for different source categories.

Ratio	Value	Source	Reference
Ant/(Ant + Phe)	< 0.1	Petrogenic	(Pies et al., 2008)
	< 0.1	Pyrogenic	(Wang et al., 2010)
Flu/(Flu+ Pyr)	< 0.4	Petrogenic	(Jamhari et al., 2014)
	0.4-0.57	Petroleum combustion	(Slezakova et al., 2013)
BaA/(BaA + Chry)	> 0.57	Biomass combustion	(Kirso et al., 2006)
	< 0.2	Petrogenic	(Yunker et al., 2002)
	0.2-0.35	Petroleum combustion	(Akyüz and Çabuk, 2008)
BaP/(BaP + Chry)	> 0.35	Biomass combustion	(Amador-Muñoz et al., 2013)
	< 0.5	Diesel	(Teixeira et al., 2012)
	> 0.5	Gasoline	(Teixeira et al., 2012)
InP/(InP + BghiP)	< 0.2	Petrogenic	(Liu et al., 2015)
	0.2-0.5	Petroleum combustion	(Wiriya et al., 2013)
	> 0.5	Biomass combustion	(Yunker et al., 2002)

(a)   (b)

(c)
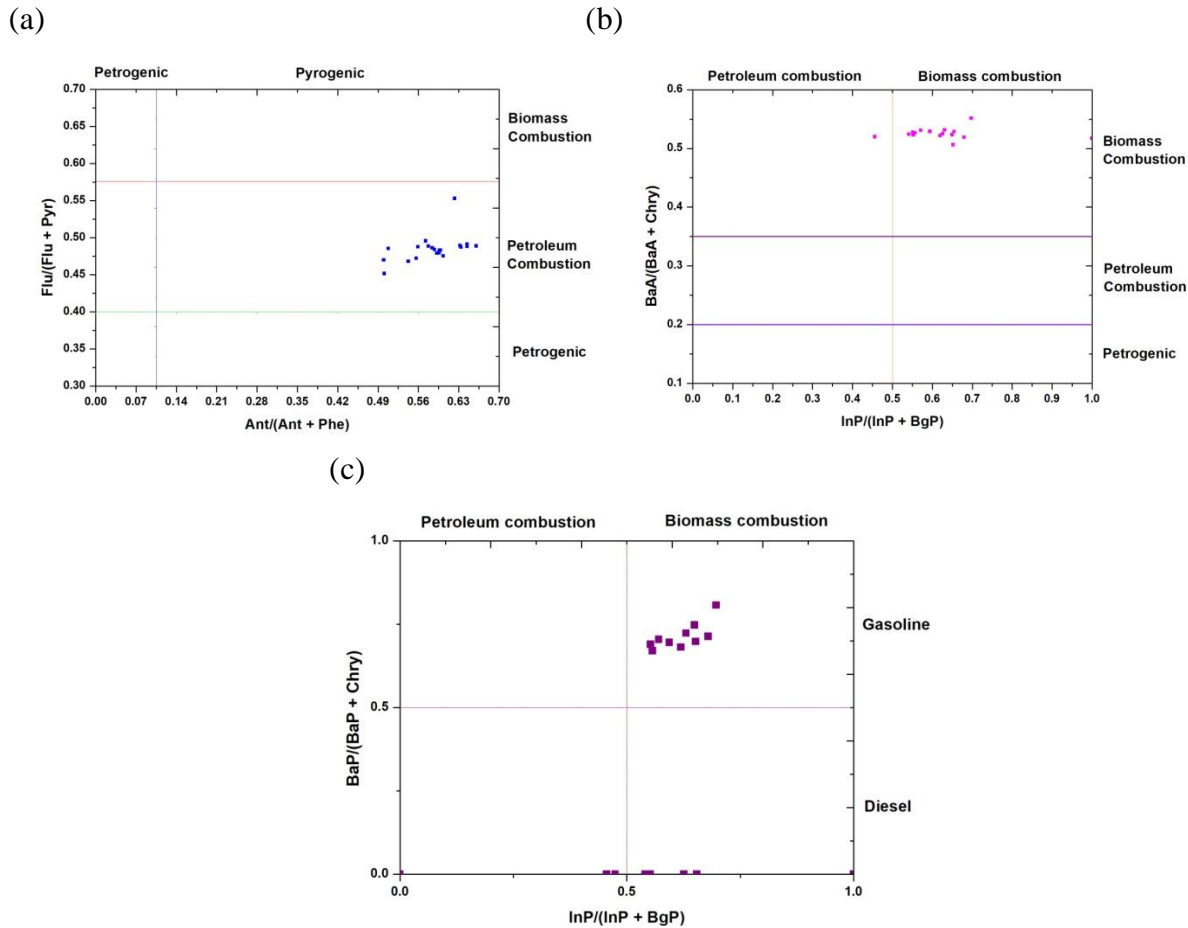
Figure 4. Scatter plots of selected PAHs ratios: (a) ratio Flu/(Flu + Pyr) vs Ant/(Ant + Phe) (b) BaA/(BaA + Chry) vs InP/(InP + BgP) (c) BaP/BaP + Chry) vs InP/(InP + BgP)

Table 3 shows some of the computed PAH diagnostic ratios selected in this study. The ratio of Ant/(Ant + Phe) is used for distinguishing between petrogenic and pyrogenic sources (Pies et al., 2008; Wang et al., 2010). The ratio of Flu/(Flu + Pyr), BaA/(BaA + Chry) and InP/(InP + BgP) can distinguishbetween petroleum combustion and biomass combustion (Akyüz and Çabuk, 2008; Amador-Muñoz et al., 2013; Liu et al., 2013; Wiriya et al., 2013; Yunker et al., 2002). The ratio of BaP/(BaP + Chry) provides a way to differentiate between gasoline and diesel emissions. In Figure 4 (a), the computed ratios are located in the area of intersection reflecting pyrogenic and petroleum combustion, suggesting that traffic emission is the main source for the 4 ring PAHs (phenanthrene, anthracene, fluoranthene and pyrene). In Figure 4 (b), only one computed ratio has a value of InP/(InP + BgP) < 0.5, other ratios are in the range of biomass combustion (0.5-1.0). This suggests that biomass combustion is an important source contributor for 5-6 ring PAH species, including benzo[a]anthracene, chrysene, indeno[1,2,3-c,d]pyrene and benzo[g,h,i]perylene. Plot (c) suggests that 5-6 ring PAH species (chrysene, benzo[a]pyrene, ndeno[1,2,3-c,d]pyrene and benzo[g,h,i]perylene) have both biomass combustion sources and traffic sources. Moreover, the traffic emissions mainly originate from gasoline vehicles. This observations are accordance with the findings with of other research groups (Bulejko et al., 2016; Callén et al., 2014; Křůmal et al., 2013; Olson and McDow, 2009; Zhang et al., 2016)

Comparison with other countries of PAHs concentrations

Recent published data of total concentrations of 16 PAH species measured in urban areas worldwide, including both European countries and China are shown in Table 4. The total PAH concentrations presented in this work had the same order of magnitude as the urban traffic site in Thessalonili (Greece) during warm seasons, whereas our data have concentrations of about one third of those in the urban background site in Thessalonili (Greece) during warmer seasons. PAH concentrations observed in winter Barcelona of PM_1 fraction were also similar to those measured in Sydney. Moreover, seasonal trends of PAHs, with higher levels during cold seasons and lower levels during warm seasons have been reported in many other locations (Bulejko et al., 2016; Manoli et al., 2016; Mohammed et al., 2016). PAH concentrations measured in winter in north eastern China, were about 100 times higher than the concentrations measured in Sydney.

Table 4. Total of 16 PAH concentrations (ng m^{-3}) measured in urban areas worldwide.

World urban areas	Total PAHs	PAHs/PM$_{2.5}$(x10^4)	Literature
Sydney (Australia) autumn PM$_{2.5}$	**2.88 ± 1.18**	**3.09**	**This study**
Sydney (Australia) winter PM$_{2.5}$	**3.32 ± 2.31**	**4.65**	**This study**
Barcelona (Spain) winter PM$_1$	1.78	nd	(Van Drooge et al., 2012)
Brno (Czech Republic) winter PM$_{10}$	61.72	nd	(Bulejko et al., 2016)
Brno (Czech Republic) summer PM$_{10}$	19.02	nd	(Bulejko et al., 2016)
Thessalonili (Greece) warm urban background PM$_{2.5}$	0.5 ± 0.4	0.28	(Manoli et al., 2016)
Thessalonili (Greece) cold urban background PM$_{2.5}$	8.9 ± 9.1	2.87	(Manoli et al., 2016)
Thessalonili (Greece) warm urban traffic PM$_{2.5}$	2.5 ± 0.9	0.81	(Manoli et al., 2016)
Thessalonili (Greece) cold urban traffic PM$_{2.5}$	11.0 ± 5.3	2.89	(Manoli et al., 2016)
Gyor (Hungary) winter PM$_{2.5}$	12.4	5.19	(Nagy et al., 2016)
Harbin (China) winter PM$_{2.5}$	376.6 ± 227.8	14.94	(Mohammed et al., 2016)
Harbin (China) summer PM$_{2.5}$	19.6 ± 14.1	1.96	(Mohammed et al., 2016)
Harbin (China) spring PM$_{2.5}$	16.1 ± 5.8	0.95	(Mohammed et al., 2016)

Carcinogenic and mutagenic potential of PAHs

Particulate PAHs represent a high risk to human health as they can deposit in the respiratory tract and aggravate negative health effects (Perera, 1997). BaP is the only species regulated by USEPA because of its carcinogenicity and mutagenicity (USEPA, 1996). The suggested upper limit value for annual BaP according to the World Health Organisation (WHO)/EU air quality standards is below 1 ng m^{-3} (EU, 2012). Time series of BaP concentrations during sampling campaign are shown in Figure 5. All samples were under this threshold, and only on 1 day was the concentration close to 1 ng m^{-3} (0.99 ng m^{-3}). Moreover, the BaP concentrations during the whole sampling campaign were significantly lower than 1 ng m^{-3} (($p < 0.01$).
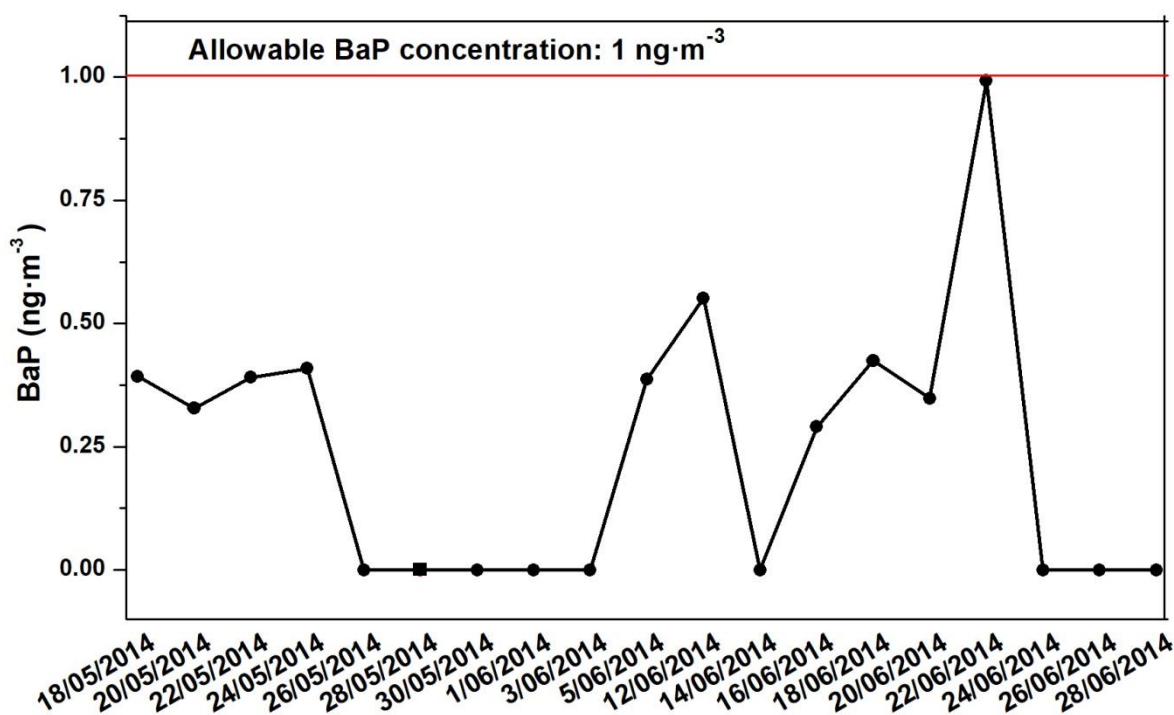
Figure 5. Time series of average daily concentrations of BaP during sampling campaign.

To evaluate the carcinogenic and mutagenic potential of PAHs, an approach using the calculated carcinogenic equivalent concentrations (BaP-teq) and the mutagenic equivalent concentrations (BaP-meq) relative to BaP was employed (Jung et al., 2010). The sum of the products of each individual PAH concentrations and its respective toxic equivalent factors (TEF) or the mutagenic potency factors (MEF) is called the BaP-teq value or BaP-meq value.

To assess the lung cancer risk via an inhalation route, the unit risk (UR) of 8.7×10^{-5} $(ng/m^3)^{-1}$ for a lifetime 70 years PAHs exposure is suggested by the World Health Organisation (Organization, 2000). This UR was based on an epidemiology study on coke-oven workers in Pennsylvania, assuming that one is exposed to the mean concentration of one unit BaP concentration ($1 ng/m^3$) (USEPA, 1996).

An estimation of the lifetime cancer risks (LCR) attributable to PAH inhalation exposure was calculated by multiplying the total of each individual BaP-teq or BaP-meq, respectively with the UR exposed to BaP levels. Table 5 shows the corresponding TEF and MEQ values adopted in this study. The TEF of light ring PAHs (naphthalene, acenaphthylene, acenaphthene, and fluorene) are from (Nisbet and LaGoy, 1992), heavy ring PAH TEF and MEQ values are from (Larsen and Larsen, 1998) and (Durant et al., 1996; Durant et al., 1999)

43

Table 5. Toxic equivalent factors (TEF) and mutagenic equivalent factors (MEQ) to calculate the BaP equivalent carcinogenicity (BaP-TEF) and the BaP-equivalent mutagenicity (BaP-MEQ).

PAH	TEF	MEQ
Naphthalene	0.001[a]	Non toxic
Acenaphthylene	0.001[a]	Non toxic
Acenaphthene	0.001[a]	Non toxic
Fluorene	0.001[a]	Non toxic
Phenanthrene	0.0005[b]	Non toxic
Anthracene	0.0005[b]	Non toxic
Fluoranthene	0.05[b]	Non toxic
Pyrene	0.001[b]	Non toxic
Benzo[a]anthracene	0.005[b]	0.082[c]
Chrysene	0.03[b]	0.017[c]
Benzo[b]fluoranthene	0.1[b]	0.25[c]
Benzo[k]fluoranthene	0.05[b]	0.11[c]
Benzo[a]pyrene	1[b]	1[c]
Indeno[1,2,3-c,d]pyrene	0.1[b]	0.31[c]
Dibenzo[a,h]anthracene	1.1[b]	0.29[c]
Benzo[g,h,i]perylene	0.02[b]	0.19[c]

a. (Nisbet and LaGoy, 1992) b. (Larsen and Larsen, 1998) c. (Durant et al., 1996; Durant et al., 1999)
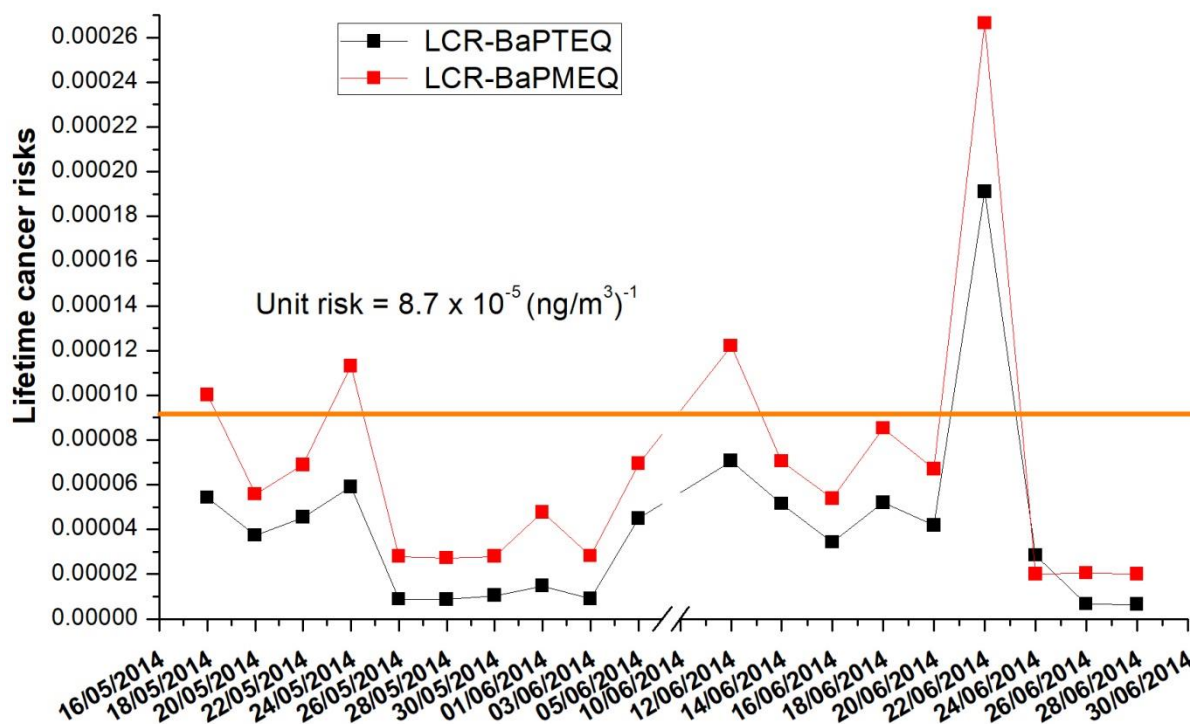
Figure 6. Time series of BaP during sampling campaign.

According to the US-EPA (2001), one in a million (10^{-6}) over an average lifetime of 70 years is the risk level considered acceptable or inconsequential, and one in ten thousand level (10^{-4}) is considered as a serious risk. As shown in Figure 6, the potential mutagenic risk from the PAH concentrations was higher than the carcinogenic potential. All sampling days were under the serious risk level (10^{-4}), however, on one day LCR-BaPTEQ in winter exceeded the WHO unit risk threshold (8.7×10^{-5} per 1 ng/m^3 of BaP). Although there were no sampling days exceeding the BaP limit value of 1 ng/m^3 for LCR-BaPMEQ, there were four days exceeding the WHO unit risk threshold, accounting for 21% of the whole sampling period.

However this analysis does not account for inhalation exposure to gas phase, and more volatile PAHs which are not bound to the particles. A more complete risk analysis would require measurements of these gas phase species. Moreover, only two seasons' exposure estimates were accounted for risk assessment for carcinogenic PAHs in this study. A more reliable and accurate risk assessment for carcinogenic PAHs would be acquired based on more exposure estimates.

Source estimation of n-alkanes

Particulate bound n-alkanes can originate from both natural and anthropogenic sources, including vehicle exhaust, tyre abrasion, biomass burning, leaf epicuticular waxes of vascular plants, vegetation debris, pollens, bacteria (Cheng et al., 2006; Chowdhury et al., 2007; Perrone et al., 2012; Young and Wang, 2002; Zheng et al., 2002). A homologous series of n-alkanes (C_{17}-C_{30}) were quantified in this work. Generally, the common source indices employed for source analysis of particle associated n-alkanes contain carbon maximum number (Cmax), carbon preference index (CPI), and plant wax n-alkanes ratio (WNA%) (Meyers, 2003). Apart from these parameters, average chain length (ACL), terrigenous to aquatic ratio (TAR) and C_{29}/C_{17} ratio also were demonstrated in some papers. (Lyu et al., 2016; Wang et al., 2015b; Wang et al., 2016b; Wang et al., 2015c). Plant wax n-alkanes could derive from both vascular higher plant, aquatic macrophytes and plankton (Sun et al., 2013). It is possible that aquatic macrophytes and plankton in the ocean could release lower odd carbon numbered alkanes, such as C_{15}, C_{17} and C_{19}, following high ocean-atmosphere exchange, these lower odd carbon numbered n-alkanes enter the atmosphere and could partition into particulate matter. The terrigenous to aquatic ratio (TAR) and C_{29}/C_{17} ratio are typically diagnostic ratios used to allocate the relative contribution of terrestrial over aquatic inputs of aliphatic hydrocarbons (Liu et al., 2013). However, as the concentrations of lower odd carbon numbered n-alkanes are extremely low in our study, terrigenous to aquatic ratio (TAR) and C_{29}/C_{17} ratio could not be used, thus, Cmax, CPI, and WNA% and average chain length (ACL) are adopted as diagnostic parameters to evaluate source attribution from anthropogenic activities and natural process.

Table 6 illustrates concentrations of n-alkanes and related indices in $PM_{2.5}$ for this study and studies in other cities around the world. The average total n-alkane concentrations in autumn in this study was slightly higher than those in winter (approximately 1.3 times). In autumn, relatively higher temperature and solar radiation could favour the emission of biogenic n-alkanes, whereas relatively lower wind speed was more beneficial for the accumulation of n-alkanes (Table 1 and Table 2). The observation that C_{27} wax and C_{29} wax were statistically different ($p < 0.05$) during autumn and winter supports this interpretation. Additionally, although n-alkanes could also partition between gas and particle phase (Guo et al., 2016; Kang et al., 2016; Lyu et al., 2016; Sun et al., 2013; Valotto et al., 2016), the ambient conditions during this sampling campaign (average daily temperature in autumn: 16.5; temperature in winter: 12.7) suggest that there will be only a minor influence on the C_{17}-C_{30} gas/particle partition ratio (Xie et al., 2014a, b). The concentrations in our study were much lower than that observed for Shanghai in 2011-2012 (Wang et al., 2016a), in the range of
46

14.72-66.40 ng/m³ during the whole sampling period. However, compared with previous studies in urban sites in America and Europe, the concentration was similar with those in other studies. Moreover, in comparison with other studies, n-alkanes in our samples made a greater contribution to $PM_{2.5}$, with a value of 0.3%, three times higher than for other studies. Likewise, fossil fuel derived n-alkanes in autumn was slightly higher than that in winter, with a mean concentration of 25.87 ng/m³

Figure 7 presents Cmax, the molecular distribution of $PM_{2.5}$ bound n-alkanes (C_{17}-C_{30}) and petrogenic n-alkanes and wax n-alkanes in individual n-alkanes. The distribution of homologuous n-alkanes in the range from C_{17}-C_{30} exhibited a unimodal pattern, with a Cmax at 30, followed by C_{29} and C_{28} in winter. In autumn the peak of the unimodal distribution centred at C_{29}, followed by C_{30} and C_{28}. Cmax (the carbon maximum number) denotes the most abundanct n-alkane in homologues, and can be used to assess anthropogenic versus biogenic source strengths. Generally, the lower molecular weight n-alkanes (n-C_{22} to n-C_{24}) are more related to vehicle emissions (Zheng et al., 2008), whereas the higher molecular weight n-alkanes, especially the odd carbon numbered (C_{27}, C_{29}) principally arise from higher carbon numbered plant waxes (Wang et al., 2016a). The differences between Cmax values in winter and autumn reflect potentially different source profiles during the two seasons. The predominant source in winter appears to be fossil fuels, whereas in autumn biogenic materials contribute more than in winter, which leads to the increased concentration of n-alkanes in autumn. This increase may not only be due to the more favourable meteorological conditions in autumn, but also can be attributed to the loss and subsequent decay of plant leaves (Yadav et al., 2013).

In summary, a remarkable shift in the n-alkane source contribution was suggested from a biogenic-influenced mode in autumn to anthropogenic-dominated pattern in winter. Specially, in our study anthropogenic sources are mainly vehicular exhaust, whereas biogenic activities mostly encompass terrestrial plant waxes (Valotto et al., 2016). Table 6 represented the Cmax values in this work and other urban sites studies in other cities. Autumn and summer in Shanghai, four seasons in a Mexican city and summer in an England city had same Cmax value (C_{29}) in comparison with our work. It was widely accepted that C_{29} n-alkane as an established marker could serve as a signature for road dust resuspension, which contains traffic and industrial emissions and surface deposited plant litter (Yadav et al., 2013). By contrast, spring and winter in Shanghai, Los Angeles and winter in an England city had featured to have the Cmax in low molecular weight n-alkanes (C_{23}, C_{24}). This suggests that seasonal variations of n-alkanes source contribution are markedly obvious in almost all cities

but this does not appear to be the case in Sydney where the temperate seasonal climatic variation is relatively small when compared to these Northern Hemisphere cities. Furthermore, different cities have different energy consumption pattern, which also leads to the variation of n-alkanes emission profiles (Huma et al., 2016).

Carbon preference index (CPI) is an indicator utilised to specify the contribution of fossil fuel combustion versus biogenic origins, which is expressed as the sum of the odd carbon number homologs divided by the sum of even carbon homologs over the same range. In our study, the CPI was defined as (Guo et al., 2016):

$$CPI_{total} = \frac{\sum(C_{17}-C_{29})}{\sum(C_{18}-C_{30})} \tag{1}$$

$$CPI_{petrogenic} = \frac{\sum(C_{17}-C_{23})}{\sum(C_{18}-C_{24})} \tag{2}$$

$$CPI_{biogenic} = \frac{\sum(C_{25}-C_{29})}{\sum(C_{26}-C_{30})} \tag{3}$$

CPI_{total} represents as the whole range of n-alkanes (C_{17}-C_{30}), while $CPI_{petrogenic}$ and $CPI_{biogenic}$ denotes petrogenic n-alkanes (C_{17}-C_{24}) and biogenic n-alkanes (C_{25}-C_{30}), respectively. The average CPI_{total}, $CPI_{petrogenic}$ and $CPI_{biogenic}$ values of n-alkanes depicted in Table 6 were 0.95, 0.53 and 0.98 in autumn in contrast to 0.78, 0.50 and 0.79 in winter. CPI values equal or lower than 1 manifest that high origin from anthropogenic sources, for example petroleum combustion residue. It is widely believed that n-alkanes almost entirely originate from terrestrial higher plant wax when CPI values are greater than 5 (Bourbonniere and Meyers, 1996; Schauer et al., 1999; Yunker et al., 1995). In our study, all CPI values were lower than 1, and in autumn the CPI values were closer to unity than those in winter. Higher CPI values imply enhanced biogenic inputs (Simoneit, 1989). Indeed, as illustrated in Table 6, lower molecular weight n-alkanes (C_{17}-C_{24}) had prominent contributions from anthropogenic activities, especially during the winter season. This conclusion is consistent with the previous discussion about Cmax. Unlike other studies in Table 6, it was notable that in our study n-alkanes displayed no or a much weaker odd/even predominance. CPI values of n-alkanes in other cities are in the range from 1.2-1.8, revealing more odd carbon numbered n-alkanes had contributed.

The wax n-alkanes percentage (WNA%) allows quantitatively differentiation of the relative contributions from anthropogenic and biogenic activities, it is computed in two steps:

$$WNA_{C_n} = C_n - 0.5(C_{n+1} + C_{n-1}) \quad (4)$$

$$WNA\% = \frac{\sum WNA_{C_n}}{\sum NA} * 100 \quad (5)$$

Where, C_n denotes the concentrations of odd carbon numbered n-alkanes, C_{n+1} and C_{n-1} represent the adjacent higher and lower even homologues concentrations, respectively. $\sum WNA_{C_n}$ is the total concentration of terrestrial plant wax n-alkanes, $\sum NA$ is the entire concentration of n-alkanes. According to the above equations, waxed% and fossil fuel derived n-alkanes are calculated, presented and plotted in Table 6, Figure 7 and 8, respectively. The results show that a lower waxed% is present in winter, only 4% when compared to the values in Shanghai. Moreover, in autumn, biogenic sources contributed approximately 5 and 3 fold more to n-alkanes, especially for C_{27} and C_{29}, than those species in winter (Figure 7). This investigation also confirms previous conclusions about Cmax and CPI, indicating that fossil fuel combustion is the major source of n-alkanes in organic aerosols at this sampling site. Additionally, it should be noted that C_{27} wax made a considerable contribution (1 ng/m^3) to n-alkane concentrations on 22/05/2014 (a bush fire day) from Figure 8, which indicate that biomass burning especially bush fires could produce C_{27} wax.

The average chain length (ACL) of higher C value n-alkanes is an additional parameter used for characterising biogenic materials and petrogenic hydrocarbon contamination. The ACL is defined as the average number of carbon atoms per molecule based on the abundance of the odd carbon numbered n-alkane homologues (Kang et al., 2016):

$$ACL(n\text{-}alkanes) = \frac{25*C_{25} + 27*C_{27} + 29*C_{29}}{C_{25} + C_{27} + C_{29}} \quad (6)$$

The ACL values found in our study were 28.03 (27.88-28.2) and 27.94 (27.75-28.09) in autumn and winter, respectively, which are very similar to those values found for fossil fuel dominated samples of PM$_{2.5}$ (Jeng, 2006). This suggests a significant input of fossil fuel combustion sources. Therefore, on the whole, all diagnostic parameters adopted in our study (Cmax, CPI, WNA% and ACL) reveal that fossil fuel combustion especially traffic exhaust

made a distinct contribution to n-alkanes. This contribution seems to be slightly higher in winter whilst in the autumn period there was a slightly higher contribution from biogenic sources.

Table 6. Summary of concentrations of n-alkanes and related indices in $PM_{2.5}$ for this study and studies in other cities around the world.

City	N-alkanes (ng m^{-3})	Fossil fuel n-alkanes (ng m^{-3})	Contribution% n-alkanes/$PM_{2.5}$	Cmax	CPI1/CPI2/CPI3[a]	Waxed %	References
Sydney (Australia) autumn 2014	29.3 ± 17.2	26.2 ± 16.4	0.3	C_{29}	1.0/0.5/1.0	12.0	This work
Sydney (Australia) winter 2014	23.1 ± 4.7	22. 1 ± 4.6	0.3	C_{30}	0.8/0.5/0.8	4.0	This work
Shanghai (China) autumn 2011	85.0 ± 87.7	42.4	0.1	$C_{29/31}$	1.5/-/-	50.1	(Wang et al., 2016a)
Shanghai (China) winter 2011	91.4 ± 59.3	83.9	0.09	$C_{23/24}$	1.2/-/-	8.2	(Wang et al., 2016a)
Shanghai (China) spring 2012	181.4 ± 100.9	170.0	0.2	$C_{23/24}$	1.8/-/-	6.3	(Wang et al., 2016a)
Shanghai (China) summer 2012	62.5 ± 31.5	31.8	0.1	$C_{29/31}$	1.8/-/-	9.8	(Wang et al., 2016a)
Monterrey (Mexico) spring 2012	34.7 ± 9.8	-	0.2	$C_{28/29}$	1.6/-/-	-	(Mancilla et al., 2016)
Monterrey (Mexico) autumn 2012	20.0 ± 10.1	-	0.1	C_{29}	1.4/-/-	-	(Mancilla et al., 2016)
Yorkville (Britain) summer 2005	20.2 (1.2-74.81)	-	0.2	C_{29}	-	-	(Yan et al., 2009)
Yorkville (Britain) winter 2006	39.3 (4.5-188.0)	-	0.2	$C_{23/24}$	-	-	(Yan et al., 2009)
Los Angeles (U.S.A) 2007	25.8	-	0.1	$C_{24/28}$	-	-	(Minguillón et al., 2008)

[a] CPI1:CPI total, CPI2: CPI petrogenic, CPI3: CPI biogenic

50
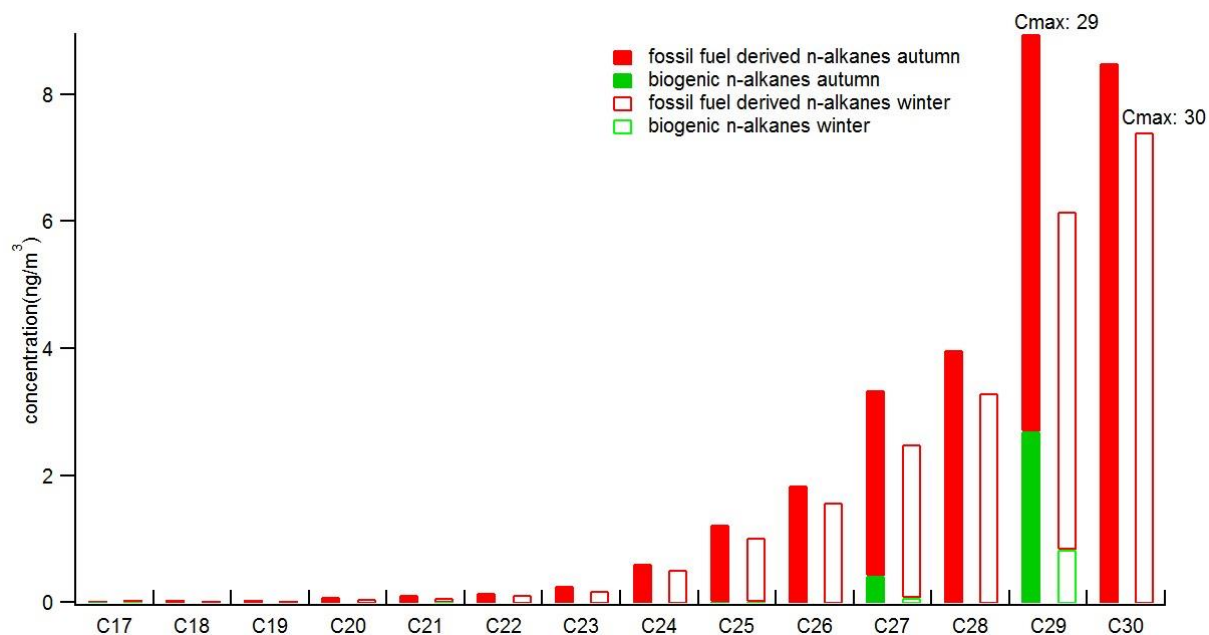
Figure 7. Cmax, molecular distribution of $PM_{2.5}$ bound n-alkanes (C_{17}-C_{30}) and petrogenic n-alkanes and wax n-alkanes in individual n-alkanes.
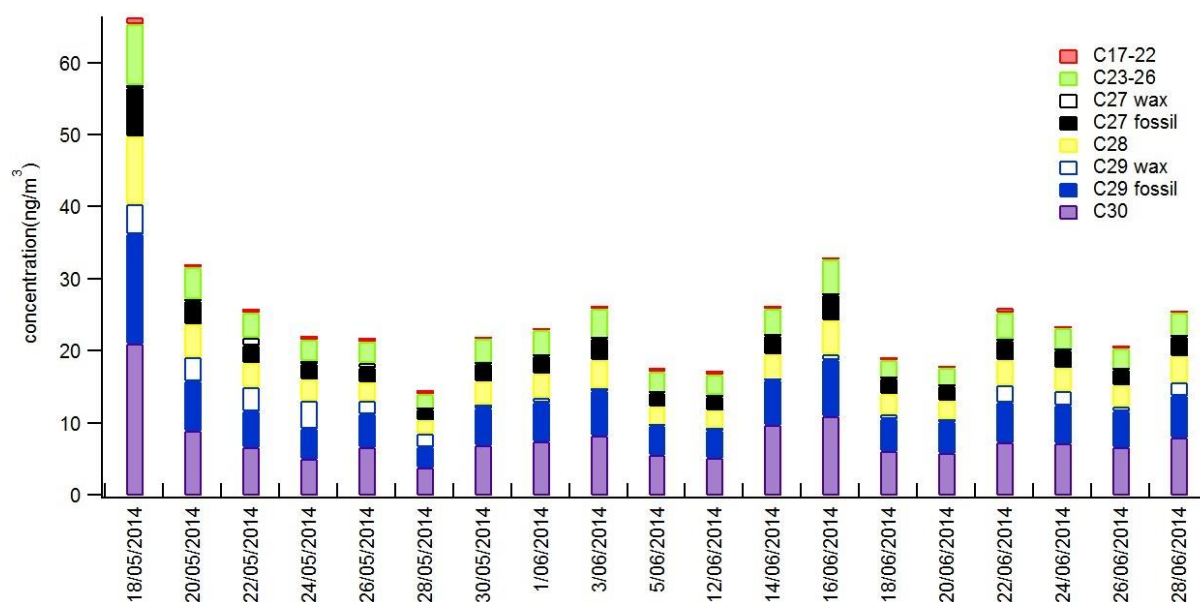
Figure 8. Temporal profiles of n-alkanes and contributions of series of n-alkanes during the whole sampling period.

Correlation analysis

Correlation analysis was carried out between individual species in n-alkanes homologous series, other related parameters (TAL: total n-alkanes, $PM_{2.5}$ and organic matter), and meteorological parameters (solar radiation, T: temperature, and WS: wind speed) and are plotted in Appendix A Supplementary Table S7. Pearson correlation analysis was performed using IBM SPSS (v23.0) to explore whether these parameters demonstrated significant correlations. Higher correlation coefficients ($\geq$ 0.9) were highlighted in yellow, lower correlation coefficients ($0.5 \leq R^2 \leq 0.9$) were highlighted in yellow. Values of $R^2 \leq 0.5$ were regarded as showing no significant correlation between individual species. On the basis of correlation coefficients in Table S7 in Supplementary material, n-alkanes homologs could be categorised into three groups, including Group 1: C_{17}, C_{19}, C_{21}; Group 2: C_{18} and C_{20}; Group 3: C_{22}-C_{30} and C_{27} fossil and C_{29} fossil. The species in each group has similar correlation coefficients to each other, which suggests that the members within each group may be derived from the same sources. We infer that C_{17}, C_{19}, C_{21}, C_{27} wax and C_{29} wax are very likely emitted from biogenic materials, for example plant wax, which can be generated from leaf fall and decay. Additionally, C_{27} wax had higher correlation coefficients with solar radiation. C_{29} wax almost had good correlations with all the other n-alkanes species, whereas C_{27} wax was not. The sources of Group 1 still could not be identified, which requires more evidence and investigation. Group 2: C_{18} and C_{20} could be deduced as possibly being the result of emissions from medium-duty diesel trucks as other studies have also shown that n-alkanes with a chain length around C_{20} mainly come from unburned fuels (Sakurai et al., 2003). The n-alkane species in Group 3 belong to sources dominated by contributions from fossil fuel combustion. It should be noted that the species in Group 3 all had low correlations with $PM_{2.5}$, OM and meteorological index, which suggests that n-alkanes and $PM_{2.5}$ and OM may have different dominant sources i.e. n-alkanes being mainly from traffic exhaust, whereas $PM_{2.5}$ and OM being mainly from biomass burning. In addition, unlike other species, such as C_{18}, C_{20}, C_{21}, $PM_{2.5}$ and OM, the species in Group 3 were less affected by atmospheric dispersion processes given a lower correlation with wind speed.

Correlation analysis between individual species of PAHs congeners, other related parameters (TAL: total n-alkanes, $PM_{2.5}$ and OM: organic matter), and meteorological parameters (solar radiation, T: temperature, and WS: wind speed) are presented in Appendix A Supplementary Table S8. Likewise, those species were categorised into three groups according to their correlation performance, referred as Group 1: fluorene and anthracene; Group 2: fluoranthene, pyrene, benzo[a]anthracene, chrysene, benzo[b]fluoranthene, benzo[k]fluoranthene, indeno[1,2,3-c,d]pyrene and Group 3: benzo[a]pyrene and dibenzo[a,h]anthracene. The specific source for Group 1 remains unexplained and needs further evidence to define a

52

common source, if this exists. The origins of Group 2 could be concluded to be dominated by biomass burning, which correspond with the discussion about PAHs diagnostic ratios of respective species. Furthermore, higher correlation values between these PAHs and wood smoke markers also validate this conclusion (Appendix D Supplementary Table S1). The main source contribution for Group 3 was probably from vehicle emissions. This investigation coincides with the results about the corresponding PAH diagnostic ratios as well. Besides, it is worth remarking that wind speed only had relatively higher negative correlation coefficient with some of PAHs, containing phenanthrene, fluoranthene, pyrene and benzo[a]pyrene. The remaining PAHs did not correlate closely with wind speed.

In order to further assist with the source identification of n-alkanes and PAHs, the correlation analysis between individual compounds of n-alkanes and PAHs were conducted in Appendix A Supplementary Table S9. From Appendix A Supplementary Table S9, C_{17} was strongly correlated with biomass burning PAH tracers (benzo[a]anthracene, chrysene, benzo[b]fluoranthene and indeno[1,2,3-c,d]pyrene), and less strongly with traffic emissions tracers (fluoranthene, pyrene, benzo[a]pyrene, dibenzo[a,h]anthracene and benzo[g,h,i]perylene), From this it may be concluded that C_{17} had a biomass burning contribution. Some lower molecular n-alkanes, such as C_{18}, C_{20} and C_{25} had moderate correlation coefficients with lower weight PAHs (naphthalene, acenaphthylene, phenanthrene and pyrene). C_{20} as mentioned previously is a tracer for unburned fuels, and C_{25} is derived from lubricating oil (He et al., 2006; Huang et al., 2006; Li et al., 2010). Unburned fuels and lubricating oil are possibly emitted from light duty diesel trucks with cold engines and falling ambient temperature (Brandenberger et al., 2005). What is more, the fact that phenanthrene serves as a reliable biomarker for diesel sources emphasizes that diesel sources contributed to some specific n-alkanes and PAHs. On the other hand, it is reasonable that PAHs biomass burning biomarkers and n-alkanes traffic biomarkers had utmost low correlations with each other. However, it should be notified that the reason that the low correlations between PAHs traffic biomarkers and n-alkanes biomarkers could be the different combustion processes they belong to. Normally, PAH traffic biomarkers are generated from incomplete combustion, whereas n-alkanes biomarkers are from petroleum residue which are combusted completely or entirely unburned.

PCA-MLR analysis of n-alkanes

PCA (Principle Component Analysis) is a very reliable statistical tool which can be applied to multiple variables to reduce their dimensionality to aid in identifying the sources of organics

in the atmosphere (Shi et al., 2009). Multivariate linear regression (MLR) can be utilised to quantify source contributions to samples. In this work, PCA and MLR were carried out by IBM SPSS (v23.0). Here only n-alkanes were used for this PCA-MLR analysis. Table 7 depicted three components generated by PCA analysis, which explained 87.4% of the total variance in n-alkanes. The first component accounted for 63.5% of the total variance, and was linked with almost all n-alkanes (C_{18}-C_{30}) including C_{27} fossil and C_{29} fossil, other than C_{17} and C_{27} wax. Therefore, this suggests that component 1 was linked to fossil fuel combustion. The second component, component 2, was enriched in lower molecular weight n-alkanes (C_{18}-C_{22}), C_{27} wax and C_{29} wax, and accounted for 14.5% of the total variance. These lower molecular weight n-alkanes are tracers of road dust and the waxed alkanes are most probably from biomass burning. Thus, component 2 reflected the possible sources from road dust and biomass burning for domestic heating during cold seasons. The third component, component 3, is related to C_{17}, C_{25}, C_{27} wax and C_{29} wax, all of which are markers for biogenic activities. This component explained 9.47% of the total variance.

MLR was conducted by applying the standardised component scores of components as independent variables and the standardised total concentrations of n-alkanes as dependent variables. Regression coefficients presenting on the following equation were procured to evaluate sources contributions.

$$\sum n\text{-}alkanes = 0.959 Component\ 1 + 0.266 Component\ 2 + 0.078 Component 3$$

Therefore, according to these coefficients, the contributions of component 1 (fossil fuel combustion), component 2 (biomass burning + road dust) and component 3 (biogenic) were 74%, 20% and 6%, respectively. This result demonstrates that anthropogenic activities were the main reason for the formation of $PM_{2.5}$ associated n-alkanes during the sampling season, contributing nearly 94% of the $PM_{2.5}$ bounded n-alkanes.

Table 7. PCA results of n-alkanes

N-alkane	Component		
	1	2	3
C_{17}	-0.024	0.213	0.651
C_{18}	0.647	0.669	-0.188
C_{19}	0.843	0.332	-0.151
C_{20}	0.605	0.586	0.051
C_{21}	0.612	0.611	-0.443
C_{22}	0.715	0.428	-0.376

54

C_{23}	0.665	-0.166	-0.546
C_{24}	0.965	-0.212	0.005
C_{25}	0.963	-0.165	0.123
C_{26}	0.941	-0.306	0.070
C_{27}	0.970	-0.122	0.180
C_{28}	0.956	-0.278	0.058
C_{29}	0.953	-0.089	0.217
C_{30}	0.925	-0.353	0.003
C_{27} fossil	0.957	-0.274	0.069
C_{27} wax	0.261	0.596	0.493
C_{29} fossil	0.942	-0.324	0.026
C_{29} wax	0.601	0.379	0.482
Explained Variance%	63.45	14.45	9.47
Identified source	fossil fuel	biomass burning + road dust	biogenic

Conclusions

In this paper, the sources of $PM_{2.5}$ associated n-alkanes and PAHs at an urban site in Sydney during the cooler months were investigated via several approaches, including diagnostic ratios, correlation analysis and PCA-MLR model. The concentrations of $PM_{2.5}$, organic fraction and n-alkanes were slightly higher in autumn than those in winter, whereas the PAHs were lower. The concentrations of total PAHs were higher during weekends than those on weekdays; however there are too few samples to make firm conclusion about this difference. Diagnostic ratios suggest fluoranthene, anthracene, pyrene, phenanthrene and benzo[a]pyrene may have a contribution from traffic emissions, whereas 5-6 rings PAHs, such as benzo[a]anthracene, chrysene, indeno[1,2,3-c,d]pyrene and benzo[g,h,i]perylene appear to arise at least in part from biomass burning.

Higher concentrations of n-alkanes were observed in autumn (mean: 29.3 ng/m^3), while lower concentrations were measured in winter (mean: 23.1 ng/m^3). Further source indices analysis (Cmax, CPI, WNA% and ACL) reveal that fossil fuel combustion especially traffic exhaust made a contribution to n-alkanes, particularly in winter, while autumn had a slightly higher contribution from biogenic materials. Correlation analysis was carried out between individual species in n-alkanes homologous series, PAH$_S$, $PM_{2.5}$, organic matter and meteorological parameters (solar radiation, temperature and wind speed), which confirm the above source identification. Finally, three sources were identified, and their contributions were estimated by a PCA-MLR model: fossil fuel (74%), biomass burning + road dust (20%) and biogenic sources (6%). It should be noted that due to lower and limited aerosol samples (< 20), PCA-

MLR results may have certain uncertainties. More reliable PCA-MLR results can be acquired from larger quantities of samples.

References

Akyüz, M., Çabuk, H., 2008. Particle-associated polycyclic aromatic hydrocarbons in the atmospheric environment of Zonguldak, Turkey. Sci Total Environ 405, 62-70.

Amador-Muñoz, O., Bazán-Torija, S., Villa-Ferreira, S., Villalobos-Pietrini, R., Bravo-Cabrera, J.L., Munive-Colín, Z., Hernández-Mena, L., Saldarriaga-Noreña, H., Murillo-Tovar, M., 2013. Opposing seasonal trends for polycyclic aromatic hydrocarbons and PM 10: Health risk and sources in southwest Mexico City. Atmos Res 122, 199-212.

Bourbonniere, R.A., Meyers, P.A., 1996. Sedimentary geolipid records of historical changes in the watersheds and productivities of Lakes Ontario and Erie. Limnology and Oceanography 41, 352-359.

Brandenberger, S., Mohr, M., Grob, K., Neukom, H.P., 2005. Contribution of unburned lubricating oil and diesel fuel to particulate emission from passenger cars. Atmospheric Environment 39, 6985-6994.

Bulejko, P., Adamec, V., Schüllerová, B., Skeřil, R., 2016. Levels, sources, and health risk assessment of polycyclic aromatic hydrocarbons in Brno, Czech Republic: a 5-year study. Environmental Science and Pollution Research, 1-12.

Callén, M.S., Iturmendi, A., López, J.M., 2014. Source apportionment of atmospheric PM2. 5-bound polycyclic aromatic hydrocarbons by a PMF receptor model. Assessment of potential risk for human health. Environmental Pollution 195, 167-177.

Cheng, Y., Li, S.-M., Leithead, A., Brook, J.R., 2006. Spatial and diurnal distributions of n-alkanes and n-alkan-2-ones on PM2. 5 aerosols in the Lower Fraser Valley, Canada. Atmospheric Environment 40, 2706-2720.

Chowdhury, Z., Zheng, M., Schauer, J.J., Sheesley, R.J., Salmon, L.G., Cass, G.R., Russell, A.G., 2007. Speciation of ambient fine organic carbon particles and source apportionment of PM2. 5 in Indian cities. Journal of Geophysical Research: Atmospheres 112.

Cohen, D.D., Stelcer, E., Garton, D., Crawford, J., 2011a. Fine particle characterisation, source apportionment and long-range dust transport into the Sydney Basin: a long term study between 1998 and 2009. Atmospheric Pollution Research 2, 182-189.

Cohen, D.D., Stelcer, E., Garton, D., Crawford, J., 2011b. Fine particle characterisation, Source Apportionment and Long Range Dust Transport into the Sydney Basin: A long term study between 1998 and 2009.

Cope, M., Keywood, M., Emmerson, K., Galbally, I., Boast, K., Chambers, S., Cheng, M., Crumeyrolle, S., Dunne, E., Fedele, R., 2013. Sydney Particle Study-Stage-II. Study undertaken by the Centre for Australian Weather and Climate Research (CAWCR) on behalf of the New South Wales Office of Environment and Heritage.

Durant, J.L., Busby, W.F., Lafleur, A.L., Penman, B.W., Crespi, C.L., 1996. Human cell mutagenicity of oxygenated, nitrated and unsubstituted polycyclic aromatic hydrocarbons associated with urban aerosols. Mutation Research/Genetic Toxicology 371, 123-157.

Durant, J.L., Lafleur, A.L., Busby, W.F., Donhoffner, L.L., Penman, B.W., Crespi, C.L., 1999. Mutagenicity of C 24 H 14 PAH in human cells expressing CYP1A1. Mutation Research/Genetic Toxicology and Environmental Mutagenesis 446, 1-14.

EPA, N., 2017. WOOD SMOKE Clean Air for NSW, in: EPA, N. (Ed.), p. 5.

EU, 2012. Air Quality Standards: Directive 2008/50/EU.

Fiore, A.M., Naik, V., Spracklen, D.V., Steiner, A., Unger, N., Prather, M., Bergmann, D., Cameron-Smith, P.J., Cionni, I., Collins, W.J., 2012. Global air quality and climate. Chemical Society Reviews 41, 6663-6683.

Gelencsér, A., May, B., Simpson, D., Sánchez-Ochoa, A., Kasper-Giebl, A., Puxbaum, H., Caseiro, A., Pio, C., Legrand, M., 2007. Source apportionment of PM2. 5 organic aerosol over Europe: Primary/secondary, natural/anthropogenic, and fossil/biogenic origin. Journal of Geophysical Research: Atmospheres (1984–2012) 112.

Goldstein, A.H., Galbally, I.E., 2007. Known and unexplored organic constituents in the earth's atmosphere. Environ Sci Technol 41, 1514-1521.

Guo, X., Li, C., Gao, Y., Tang, L., Briki, M., Ding, H., Ji, H., 2016. Sources of organic matter (PAHs and n-alkanes) in PM 2.5 of Beijing in haze weather analyzed by combining the C–N isotopic and PCA-MLR analyses. Environmental Science: Processes & Impacts 18, 314-322.

Gupta, P., Christopher, S.A., Box, M.A., Box, G.P., 2007. Multi year satellite remote sensing of particulate matter air quality over Sydney, Australia. International Journal of Remote Sensing 28, 4483-4498.

He, L.-Y., Hu, M., Huang, X.-F., Zhang, Y.-H., Yu, B.-D., Liu, D.-Q., 2006. Chemical characterization of fine particles from on-road vehicles in the Wutong tunnel in Shenzhen, China. Chemosphere 62, 1565-1573.

Heo, J., de Foy, B., Olson, M.R., Pakbin, P., Sioutas, C., Schauer, J.J., 2015. Impact of regional transport on the anthropogenic and biogenic secondary organic aerosols in the Los Angeles Basin. Atmospheric Environment 103, 171-179.

Heo, J., Dulger, M., Olson, M.R., McGinnis, J.E., Shelton, B.R., Matsunaga, A., Sioutas, C., Schauer, J.J., 2013. Source apportionments of PM 2.5 organic carbon using molecular marker Positive Matrix Factorization and comparison of results from different receptor models. Atmospheric Environment 73, 51-61.

Hine, D.W., Marks, A.D., Nachreiner, M., Gifford, R., Heath, Y., 2007. Keeping the home fires burning: The affect heuristic and wood smoke pollution. Journal of Environmental Psychology 27, 26-32.

Hinwood, A.L., Rodriguez, C., Runnion, T., Farrar, D., Murray, F., Horton, A., Glass, D., Sheppeard, V., Edwards, J.W., Denison, L., 2007. Risk factors for increased BTEX exposure in four Australian cities. Chemosphere 66, 533-541.

Ho, K., Ho, S.S.H., Lee, S., Cheng, Y., Chow, J.C., Watson, J.G., Louie, P.K.K., Tian, L., 2009. Emissions of gas-and particle-phase polycyclic aromatic hydrocarbons (PAHs) in the Shing Mun Tunnel, Hong Kong. Atmospheric Environment 43, 6343-6351.

Huang, X.-F., He, L.-Y., Hu, M., Zhang, Y.-H., 2006. Annual variation of particulate organic compounds in PM2. 5 in the urban atmosphere of Beijing. Atmospheric Environment 40, 2449-2458.

Huma, B., Yadav, S., Attri, A.K., 2016. Profile of particulate-bound organic compounds in ambient environment of Srinagar: a high-altitude urban location in the North-Western Himalayas. Environmental Science and Pollution Research 23, 7660-7675.

Jamhari, A.A., Sahani, M., Latif, M.T., Chan, K.M., Tan, H.S., Khan, M.F., Tahir, N.M., 2014. Concentration and source identification of polycyclic aromatic hydrocarbons (PAHs) in PM 10 of urban, industrial and semi-urban areas in Malaysia. Atmospheric Environment 86, 16-27.

Jeng, W.-L., 2006. Higher plant n-alkane average chain length as an indicator of petrogenic hydrocarbon contamination in marine sediments. Marine Chemistry 102, 242-251.

Johnston, F., Hanigan, I., Henderson, S., Morgan, G., Bowman, D., 2011. Extreme air pollution events from bushfires and dust storms and their association with mortality in Sydney, Australia 1994–2007. Environmental research 111, 811-816.

Jung, K.H., Yan, B., Chillrud, S.N., Perera, F.P., Whyatt, R., Camann, D., Kinney, P.L., Miller, R.L., 2010. Assessment of benzo (a) pyrene-equivalent carcinogenicity and mutagenicity of residential indoor versus outdoor polycyclic aromatic hydrocarbons exposing young children in New York City. Int J Env Res Pub He 7, 1889-1900.

Kanakidou, M., Seinfeld, J., Pandis, S., Barnes, I., Dentener, F., Facchini, M., Dingenen, R.V., Ervens, B., Nenes, A., Nielsen, C., 2005. Organic aerosol and global climate modelling: a review. Atmospheric Chemistry and Physics 5, 1053-1123.

Kang, M., Fu, P., Aggarwal, S.G., Kumar, S., Zhao, Y., Sun, Y., Wang, Z., 2016. Size distributions of n-alkanes, fatty acids and fatty alcohols in springtime aerosols from New Delhi, India. Environmental Pollution.

Kingham, S., Dorset, W., 2011. Assessment of exposure approaches in air pollution and health research in Australia and New Zealand.

Kirso, U., Urb, G., Laja, M., Teinemaa, E., Reinik, J., Gebefügi, I., Kettrup, A., 2006. PAH in airborne particulate matter. Polycyclic Aromatic Compounds 26, 111-119.

Knibbs, L.D., de Dear, R.J., Morawska, L., Mengersen, K.L., 2009. On-road ultrafine particle concentration in the M5 East road tunnel, Sydney, Australia. Atmospheric Environment 43, 3510-3519.

Křůmal, K., Mikuška, P., Večeřa, Z., 2013. Polycyclic aromatic hydrocarbons and hopanes in PM1 aerosols in urban areas. Atmospheric Environment 67, 27-37.

Larsen, J.C., Larsen, P.B., 1998. Chemical carcinogens. Issues in Environmental Science and Technology 10, 33-56.

Li, W., Peng, Y., Bai, Z., 2010. Distributions and sources of n-alkanes in PM2. 5 at urban, industrial and coastal sites in Tianjin, China. Journal of Environmental Sciences 22, 1551-1557.

Liu, J., Man, R., Ma, S., Li, J., Wu, Q., Peng, J., 2015. Atmospheric levels and health risk of polycyclic aromatic hydrocarbons (PAHs) bound to PM 2.5 in Guangzhou, China. Marine pollution bulletin 100, 134-143.

Liu, L.-Y., Wei, G.-L., Wang, J.-Z., Guan, Y.-F., Wong, C.S., Wu, F.-C., Zeng, E.Y., 2013. Anthropogenic Activities Have Contributed Moderately to Increased Inputs of Organic Materials in Marginal Seas off China. Environ Sci Technol 47, 11414-11422.

Lu, C.-F., Yuan, X.-Y., Li, L.-Z., Zhou, W., Zhao, J., Wang, Y.-M., Peng, S.-Q., 2015. Combined exposure to nano-silica and lead induced potentiation of oxidative stress and DNA damage in human lung epithelial cells. Ecotoxicology and environmental safety 122, 537-544.

Lyu, Y., Xu, T., Yang, X., Chen, J., Cheng, T., Li, X., 2016. Seasonal contributions to size-resolved n-alkanes (C 8–C 40) in the Shanghai atmosphere from regional anthropogenic activities and terrestrial plant waxes. Sci Total Environ.

Maleknia, S.D., Bell, T.L., Adams, M.A., 2009. Eucalypt smoke and wildfires: temperature dependent emissions of biogenic volatile organic compounds. International Journal of Mass Spectrometry 279, 126-133.

Mancilla, Y., Mendoza, A., Fraser, M., Herckes, P., 2016. Organic composition and source apportionment of fine aerosol at Monterrey, Mexico, based on organic markers. Atmospheric Chemistry and Physics 16, 953-970.

Manoli, E., Kouras, A., Karagkiozidou, O., Argyropoulos, G., Voutsa, D., Samara, C., 2016. Polycyclic aromatic hydrocarbons (PAHs) at traffic and urban background sites of northern Greece: source apportionment of ambient PAH levels and PAH-induced lung cancer risk. Environmental Science and Pollution Research 23, 3556-3568.

Meyers, P.A., 2003. Applications of organic geochemistry to paleolimnological reconstructions: a summary of examples from the Laurentian Great Lakes. Organic geochemistry 34, 261-289.

Mikuška, P., Křůmal, K., Večeřa, Z., 2015. Characterization of organic compounds in the PM2. 5 aerosols in winter in an industrial urban area. Atmospheric Environment.

Minguillón, M.C., Arhami, M., Schauer, J.J., Sioutas, C., 2008. Seasonal and spatial variations of sources of fine and quasi-ultrafine particulate matter in neighborhoods near the Los Angeles–Long Beach harbor. Atmospheric Environment 42, 7317-7328.

Mohammed, M.O., Song, W.-w., Ma, Y.-l., Liu, L.-y., Ma, W.-l., Li, W.-L., Li, Y.-F., Wang, F.-y., Qi, M.-y., Lv, N., 2016. Distribution patterns, infiltration and health risk assessment of PM2. 5-bound PAHs in indoor and outdoor air in cold zone. Chemosphere 155, 70-85.

Nagy, A.S., Szabó, J., Csanádi, Z., Erdős, J., 2016. Characterization of Polycyclic Aromatic Hydrocarbons in Ambient Air PM2. 5 in an Urban Site of Győr, Hungary. World Academy of Science, Engineering and Technology, International Journal of Environmental, Chemical, Ecological, Geological and Geophysical Engineering 10, 873-876.

Nisbet, I.C., LaGoy, P.K., 1992. Toxic equivalency factors (TEFs) for polycyclic aromatic hydrocarbons (PAHs). Regulatory toxicology and pharmacology 16, 290-300.

Olson, D.A., McDow, S.R., 2009. Near roadway concentrations of organic source markers. Atmospheric Environment 43, 2862-2867.

Organization, W.H., 2000. Air quality guidelines for Europe.

Perera, F.P., 1997. Environment and cancer: who are susceptible? Science 278, 1068-1073.

Perrone, M., Larsen, B., Ferrero, L., Sangiorgi, G., De Gennaro, G., Udisti, R., Zangrando, R., Gambaro, A., Bolzacchini, E., 2012. Sources of high PM2. 5 concentrations in Milan, Northern Italy: molecular marker data and CMB modelling. Science of the Total Environment 414, 343-355.

Philip, S., Martin, R.V., van Donkelaar, A., Lo, J.W.-H., Wang, Y., Chen, D., Zhang, L., Kasibhatla, P.S., Wang, S., Zhang, Q., 2014. Global chemical composition of ambient fine particulate matter for exposure assessment. Environ Sci Technol 48, 13060-13068.

Pies, C., Hoffmann, B., Petrowsky, J., Yang, Y., Ternes, T.A., Hofmann, T., 2008. Characterization and source identification of polycyclic aromatic hydrocarbons (PAHs) in river bank soils. Chemosphere 72, 1594-1601.

Ravindra, K., Sokhi, R., Van Grieken, R., 2008. Atmospheric polycyclic aromatic hydrocarbons: source attribution, emission factors and regulation. Atmospheric Environment 42, 2895-2921.

Sakurai, H., Tobias, H.J., Park, K., Zarling, D., Docherty, K.S., Kittelson, D.B., McMurry, P.H., Ziemann, P.J., 2003. On-line measurements of diesel nanoparticle composition and volatility. Atmospheric Environment 37, 1199-1210.

Schauer, J.J., Kleeman, M.J., Cass, G.R., Simoneit, B.R., 1999. Measurement of emissions from air pollution sources. 2. C1 through C30 organic compounds from medium duty diesel trucks. Environ Sci Technol 33, 1578-1587.

Shi, G.-L., Li, X., Feng, Y.-C., Wang, Y.-Q., Wu, J.-H., Li, J., Zhu, T., 2009. Combined source apportionment, using positive matrix factorization–chemical mass balance and principal component analysis/multiple linear regression–chemical mass balance models. Atmospheric Environment 43, 2929-2937.

Simoneit, B.R., 1989. Organic matter of the troposphere—V: application of molecular marker analysis to biogenic emissions into the troposphere for source reconciliations. Journal of Atmospheric Chemistry 8, 251-275.

Singare, P.U., 2015. Studies on polycyclic aromatic hydrocarbons in surface sediments of Mithi River near Mumbai, India: Assessment of sources, toxicity risk and biological impact. Marine pollution bulletin 101, 232-242.

Slezakova, K., Castro, D., Delerue–Matos, C., da Conceição Alvim–Ferraz, M., Morais, S., do Carmo Pereira, M., 2013. Impact of vehicular traffic emissions on particulate-bound PAHs: Levels and associated health risks. Atmos Res 127, 141-147.

Sun, Q., Xie, M., Shi, L., Zhang, Z., Lin, Y., Shang, W., Wang, K., Li, W., Liu, J., Chu, G., 2013. Alkanes, compound-specific carbon isotope measures and climate variation during the last millennium from varved sediments of Lake Xiaolongwan, northeast China. Journal of paleolimnology 50, 331-344.

Teixeira, E.C., Agudelo-Castañeda, D.M., Fachel, J.M.G., Leal, K.A., de Oliveira Garcia, K., Wiegand, F., 2012. Source identification and seasonal variation of polycyclic aromatic hydrocarbons associated with atmospheric fine and coarse particles in the Metropolitan Area of Porto Alegre, RS, Brazil. Atmos Res 118, 390-403.

USEPA, P.P., 1996. Code of Federal Regulations. Title.

Valotto, G., Rampazzo, G., Gonella, F., Formenton, G., Ficotto, S., Giraldo, G., 2016. Source apportionment of PAHs and n-alkanes bound to PM 1 collected near the Venice highway. Journal of Environmental Sciences.

van Drooge, B., Grimalt, J., 2015. Particle size-resolved source apportionment of primary and secondary organic tracer compounds at urban and rural locations in Spain. Atmos Chem Phys 15, 7735-7752.

Van Drooge, B.L., Crusack, M., Reche, C., Mohr, C., Alastuey, A., Querol, X., Prevot, A., Day, D.A., Jimenez, J.L., Grimalt, J.O., 2012. Molecular marker characterization of the

organic composition of submicron aerosols from Mediterranean urban and rural environments under contrasting meteorological conditions. Atmospheric Environment 61, 482-489.

Wang, F., Guo, Z., Lin, T., Rose, N.L., 2016a. Seasonal variation of carbonaceous pollutants in PM 2.5 at an urban 'supersite' in Shanghai, China. Chemosphere 146, 238-244.

Wang, G., Cheng, S., Li, J., Lang, J., Wen, W., Yang, X., Tian, L., 2015a. Source apportionment and seasonal variation of PM2. 5 carbonaceous aerosol in the Beijing-Tianjin-Hebei Region of China. Environmental monitoring and assessment 187, 1-13.

Wang, J., Ho, S.S.H., Cao, J., Huang, R., Zhou, J., Zhao, Y., Xu, H., Liu, S., Wang, G., Shen, Z., 2015b. Characteristics and major sources of carbonaceous aerosols in PM 2.5 from Sanya, China. Sci Total Environ 530, 110-119.

Wang, Q., Feng, Y., Huang, X., Griffith, S.M., Zhang, T., Zhang, Q., Wu, D., Yu, J.Z., 2016b. Nonpolar organic compounds as PM2. 5 source tracers: Investigation of their sources and degradation in the Pearl River Delta, China. Journal of Geophysical Research: Atmospheres 121.

Wang, Q.Q., Huang, X.H., Zhang, T., Zhang, Q., Feng, Y., Yuan, Z., Wu, D., Lau, A.K., Yu, J.Z., 2015c. Organic tracer-based source analysis of PM 2.5 organic and elemental carbon: A case study at Dongguan in the Pearl River Delta, China. Atmospheric Environment 118, 164-175.

Wang, W., Simonich, S.L.M., Xue, M., Zhao, J., Zhang, N., Wang, R., Cao, J., Tao, S., 2010. Concentrations, sources and spatial distribution of polycyclic aromatic hydrocarbons in soils from Beijing, Tianjin and surrounding areas, North China. Environmental Pollution 158, 1245-1251.

Wiriya, W., Prapamontol, T., Chantara, S., 2013. PM10-bound polycyclic aromatic hydrocarbons in Chiang Mai (Thailand): seasonal variations, source identification, health risk assessment and their relationship to air-mass movement. Atmos Res 124, 109-122.

Xie, M., Hannigan, M.P., Barsanti, K.C., 2014a. Gas/particle partitioning of n-alkanes, PAHs and oxygenated PAHs in urban Denver. Atmospheric Environment 95, 355-362.

Xie, M., Hannigan, M.P., Barsanti, K.C., 2014b. Impact of gas/particle partitioning of semivolatile organic compounds on source apportionment with positive matrix factorization. Environ Sci Technol 48, 9053-9060.

Yadav, S., Tandon, A., Attri, A.K., 2013. Monthly and seasonal variations in aerosol associated n-alkane profiles in relation to meteorological parameters in New Delhi, India. Aerosol and Air Quality Research 13, 287-300.

Yan, B., Zheng, M., Hu, Y., Ding, X., Sullivan, A.P., Weber, R.J., Baek, J., Edgerton, E.S., Russell, A.G., 2009. Roadside, urban, and rural comparison of primary and secondary organic molecular markers in ambient PM2. 5. Environ Sci Technol 43, 4287-4293.

Young, L.-H., Wang, C.-S., 2002. Characterization of n-alkanes in PM2. 5 of the Taipei aerosol. Atmospheric Environment 36, 477-482.

Yunker, M.B., Macdonald, R.W., Veltkamp, D.J., Cretney, W.J., 1995. Terrestrial and marine biomarkers in a seasonally ice-covered Arctic estuary—integration of multivariate and biomarker approaches. Marine chemistry 49, 1-50.

Yunker, M.B., Macdonald, R.W., Vingarzan, R., Mitchell, R.H., Goyette, D., Sylvestre, S., 2002. PAHs in the Fraser River basin: a critical appraisal of PAH ratios as indicators of PAH source and composition. Organic geochemistry 33, 489-515.

Zhang, L., Chen, R., Lv, J., 2016. Spatial and Seasonal Variations of Polycyclic Aromatic Hydrocarbons (PAHs) in Ambient Particulate Matter (PM10. B Environ Contam Tox 96, 827-832.

Zheng, M., Cass, G.R., Schauer, J.J., Edgerton, E.S., 2002. Source apportionment of PM2. 5 in the southeastern United States using solvent-extractable organic compounds as tracers. Environmental science & technology 36, 2361-2371.

Zheng, M., Kester, D.R., Wang, F., Shi, X., Guo, Z., 2008. Size distribution of organic and inorganic species in Hong Kong aerosols during the wet and dry seasons. Journal of Geophysical Research: Atmospheres 113.

Zhu, Y., Yang, L., Meng, C., Yuan, Q., Yan, C., Dong, C., Sui, X., Yao, L., Yang, F., Lu, Y., 2015. Indoor/outdoor relationships and diurnal/nocturnal variations in water-soluble ion and PAH concentrations in the atmospheric PM 2.5 of a business office area in Jinan, a heavily polluted city in China. Atmos Res 153, 276-285.

Zhu, Y., Yang, L., Yuan, Q., Yan, C., Dong, C., Meng, C., Sui, X., Yao, L., Yang, F., Lu, Y., 2014. Airborne particulate polycyclic aromatic hydrocarbon (PAH) pollution in a background site in the North China Plain: concentration, size distribution, toxicity and sources. Sci Total Environ 466, 357-368.

CHAPTER 3

Paper Two

Chemical characterization of polar organic compounds in PM$_{2.5}$ aerosols at an urban site in Sydney

Meng, C., Nelson, P.F.

Draft for submission to *Atmospheric Environment*

In this paper concentrations of typical polar organic compounds of six compound classes in ambient PM$_{2.5}$ samples from an urban Sydney site during 2014 autumn and winter are presented. Correlation analysis and principal component analysis (PCA) techniques are used to assess correlations between concentrations of the selected polar organic compounds and to interpret the respective sources. This study discusses the seasonal variation of typical polar organic compounds in PM$_{2.5}$ and identifies their possible sources in autumn and winter.

Chemical characterization of polar organic compounds in $PM_{2.5}$ aerosols at an urban site in Sydney

Chuanping Meng [*], Peter F. Nelson

Department of Environmental Sciences, Faculty of Science and Engineering, Macquarie University, North Ryde, Sydney, New South Wales, 2109, Australia

[*] Corresponding author e-mail: Chuanping.meng@students.mq.edu.au

ABSTRACT

Atmospheric particulates are of worldwide concern and significantly affect climate and human health. Carbonaceous aerosols are one of the most abundant components (20–80%) of atmospheric fine particulate matter ($PM_{2.5}$) and for regulatory purposes, it is important to understand $PM_{2.5}$ formation and evolution pathways from their sources to the ultimate receptors. The aim of this study is to characterize the emission and sources of carbonaceous aerosols. Twenty one airborne particulate matter samples ($PM_{2.5}$), including field blanks were collected at 48 h intervals from a location on the Macquarie campus in Sydney, Australia using a high volume sampler and quartz filters during the period 17/05/2014–31/05/2014 (autumn, n = 7) and 31/05/2014–30/06/2014 (winter, n = 12).

Twelve polar organic species were identified, belonging to six compound classes, including 3 fatty acids ($C_{16:0}$, $C_{18:0}$ and $C_{18:1}$), 3 monosaccharide anhydrides (levoglucosan, mannosan and galactosan), dehydroabietic acid, syringic acid for anthropogenic primary organic aerosol markers; 2 dicarboxylic acid (succinic acid and azelaic acid) and 2 aromatic derived compounds (terephthalic acid and phthalic acid) for anthropogenic secondary organic aerosol markers.

The concentrations of the selected trace chemical compounds analysed are presented and discussed. Palmitic acid had the highest observed (22/05/2014) concentration up to 655.4 ng $\cdot m^{-3}$, followed by monosaccharide anhydrides, with a highest concentration of 593.5 ng $\cdot m^{-3}$ (22/06/2014), and syringic acid, with a highest concentration of 263.4 ng $\cdot m^{-3}$ (22/06/2014). Oleic acid and succinic acid were less abundant.

64

Three primary sources and two secondary sources were preliminarily identified according to several diagnostic ratios and correlation analysis for individual organic species. These are wood burning, traffic, anthropogenic secondary organic aerosol (SOA), and aromatic derived anthropogenic SOA.

The chemical analysis suggests that the site was significantly influenced by the emissions from wintertime domestic wood combustion and controlled bushfire prevention burns during autumn. In autumn, hardwood was found as a predominant source combined with some softwood burning, whereas in winter hardwood and grass combustion are the main type of biomass burnt. It is apparent that during the cold seasons the primary sources of the polar fraction of the organic component of PM are biomass combustion.

Keywords: $PM_{2.5}$, polar organic compounds, emission sources, urban area

Introduction

Airborne particulate matter is composed of ionic species, sea salts, heavy metals and a carbonaceous component, the latter of which has received increasing attention, owing to its adverse and detrimental impacts on human health (Franklin et al., 2008; Franklin et al., 2007; Turpin and Lim, 2001; Van Donkelaar et al., 2010) and potential climatic influence (Bond et al., 2013; Dawson et al., 2014; Fuzzi et al., 2015). Carbonaceous substances are comprised of organic carbon and elemental carbon (Keywood et al., 2011; Ng et al., 2006). Elemental carbon is a primary pollutant emitted into the atmosphere by incomplete combustion, whilst organic carbon is a complex mixture of many classes of organic compounds that originate from both primary sources and secondary photo-chemical reactions (Keywood et al., 2013; Reisen et al., 2013). Fine inhalable particles (particulate matter with aerodynamic diameters 2.5 microns and smaller designated as $PM_{2.5}$) have a direct and indirect influence on many diseases, such as stroke, heart disease, lung cancer, and both chronic and acute respiratory diseases, including asthma (Bell et al., 2007; Boldo et al., 2006; Franklin et al., 2007; Kampa and Castanas, 2008; Mar et al., 2006). There has been considerable research on the carbonaceous constituents of $PM_{2.5}$ aerosol in America, China, Europe, Southeast Asia and India (Dusek et al., 2017; Masalaite et al., 2017; Meena et al., 2017; Pant et al., 2017; Singh et al., 2017; Xiang et al., 2017; Zhou et al., 2017). This research has been driven in part because not only are these carbonaceous components a major constituent of the aerosol, but also

because of the broad and complex range of compounds involved information remains limited (Choi et al., 2017; Huang et al., 2014; Khan et al., 2016; Park and Son, 2017). Moreover, in Oceania including Australia research on carbonaceous aerosols is rare (Krivácsy et al., 2006; Zhang et al., 2007). Furthermore, most of that research is focused on the effects of carbonaceous aerosol on climate change (Rotstayn et al., 2009; Zhang et al., 2007), and relatively few studies have concentrated on the apportionment of sources and health risk of carbonaceous aerosols (Chan et al., 1999; Keywood et al., 2011). Australia has some distinctive features, which can result in deterioration of air quality. For example, higher forest coverage combined with a dry climate can lead to frequent bushfires (Blake et al., 2009; De Vos et al., 2009; Jordan et al., 2006), and high levels of solar radiation can create favourable conditions for the formation of secondary organic aerosols (Iinuma et al., 2008; Iinuma et al., 2016; Maleknia et al., 2009). With the combination of such conditions elevated particulate matter levels can be observed and air pollution events such as haze occur (Finlay et al., 2012; Miranda et al., 2012).

Sydney is the largest urban city in Australia with a population estimated around 4.92 million and as a world famous harbour city, located in an ear-shaped basin (part of the Sydney Basin) with a narrow sea-outlet. This geographical position (Sydney Basin) favours photo-chemical reactions and accumulation of secondary organic aerosols (Churches and Corbett, 1991; Jalaludin et al., 2006). For the implementation of effective abatement measures, an insight into the characterisation of organic tracers in $PM_{2.5}$ can aid further source apportionment and ultimately lead to management and reduction of airborne particles. Organic molecular markers are source indicators and tracers for specific sources and these markers have been widely used as powerful tools for the identification of the origin of particulate matter, (Feng et al., 2013; Medeiros and Simoneit, 2008; Simoneit, 2002). Although gas chromatography-mass spectrometry (GC/MS) techniques only allows the detection of a small fraction of the organic aerosol mass (usually < 5%), once detected these tracer organic compounds can be used as inputs for source apportionment during the process of developing receptor and climate models (Schauer et al., 1996; Stone et al., 2009; Wang et al., 2012).

In order to identify the sources of atmospheric aerosols and assess natural versus anthropogenic contributions to the carbonaceous aerosols, source specific chemical organic compounds (or ratios between compounds) can be used as molecular biomarkers or tracers. Many of the tracers have the same traits in that they are relatively stable or react slowly in the atmosphere and do not partition to the gas phase during transport (Alves, 2008; Jaeckels et al.,

2007; Lin et al., 2010). Many studies have been conducted which focus on the organic characterisation of specific source emissions, such as motor vehicle exhausts, coal combustion in the large power stations, cooking operations and biomass burning (Alves et al., 2012; Cass, 1998; Fine et al., 2002; Morawska and Zhang, 2002; Robinson et al., 2006).

Thus, after qualitative analysis, quantitative analysis of the solvent extractable organic fraction in the samples collected for this study was conducted. Based on the discussion above, a sampling campaign (48h sampling periods) during autumn and winter to collect $PM_{2.5}$ in the Sydney urban area was carried out. The composition of the solvent extractable organic fraction was first investigated using GC/MS by qualitative identification of major peaks. After this comprehensive qualitative analysis, to gain insight into the compositions, sources, formation and processing of organic fine particulate matter during the cooler months, this work presents an autumn and winter study of selected major polar particulate organic compounds in $PM_{2.5}$ collected at an urban site in north western Sydney. The polar compounds extracted included three fatty acids (palmitic acid $C_{16:0}$, stearic acid $C_{18:0}$ and oleic acid $C_{18:1}$), three monosaccharide anhydrides (levoglucosan, mannosan and galactosan), dehydroabietic acid and syringic acid (identified as primary organic aerosol markers) (Lewandowski et al., 2008); two dicarboxylic acids (succinic acid C_4, and azelaic acid C_9) and aromatic derived compounds (terephthalic acid + phthalic acid) (identified as anthropogenic secondary organic aerosol markers) (Feng et al., 2013). The selection of the monosaccharide anhydrides, C_9 dicarboxylic acid and aromatic dicarboxylic acid are based on their representation of organic aerosol emission sources, whereas palmitic acid $C_{16:0}$ and dehydroabietic acid were selected to be quantified due to their significant enrichment in $PM_{2.5}$ samples.

The concentrations of $PM_{2.5}$, organic molecular markers and preliminary analysis of the source of specific molecular markers are discussed. Compositional information on the sources of ambient $PM_{2.5}$ particles is important for future toxicological research in understanding the potential influence of aerosol-associated organic materials on human health and global ecosystems and to aid the development of emission inventories and for establishment of effective abatement plans.

Experimental Section

Description of sampling

The sampling site (Figure 1) for the study was located in Macquarie University Automatic Weather Station (AWS) at North Ryde, Sydney, Australia (33 °45' 55.1" South, 151 °7' 3.2" East and 66.8 m above mean sea level). The AWS site is situated in a residential area approximately 20 km northwest of the Sydney central business district (CBD), located to the north of the university, on the northern side of the M2 Hills motorway, within the sports grounds of Macquarie University at North Ryde, NSW, Australia, and adjacent to a vegetated and wooded area of Lane Cove River State Park. The site is shown on a satellite image in Figure 1.

Figure 1. Map of the site location-automatic weather station in Macquarie University sports field (Map data source: Google, DigitalGlobe).

Nineteen $PM_{2.5}$ quartz filters were collected from 17 May to 29 June 2014 (autumn and winter), under the operation of an Ecotech 3000 high volume sampler (Ecotech Pty Ltd) equipped with a $PM_{2.5}$ size selective inlet for 48 h periods with a sampling rate of 67.8 m³/h. The filters (Pall Life Sciences; Tissuquartz^{TM} 8 x 10 inch 2500QAT-UP), were prebaked at 550 °C for 24 h and prior to sampling filters were equilibrated under constant temperature and humidity conditions (temperature of 20 °C, relative humidity of 50%) for 24 h and then weighted to a resolution of 0.1 mg (Sartorius, BP 221S). After collection, the same procedure

68

of filter equilibration was performed. After gravimetric determination of the weight of PM collected on the filters, they were wrapped in clean aluminium foil, sealed in individual polyethylene bags and stored at -18 ℃ until further analysis. Two field blanks collected during the campaign were obtained by placing the filter on the filter cartridge of the sampler for a few seconds without activating the air pump and stored following the same procedure.

Analytical procedure

Each sample was solvent extracted and analysed by GC/MS. Solvent extraction used an accelerated pressurized solvent extraction device (ASE, Dionex 300), performing with following parameters: preheat = 5 min; heat = 5 min; static = 5 min; pressure = 1500 psi; flush = 70%, purge = 300 sec; cycles = 3; temperature = 100 ℃; solvent = dicholoromethane/methanol mixture (Honeywell, Australia, 9:1, v/v). Resulting extracts were reduced by a rotary evaporator and blown down to dryness by a gentle stream of ultrapure nitrogen on a heating block at 60 ℃ cooled and then gravimetrically quantified. For analysis extracts were resuspended in dichloromethane-hexane (Honeywell, Australia, 1:1, v/v) to 1 ml. Any insoluble particles observed in the extracts were removed by glass wool filled Pasteur pipettes. Extraction recoveries are > 75%.

Homogenised 1 ml volume extracts were split into two 0.5 ml vials. One of 0.5 ml aliquots was analysed for non-polar compound content, including C_{17}-C_{30} alkanes and 16 PAHs, the results of which are discussed elsewhere (chapter 2). The second aliquot was evaporated to dryness by a gentle stream of ultrapure nitrogen and then derivatized with 50 μL of N,O-Bis (trimethylsilyl)-trifluoroacetamide containing 1% trimethyl-chlorosilane (BSTFA + 1% TMCS) for 2 hours at 70 ℃ on a heating block in order to convert the carboxyl and hydroxyl compounds into their corresponding trimethylsilyl esters and ethers, before GC/MS analysis (Nirmalkar et al., 2015; Simoneit, 1999). After derivatization, extracts were resuspended in dichloromethane-methanol (Honeywell, Australia, 1:1, v/v) to 1 ml. Before injection into the gas chromagraph coupled to the MS, internal standards (methyl β-L-arabinopyranoside for sugars and *cis*-ketopinic for acids) were added into each of the polar organic compound vials, in accordance with USEPA method TO-13A (U.S.EPA, 1999).

Polar organic compounds were determined by gas chromatography coupled with mass selective detection (GC/MSD, Agilent, 7890A, 5977B, operated in electron ionization (EI) mode). The GC was equipped with a capillary column (HP5-MS) of 0.25 mm film thickness,

0.25 mm inside diameter and a length of 30 m. A split injection (split ratio 20) with pressure pulse of 30 psi and pulse hold time of 0.7 minute was used to minimize flashback and maximise (560 m/z) molecular weight discrimination. Auto-injections of 1.0 μL were conducted at an inlet temperature of 280 ℃ and purge time of 0.5 minute using an Agilent single-taper, deactivated inlet liner with glass wool. The MS transfer line temperature was maintained at 320 ℃. The MSD was optimised for maximum mass-ion signal response operated at source and quadrupole temperatures of 300 ℃ and 200 ℃, respectively. Ultra-high-purity He (99.99%) at a constant flow rate at 1 mL/min was used as the carrier gas. The oven temperature was set to start to heat from 45 ℃ for 2 minutes; to 180 ℃ at 10 ℃/min, hold for 2 minutes; then ramp to 280 ℃ at 2 ℃/min, hold 2 minutes; ramp to 320 ℃ at 2 ℃/min, hold for a further 10 minutes.

Compounds were identified by chromatogram deconvolution. Agilent GC/MS MassHunter Acquisition software (Agilent Technologies, USA) was employed to identify a comprehensive collection of the organic compounds detected. Qualitative identification was based on the retention time of the authentic target analyte standard quantitation ion and on the relative abundance of the quantitation and qualifier ions. Quantification of target compounds was performed by running a series of external standard solutions (7 points, quadratic fitting) spiked with a 30 μl internal standard. This allowed a response factor to be determined by calibrating the response to seven different concentrations of each target analyte. The recovery is calculated by using internal standards. In these cases, the final mass amount of each target compound was determined by converting peak area ratios to mass ratios using calibration curves and known mass of pre-spiked internal standard in MS quantitative analysis software MassHunter (Agilent Technologies, USA). No organic compounds were detected on field blanks.

Polar organic compounds discussed in this present study were selected as representatives of primary organic aerosol emission sources, secondary organic aerosol formation and because of their enrichment in $PM_{2.5}$. Higher abundance organic compounds were more likely to be selected, their corresponding concentrations can assist to reflect the emission sources' pollution extent. Detailed concentrations of each quantified species in this study are provided in Appendix B, Supplementary Table S1-S2.

Statistical analysis

Multiple comparison tests (T test, non-parametric Kruskal-Wallis H test and Mann-Whitney U test) in SPSS software version 23.0 were applied to test whether each individual indices including $PM_{2.5}$, organic fraction, meteorological variables (temperature, wind speed and solar radiation, which are presented in daily averages) and polar organic compounds were significantly different among four sampling periods (autumn weekdays, autumn weekend, winter weekdays and winter weekend) (Meng et al., 2005). Effects were designated significant if $p < 0.01$. To determine dependence between the above species, a correlation analysis resulting in a univariate Pearson correlation coefficient was performed (Yao et al., 2002).

Results and Discussion

Meteorological conditions

Meteorological data (daily averages) were automatically measured at the sampling site and recorded at 15 minute intervals. Data recorded included dry bulb temperature, wind speed, wind direction and solar radiation. Temperature showed strong seasonal variation between autumn and winter ($p = 0.01 < 0.05$). Unlike temperature, wind speed and solar radiation were not significantly different during autumn and winter. However, wind speed and solar radiation appears to have had a strong effect on the $PM_{2.5}$ and organic fraction concentrations. A linear negative dependence of wind speed with $PM_{2.5}$ and organic fraction concentrations was observed ($R^2 = -0.6$, $p < 0.01$, Appendix B, Supplementary Table S3), which indicates as expected that wind driven dispersion had the effect of reducing PM level and dispersing organic compounds emissions. The correlation between solar radiation and $PM_{2.5}$ and organic fraction concentrations suggests that solar radiation has a role in boosting PM levels particularly the organic fraction ($R^2 = 0.5$, $p < 0.05$, Appendix B, Supplementary Tables S3).

Qualitative analysis

By means of Agilent MassHunter software (Agilent Technologies, USA), several classes of organic compounds were identified, including diols, dicarboxylic acid, polyols, fatty acids (saturated fatty acid and unsaturated fatty acid), aromatic acid and sugars (monosaccharide

and disaccharide). All peaks were identified and there were no large unknown peaks. Eighty-three identified organic compounds and their corresponding retention times are listed in Table 1. Polar organic compounds quantified in this study are representative of the major species which appeared in each sample and relatively higher concentrations.

Table 1. Identified organic species and their corresponding retention times.

Name	Retention Time	Name	Retention Time
1,2-Butanediol	6.20	1,2-Ethenediol	15.81
Levulinic acid	6.71	Propanedioic acid	15.96
3-Pyridinol	6.75	3-Methyladipic acid	16.41
Hydracrylic acid	6.87	Butanedioic acid	16.76
2-Ethoxyethanol	7.07	4-Hydroxybenzoic acid	16.95
1-Methoxy-2-propanol	7.21	Xylose	18.50
Isopropyl alcohol	7.22	Levoglucosan[*]	18.60
L-Valine	7.29	Mannosan[*]	18.70
Malonic acid	7.78	Suberic acid	18.85
1-Methoxy-2-propanol	7.97	Galactosan	19.40
1-Nonanol	8.31	Sedoheptulose	19.43
Diethylene glycol	8.43	D-Lyxose	19.74
Benzoic acid	8.44	Arabinitol	20.03
1-Phenyl-1,2-ethanediol	8.69	Xylitol	20.03
Glycerol	9.06	D-2-Deoxyribose	20.26
Succinic acid	9.70	Vanillic Acid	20.49
Ethylmalonic acid	9.95	Triethylene glycol	20.55
Glyceric acid	10.18	Terephthalic acid	21.08
2,3-Butanediol	10.52	Azelaic acid	21.28
Nonanoic acid	10.57	Myristic acid	22.38
phenoxyethanol	10.68	1,5-Anhydrohexitol	23.04
Ethylene glycol	11.38	Inositol	23.56
Vanillin	11.42	Syringic acid	23.84
Glutaric acid	11.60	Pentadecanoic acid	24.74
2-Butanol	11.77	D-Glucitol	25.23
Cyclobutanol	11.94	D-Lyxose	26.21
4-Dodecanol	12.07	D-Mannose	26.51
Pinonic acid	12.29	Palmitic Acid	27.04
3-Ethoxypropanol	13.17	Oleic Acid	30.78
4-Pentenoic acid	13.31	Stearic acid	31.38
2,4-Dimethyl-3-pentanol	13.63	Dehydroabietic acid	34.31
Malic acid	13.79	Eicosanoic acid	35.39
2-Methyl-1,3-butanediol	13.87	Docosanoic acid	37.01
Triethylene glycol	13.99	Docosanol	37.49
Butyric Acid	14.01	Behenic acid	39.14
4-Hydroxybutanoic acid	14.36	Sucrose	40.39
Erythritol	14.46	1-Tetracosanol	41.07
2-methylthreitol	15.06	Lignoceric acid	42.63
Pyruvic acid	15.39	Hexacosanoic acid	45.90
1-Dodecanol	15.41	1-Octacosanol	47.56
2-methylerythritol	15.56	beta-Sitosterol	50.65
3-Methyl-2-oxovaleric acid	15.80	Ursolic acid	54.59

[*] levoglucosan and mannosan were not chromatographically separated completely (double peaks) since the same m/z in mass spectra. Thus, manually peak splitting was performed for quantitative analysis.

PM$_{2.5}$ and organic fraction concentrations

A summary of average mass concentrations of PM$_{2.5}$ aerosols collected, polar organic compounds determined and the range of meteorological variables, and their ranges during four sampling periods (autumn weekdays, autumn weekend, winter weekdays and winter weekend) are listed in Table 1. The average mass concentrations of PM$_{2.5}$ in autumn and winter were 9.4 $\pm$ 2.6 μg·m^{-3} and 7.1 $\pm$ 2.4 μg·m^{-3}, respectively, which are comparable to winter Rozelle (a more highly populated urban Sydney area) PM$_{2.5}$ concentrations (8.1 μg·m^{-3}) in a report (Nelson et al., 2009). Hazard reduction burns which occurred from 22nd May to 30th May 2014 (RFS, 2014) could be a reason for the slightly higher concentrations in autumn. Enhanced extractable organic concentrations in autumn provided some evidence for this occurrence (autumn: 4.3 μg·m^{-3}, winter: 2.9 μg·m^{-3}, $p > 0.01$). Organic constituents range from 40–61% and 12–78% of PM$_{2.5}$ mass during autumn and winter, with average values of 46 $\pm$ 7% and 38 $\pm$ 20%, respectively.

The solvent-extractable organic fraction consisted of 10–80% of the total PM$_{2.5}$ mass, furthermore, there was a very good correlation between the concentration of the solvent-extractable organic fraction and PM$_{2.5}$ concentration (R^2 = 0.8 $p < 0.01$, Appendix B, Supplementary Table S3). The strength of the correlation coefficient between the concentration of solvent-extractable organic fraction and PM$_{2.5}$ concentration suggests that increases in the organic fraction may be a significant contributor to elevated PM$_{2.5}$ concentrations. Nevertheless, the concentrations of solvent-extractable organic fraction during four sampling campaign periods (autumn weekday, autumn weekend, winter weekday and winter weekend) were not significantly different from each other.

Table 2. Concentrations of PM$_{2.5}$, organic fraction, organic tracer compounds (ng/m^3), particulate organic groups and values for meteorological variables (daily averages). Ranges of results are bracketed ( ).

	Autumn (n = 7)		Winter (n = 12)	
	Weekday n = 5	Weekend n = 2	Weekday n = 8	Weekend n = 4
Temperature (℃)	16.4	16.4	12.8	12.9
Wind Speed (m/s)	0.9	0.8	1.2	1.4
Solar radiation (w/m^2)	41.6	39.3	28.3	30.5
PM$_{2.5}$ (μg·m^{-3})	9.0 $\pm$ 3.0	10.6 $\pm$ 0.2	6.8 $\pm$ 2.1	7.7 $\pm$ 3.1
Organic fraction (μg·m^{-3}) [a]	4.2 (3.1-6.2)	4.5 (4.3-4.6)	2.6 (0.6-5.5)	3.4 (0.6-7.4)
Organic fraction/PM$_{2.5}$	0.5 (0.4-0.6)	0.4 (0.4-0.4)	0.4 (0.1-0.8)	0.4 (0.1-0.6)
Organic tracer compounds				

Monosaccharide anhydrides			
Levoglucosan	215.2 (0-402.6)	375.1 (297.7-452.5)	216.5 (0-498.0)	440.6 (269.8-593.5)
Mannosan	1.0 (0-4.8)	n.d.	2.9 (0-10.6)	n.d.
Galactosan	33.5 (0-128.0)	63.2 (0-126.4)	2.9 (0-9.9)	n.d.
Total MAs	249.7 (0-530.6)	438.3 (297.7-578.9)	222.4 (0-498.0)	440.6 (269.8-593.5)

Resin acid			
Dehydroabietic acid	46.2 (0-96.8)	62.0 (50.8-73.1)	9.4 (0-75.5)	82.5 (69.6-100.6)

Methoxyphenol			
Syringic acid	0.0	112.9 (92-133.7)	71.6 (0-165.0)	137.2 (0-263.4)

Fatty acids			
Palmitic acid $C_{16:0}$	369.3 (0-655.4)	n.d.	244.7 (0-510.8)	371.8 (0-557.0)
Stearic acid $C_{18:0}$	11.0 (6.4-13.8)	n.d.	9.0 (4.3-13.5)	15.8 (7.9-28.2)
Oleic acid $C_{18:1}$	1.3 (0-6.6)	n.d.	5.0 (0-22.6)	0.7 (0-2.8)
Total fatty acids	381.6(6.4-675.8)	n.d.	258.7 (4.3-546.9)	388.3 (7.9-588.0)

Dicarboxylic acids			
Succinic acid(C_4)	5.0 (0-10.5)	0.0	0.6 (0-1.7)	0.0
Azelaic acid(C_9)	9.8 (0-17.4)	7.0 (0-14.1)	7.5 (0-11.2)	8.6 (0-12.6)
Phthalic+Terephthalic acid (Ph+tPh)	11.8 (0-40.2)	7.2 (0-14.4)	1.1 (0-5.2)	8.9 (0-20.8)
Total dicarboxylic acid	26.6 (0-68.1)	14.2 (0-28.5)	9.2 (0-18.1)	17.5 (0-33.4)
Total polar compounds	704.1 (25.9-1191.1)	643 (542.6-743.5)	571.4 (42.9-1002.5)	1100.7 (954.8-1239.8)

n.d.: not detected.

[a] : solvent extractable material

Primary Organic tracers

Monosaccharide anhydrides

Australia has relatively high forest coverage, with approximately 123 million hectares of native forest, and this comprises about 16% of Australia's total land area. Given also Australia's often hot and dry climate, controlled and uncontrolled bushfires are frequent events in Australia (Harris et al., 2017; Muir et al., 2017). Bushfires are increasingly being identified as a major contributor to air pollution in a number of Australian cities (Guerin, 2017; Rawluk et al., 2017). Our autumn sampling campaign coincided with the regular period of hazard reduction burns (controlled bushfires) every year in urban Sydney. In addition, the use of wood heaters for residential domestic heating during colder seasons can also be a significant contributor to an increase in the level of air pollutants (Jordan et al., 2006; Reisen et al., 2013).

Table 3. Ratios of anhydrosugars in $PM_{2.5}$ emitted from several sources.

	Levoglucosan/Mannosan	Levoglucosan/(Mannosan + Galactosan)
This study	41.5 ±22.0	18.0 ±15.2
Autumn	26.2	8.3 ±6.9
Winter	44.0 ±28.7	19.1 ±6.1
Hardwood burning[1]	13-24	10-14
Grasses burning [1]	108-202	54-66
Softwood burning [1]	6.7-6.9	2.9-5.0

[1] (Engling et al., 2006)

Monosaccharide anhydrides including levoglucosan, mannosan and galactosan are cellulose and hemicellulose pyrolysis products created by thermal alteration and are detected in large quantities in any emissions resulting from wood burning. As a result, they are widely regarded as unique tracers for wood combustion (Corsini et al., 2017; Singh et al., 2017; Wan et al.). The average concentration of levoglucosan in this study was 271.1 ±170.3 ng/m^3, and this concentration is of the same order of magnitude as that detected in the Sydney Particle Study in autumn 2012 (May), and other periods when fire management burns were occurring (Cope et al., 2013). Compared to studies in Southeast Asia and Central Europe, the levels of monosaccharide anhydrides in our study were somewhat lower but still comparable to the ambient values taken from the literature (Engling et al., 2011; Herich et al., 2014; Rada et al., 2012; Streets et al., 2003). The high concentrations (usually up to thousands ng/m^3) see in these other localities are suggested to be due to the intense use of wood fuel for domestic heating in combination with topography that favours the accumulation of air pollutants in a shallow surface layer (Central Europe-Alpine area cases) or due to the many continuous days of uncontrolled biomass burning (Southeast Asia cases).

Among levoglucosan, mannosan and galactosan, only galactosan revealed significant differences between autumn and winter ($p < 0.01$). Levoglucosan and mannosan showed no differences between the four sampling periods. Concentrations of monosaccharide anhydrides were found ranging from 0 (non-detection, n.d.) to 578.9 ng/m^3 and from n.d. to 593.5 ng/m^3 during the respective autumn and winter periods. Levoglucosan is the most abundant species, followed by galactosan, while mannosan was not observed in all sampling periods, but was only found on the five sampling periods shown in Figure 3.

Different types of wood materials consist of different proportions of structural chemical components, and thus this can result in different levoglucosan/mannosan and levoglucosan/(mannosan + galactosan) ratios when the woody material is combusted. As a result these characteristic ratios, compiled from experiment data, can be used to distinguish combustion sources from different woody materials (Engling et al., 2006).

Wood types normally classified into hardwood such as oak and beech and softwood such as pine and spruce. In Australia, eucalypts are the most common hardwood type (Forrester et al., 2010). Therefore the proportion of soft and hard woods used during combustion can be estimated by the levoglucosan/mannosan ratio and levoglucosan/(mannosan + galactosan) ratios (Schmidl et al., 2008). Combustion of softwoods produces low levoglucosan/mannosan and levoglucosan/(mannosan + galactosan) ratios, while hardwood burning is associated with higher ratios (Iinuma et al., 2007). However, grass burning has much higher levoglucosan/mannosan and levoglucosan/(mannosan + galactosan) ratios, 5-10 times more than hardwood and softwood burning (Engling et al., 2006; Schmidl et al., 2008).

In the present study, the average ratios of levoglucosan to mannosan are 24.2 and 44.0 in autumn and winter, respectively, slightly higher than the experimental hardwood burning data in literature, suggesting that the wood types in autumn and winter were dominated by hardwood burning and grass burning. The levoglucosan/(mannosan + galactosan) and levoglucosan/mannosan ratios in winter were similar to those found in autumn, both being slightly higher than expected for hardwood burning, which confirm that in winter more grass burning was contributed than those in autumn.

Figure 3 shows a temporal series of monosaccharide anhydride concentrations measured during the sampling campaign and indicates that wood smoke was present in most of the sampling periods (16 out of 18). Amongst the three monosaccharide anhydrides measured, levoglucosan was in the highest proportion, varying from 75.9–100.0%, followed by galacosan and mannosan, with the percentages of 0.0–3.8% and 0.0–24.1%, respectively. In winter slightly higher monosaccharide anhydrides concentrations were measured compared with autumn. A large spike in monosaccharide anhydrides concentrations detected at the start of autumn sampling campaign is likely related to the controlled bushfires burn for hazardous reduction carried out at this time. The build-up of monosaccharide anhydrides in winter is probably related to the onset of cooler ambient temperatures and therefore results from higher

wood heater contribution (Cope et al., 2013). Relatively higher galactosan concentration mostly appeared in autumn rather than in winter, whereas mannosan was basically only observed in winter. This could suggest that in autumn and winter there might be combustion of different wood types. In winter, the ratios obtained suggest that wood combustion was mainly from bushfire management burns. In contrast, in winter, residential heating from wood heaters may contribute more to monosaccharide anhydride concentrations. Therefore, this suggests that the two seasons had different proportions of monosaccharide anhydride isomers.
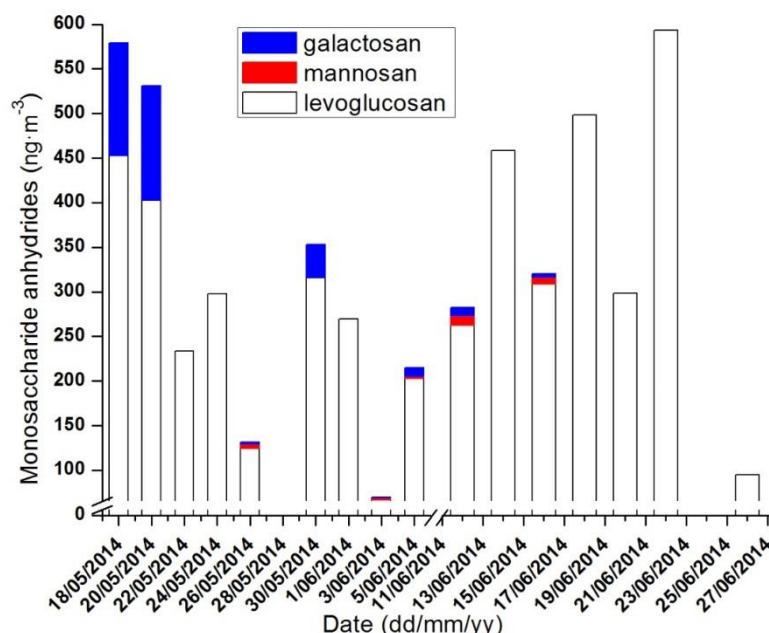
Figure 2. Time series plot of the biomass burning tracers (monosaccharide anhydrides) as observed during the sampling campaign.

Resin acids

Resin acids are produced via a series of biosynthetic reactions of gymnosperms (mainly pine and spruce), and are usually reported in high concentrations particularly in temperate regions (Zheng et al., 2005). There are two types of resin acids, unaltered (pimaric-type acids) and thermal degradation products (abietic-type acids). Therefore, abietic-type acids can be used as wood smoke tracers. In our study, the thermal degradation product, dehydroabietic acid was found in significant concentrations. Moreover, dehydroabietic acid has been proposed as a candidate marker compound for coniferous wood combustion (Oliveira et al., 2007). As the major quantified resin acid in the aerosols, dehydroabietic acid was present in concentrations varying from 50.8 to 100.6 ng/m^3 during the sampling campaign. The minimum concentrations are similar, but the maximum concentrations are slightly lower than those

77

which have been measured in some European cities where wood is used for heating, where concentrations measured ranged from 48 to 440 ng/m^3 (Oliveira et al., 2007). Dehydroabietic acid was not detected in every sampling period; in winter (n = 11), dehydroabietic acid was only found in four samples, three on the weekends and on only one collected during the working week. This suggests the absence of a significant contribution from conifer wood combustion during most of the winter sampling periods. Moreover, statistically significant differences were investigated between autumn weekday samples and winter weekend samples ($p < 0.05 = 0.04$, Table S1). These appear to indicate that there was more softwood burning during autumn. During the autumn sampling campaign, the regular hazard reduction burns which take place every year in the forested areas of Sydney were apparent. It should also be stressed that dehydroabietic acid concentrations had a high correlation with PM$_{2.5}$ concentrations ($R^2 = 0.7$, $p < 0.01$, Appendix B, Supplementary Table S3). This relationship could indicate that the increases in PM$_{2.5}$ concentrations are due to a sizeable contribution from softwood combustion (Leithead et al., 2006). Dehydroabietic acid also showed a relatively good correlation with levoglucosan as well ($R^2 = 0.7$, $p < 0.05$, Appendix B, Supplementary Table S3). Obviously, dehydroabietic acid showed lower concentration levels amongst the biomass burning tracers, mainly in comparison with syringic acid, which emphasises that the burning of softwood particularly wood from conifers was uncommon. This is not surprising given the very different tree and vegetation species in the Sydney region.

Methoxyphenol

Dehydroabietic acid, similarly to syringic acid, also derives from wood combustion and can therefore also be used as a wood burning tracer (Mikuška et al., 2016). Syringic acid is emitted to the atmosphere following pyrolysis of wood lignin (Zangrando et al., 2016b), unlike dehydroabietic acid which is produced by softwood combustion (Fujii et al., 2016). In this study, concentrations of syringic acid fluctuated from 92.0 to 263.4 ng/m^3. The concentration of syringic acid was around a factor of three times those of levoglucosan, and approximately an order of magnitude higher than dehydroabietic acid (Figure 4). Syringic acid concentration in the PM was significantly correlated with levoglucosan ($R^2 = 0.7$, $p < 0.01$, Appendix B, Supplementary Table S3), as well as with stearic acid ($R^2 = 0.6$, $p < 0.01$, Appendix B, Supplementary Table S3), which suggests that syringic acid, levoglucosan and stearic acid may have arisen from the same source, namely, wood burning. Unlike dehydroabietic acid (a typical organic tracer for the burning of conifer trees (softwood)) where occurrences were found mostly in autumn, syringic acid (lignin pyrolysis products)

were found mainly in winter. This suggests that dehydroabietic acid and syringic acid may have originated from combustion of different wood types. This hypothesis is supported by the extremely low correlation between dehydroabietic acid and syringic acid ($R^2 = 0.3$, Appendix B, Supplementary Table S3). In contrast to monosaccharide anhydrides like levoglucosan, syringic acid is the subject of interest in a much smaller number of research papers. The concentration of syringic acid found in our study was approximately 5-10 times higher than that found in PM in the Czech Republic, Portugal and Malaysia (Fujii et al., 2016; Mikuška et al., 2016; Zangrando et al., 2016a). This indicates that the burning of hardwood is an important contributor to the concentration levels of urban $PM_{2.5}$ aerosols in Sydney during the autumn and winter seasons.
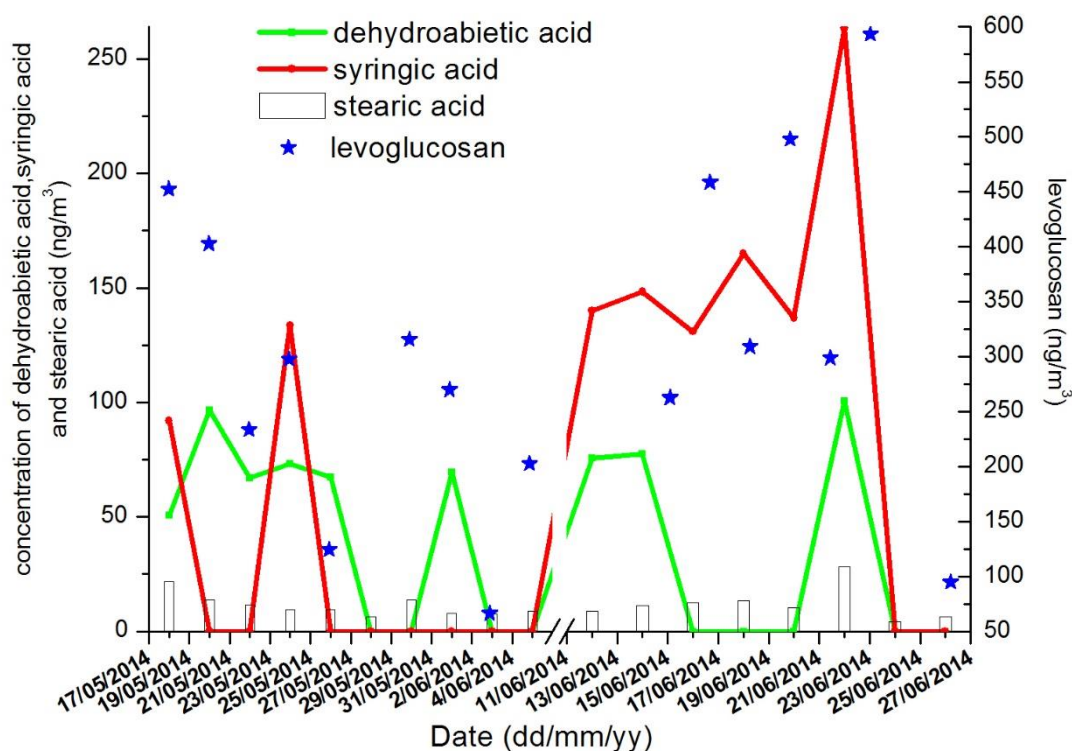
Figure 3. The distribution of the absolute concentrations of different wood burning markers (dehydroabietic acid, syringic acid, stearic acid and levoglucosan) during autumn and winter sampling campaign.

Fatty acids

Fatty acids could significantly contribute to the acidity of rainwater in urban and rural environments (Kourtchev et al., 2008), and therefore have the potential to alter hygroscopic properties of airborne aerosols, and to change the global radiation balance as well as causing

health problems (Guo et al., 2015). In our work palmitic acid was the most abundant fatty acid species detected followed by stearic acid. The concentrations of palmitic acid and stearic acid showed apparent seasonal variations between autumn and winter, and this difference was significant between the two seasons ($p < 0.05$). Palmitic acid has various emission sources (both biogenic and anthropogenic sources) (Deshmukh and Boreddy, 2016; George et al., 2016; Pei et al., 2016; Popovicheva et al., 2016; Urban et al., 2016), and can be emitted directly from vegetation, and also from human activities such as combustion of fossil fuel, biomass and cooking. (Ho et al., 2011; Li et al., 2013). In our study, palmitic acid concentrations appear to be correlated ($R^2 = 0.5$, $p < 0.05$) with traffic tracers (C_{23} n-alkanes).

The extent of aging process of aerosols can be gauged by the ratio between the concentrations of the saturated C_{18} alkanoic acid – stearic acid ($C_{18:0}$) and the mono-unsaturated C_{18} acid – oleic acid ($C_{18:1}$) (Li et al., 2013). Oleic acid ($C_{18:1}$) in the urban ambient air may have numerous sources, such as traffic, cooking and biogenic sources (Eveleigh et al., 2015; Sevimoglu and Rogge, 2015; Yang et al., 2016). As the mono-unsaturated acid is broken down more quickly by free radicals, ozone and other atmospheric oxidants than the saturated homologues, ratios of these corresponding compounds can be used as an aerosol age indicator and to indicate a relative decomposition rate (Katrib et al., 2005; Li et al., 2013). Lower oleic acid ($C_{18:1}$)/stearic acid ($C_{18:0}$) ratios indicate that significant oxidation of oleic acid has occurred resulting in the production of diacids and corresponding compounds (Hoque and Kawamura, 2016). The more aged aerosols often show lower ratios of oleic acid ($C_{18:1}$)/stearic acid ($C_{18:0}$). In the present study, oleic acid ($C_{18:1}$) was not identified in every sample. In autumn, oleic acid ($C_{18:1}$) was only detected in one sample. However, on five out of twelve sampling periods in winter samples were observed to contain oleic acid ($C_{18:1}$). The concentration of oleic acid ($C_{18:1}$) determined ranged from 2.8 to 22.6 ng/m^3. The highest concentration of oleic acid ($C_{18:1}$) was observed for a sample collected on 12 June 2014 under relatively stable atmospheric conditions (solar radiation: 37.7 w/m^2, temperature: 6.9 °C, wind speed: 0.62 m/s). The lack of substantial oleic acid concentrations in the samples might be due to the chemical instability of this unsaturated fatty acid and/or result from rapid oxidation to other compounds in the urban atmosphere (Ho et al., 2015; Hoque and Kawamura, 2016; Saffari et al., 2016). In the present study, ratios of oleic acid/stearic acid were in the range of 0.2-2.1, higher than those determined in Beijing and Hong Kong (Hu et al., 2010; Li et al., 2013), which appears to indicate that aerosols in Sydney were less degraded than those in other urban cities. It should be noted that oleic acid ($C_{18:1}$) had a good correlation with mannosan ($R^2 = 0.6$, $p < 0.05$, Appendix B, Supplementary Table S3), a marker for biomass

burning. Likewise, stearic acid ($C_{18:0}$) was well correlated with levoglucosan and syringic acid, respectively ($R^2 = 0.8$ and 0.6, $p < 0.01$, Appendix B, Supplementary Table S3).

Even though palmitic acid ($C_{16:0}$) and stearic acid ($C_{18:0}$) are not source specific organic compounds, the abundance of stearic acid ($C_{18:0}$) when compared to palmitic acid ($C_{16:0}$) is unique, and thus, can be used to assess source apportionment (Ho et al., 2015). Low ratios determined (< 0.25) in collected $PM_{2.5}$ suggest likely origins from wood smoke, waxy leaf surface abrasions and foliar vegetation combustion; ratios that vary from 0.25 to 0.5 are indicative of traffic exhaust origins (Ho et al., 2010). Stearic acid/palmitic acid ratios in our study had a range from 0.01-0.26, with an average of 0.07, indicating the principal sources are from wood burning and vegetative material is the main source combined with vehicle exhausts.

Secondary organic tracers

Dicarboxylic acids

Succinic acid has been reported to be abundant in emissions from biomass burning as well as involved in photochemical reactions of the combustion products, principally SOA (Li et al., 2015; Yao et al., 2004; Zhao et al., 2014). In our study succinic acid was weakly negatively correlated with several biomass burning markers (levoglucosan: $R^2 = 0.2$; galactosan: $R^2 = 0.1$; syringic acid: $R^2 = 0.4$; stearic acid: $R^2 = 0.2$, Appendix B, Supplementary Table S3), but there was also a moderate to high degree collinearity between succinic acid with other two dicarboxylic acids (azelaic acid: $R^2 = 0.5$ $p < 0.05$; Phthalic+Terephthalic acid: $R^2 = 0.6$, $p < 0.01$, Appendix B, Supplementary Table S3). These relationships suggest that biomass burning SOA is possibly the main source of the observed concentrations of succinic acid. Succinic acid did not appear in every sample, only were found in one third of sampling periods, varying from 1.1 to 10.5 ng/m^3.

Azelaic acid (C_9 dicarboxylic acid) identified as an aged anthropogenic secondary product usually was observed during the daytime (Claeys et al., 2007), and was described as the "urban oxygenated organic compound" due to its frequent observations in urban areas (Alier et al., 2014; Alier et al., 2013). Negative correlation analyses between galactosan (GN) and azelaic acid (C_9 dicarboxylic acid) ($R^2 = 0.6$, $p < 0.01$, Appendix B, Supplementary Table S3) suggests that galactosan (GN) might be oxidized by some atmospheric oxidants, such as OH

radicals, O_3 and NO_X. Azelaic acid (C_9 dicarboxylic acid) was generated via photochemical atmospheric processing (Xingru et al., 2009). Several studies by others have revealed that diluted emissions from biomass burning produce large quantities of SOA (Alier et al., 2014; Alier et al., 2013; Grieshop et al., 2009), these studies have also confirmed that galactosan (GN) could form azelaic acid (C_9 dicarboxylic acid) as a result of atmospheric oxidation processes. In other studies, the presence of azelaic acid was proved to be related to fast oxidation of unsaturated fatty acids (i.e. oleic acid) or biogenic precursors by ozone and other radicals (Ho et al., 2011; Moise and Rudich, 2002; Zhang et al., 2010). Nevertheless, in our study, there is no robust evidence to demonstrate the above conclusions. Azelaic acid (C_9 dicarboxylic acid) had the highest frequency of occurrence among the analyzed dicarboxylic acids,; it was detected almost in every sample (15 occasions; succinic acid C_4: 6 occasions; aromatic dicarboxylic acid: 8 occasions). The concentrations of azelaic acid (C_9 dicarboxylic acid) varied from 7.3 to 17.4 ng/m^3, and were much higher than those investigated in Barcelona (3-6 ng/m^3) (Alier et al., 2013).

Aromatic dicarboxylic acids (DCA) – Phthalic + Terephthalic acid are secondary organic tracers formed by degradation of lower molecular weight PAHs (for example, naphthalenes: Nap). Some volatile PAHs such as naphthalene can take part in photochemical reactions as precursors to generate terephthalic acid, methyl phthalic acid and phthalic acid (Ho et al., 2015). Ho et al. (2015) found that aged anthropogenic secondary organic compounds (SOA aged) appeared to accumulate under stagnant atmospheric conditions. This outcome has corroborated the work by Ding et al. (Ding et al., 2012) who reported that > 75% of SOA stemmed from aromatic precursors during fall and winter in the Pearl River delta, South China, one of the most industrialized and densely populated regions in China. When compared with the winter sampling periods, samples collected in autumn possessed higher phthalic + terephthalic acid concentrations up to 40.2 ng/m^3, which matched the period with highest average solar radiation, a higher temperature and lower wind speed (average solar radiation: 50.6 w/m^2, average temperature: 8.9 ℃, average wind speed: 0.8 m/s). Furthermore, relatively higher correlation coefficients were recorded between phthalic + terephthalic acid and other dicarboxylic acids (C_4 succinic acid and C_9 azelaic acid), both with R^2 values of 0.6 ($p < 0.01$, Appendix B, Supplementary Table S3). Also, some correlation was found between phthalic + terephthalic acid and solar radiation ($R^2 = 0.5$, $p < 0.01$, Appendix B, Supplementary Table S3).
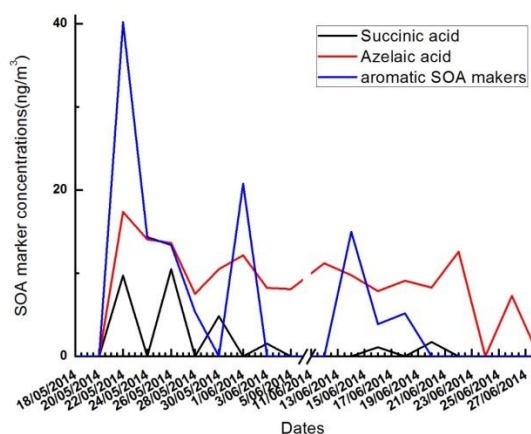
Figure 4. Temporal change in SOA markers across the monitoring periods.

Principal Component Analysis

Table 4 demonstrates the results of principle component analysis (PCA) for all examined organic species in this study. Four groups are categorized, which makes up 80% of all the data variation. The first principle component (PC1) shows predominant constituents of levoglocosan, dehydroabietic acid, syringic acid and stearic acid, which thus is identified as biomass burning. The second principal component (PC2) is characterised by high loadings of dicarboxylic acids, which might be ascribed to the formation of secondary organic aerosols. Mannosan and oleic acid comprise the third principal component (PC3). The specific sources are still unknown according to the current information. The fourth principal component (PC4) is likely to be a mixed source of biomass burning and traffic owing to the domination of mannosan, galactosan, palmitic acid and oleic acid.

Table 4. Rotated component matrix.

	Component			
Organic compounds	PC1	PC2	PC3	PC4
Levoglucosan	0.89	-0.31	-0.16	-0.03
Mannosan	-0.04	-0.14	*0.59*	*0.61*
Galacotsan	0.05	-0.26	-0.78	0.45
Dehydroabietic acid	0.72	0.16	-0.18	0.33
Syringic acid	0.72	-0.49	0.40	-0.17
Palmitic acid	0.16	0.27	-0.44	*0.58*
Stearic acid	0.85	-0.25	-0.14	-0.16
Oleic acid	-0.05	-0.33	*0.58*	*0.60*
Succinic acid	0.09	0.80	0.04	0.12
Azelaic acid	*0.54*	*0.63*	0.46	-0.02

	Biomass burning	Secondary sources	Unknown sources	Biomass burning + traffic
Phthalic + Terephthalic acid	0.30	0.85	0.02	-0.03
Explained Variance%	26.94%	22.21%	17.59%	13.20%
Sources	Biomass burning	Secondary sources	Unknown sources	Biomass burning + traffic

Values higher than 0.7 are highlighted in yellow; values higher than 0.5 and lower than 0.7 in **bold** and in *italics*; values lower than 0.5 in regular font.

Conclusions

The quantification of solvent-extractable and chromatographically identifiable organic compounds in PM$_{2.5}$ samples demonstrated that biomass burning, represented the chief sources of identifiable polar organic aerosol constituents.

Palmitic acid and monosaccharide anhydrides were dominant analysed polar organic compounds during autumn and winter sampling campaign. Dehydroabietic acid and syringic acid had nearly opposite distribution during autumn and winter sampling campaign. Dehydroabietic acid mostly appeared in autumn and was nearly absent in winter. By contrast, syringic acid was detected mostly in winter rather than in autumn. Ratios of monosaccharide anhydrides reveal different contributions of different wood types during the two sampling seasons; in autumn wood combustion consisted of a major contribution from hardwood burning and a minor contribution from softwood burning. In winter hardwood and grass burning were the major contributors. Dicarboxylic acids were formed through photo-chemical processing from anthropogenic precursors. The results of principle component analysis (PCA) elicit four groups, reflecting the contribution of biomass burning, secondary activities and traffic to PM$_{2.5}$. Furthermore, owing to limited samples in this study (< 20), PCA results of polar compounds might be biased. Additional samples could increase reliability of PCA results.

Overall, the polar organic fractions of PM$_{2.5}$ had contributions from biomass burning, vehicular traffic combined with anthropogenic secondary sources during autumn and winter sampling campaign. Identified sources are a crucial aid to developing State and National abatement policy for reducing the levels of population exposure to PM$_{2.5}$.

84

References

Alier, M., Osto, M.D., Lin, Y.-H., Surratt, J., Tauler, R., Grimalt, J., van Drooge, B., 2014. On the origin of water-soluble organic tracer compounds in fine aerosols in two cities: the case of Los Angeles and Barcelona. Environmental Science and Pollution Research 21, 11649-11660.

Alier, M., Van Drooge, B.L., Dall'Osto, M., Querol, X., Grimalt, J.O., Tauler, R., 2013. Source apportionment of submicron organic aerosol at an urban background and a road site in Barcelona (Spain) during SAPUSS. Atmos Chem Phys 13, 10353-10371.

Alves, C., Vicente, A., Pio, C., Kiss, G., Hoffer, A., Decesari, S., Prevôt, A.S., Minguillón, M.C., Querol, X., Hillamo, R., 2012. Organic compounds in aerosols from selected European sites–Biogenic versus anthropogenic sources. Atmospheric Environment 59, 243-255.

Alves, C.A., 2008. Characterisation of solvent extractable organic constituents in atmospheric particulate matter: an overview. Anais da Academia Brasileira de Ciências 80, 21-82.

Bell, M.L., Dominici, F., Ebisu, K., Zeger, S.L., Samet, J.M., 2007. Spatial and temporal variation in PM2. 5 chemical composition in the United States for health effects studies. Environmental health perspectives, 989-995.

Blake, D., Hinwood, A.L., Horwitz, P., 2009. Peat fires and air quality: Volatile organic compounds and particulates. Chemosphere 76, 419-423.

Boldo, E., Medina, S., Le Tertre, A., Hurley, F., Mücke, H.-G., Ballester, F., Aguilera, I., 2006. Apheis: Health impact assessment of long-term exposure to PM2. 5 in 23 European cities. European journal of epidemiology 21, 449-458.

Bond, T.C., Doherty, S.J., Fahey, D., Forster, P., Berntsen, T., DeAngelo, B., Flanner, M., Ghan, S., Kärcher, B., Koch, D., 2013. Bounding the role of black carbon in the climate system: A scientific assessment. Journal of Geophysical Research: Atmospheres 118, 5380-5552.

Cass, G.R., 1998. Organic molecular tracers for particulate air pollution sources. TrAC Trends in Analytical Chemistry 17, 356-366.

Chan, Y., Simpson, R., Mctainsh, G., Vowles, P., Cohen, D., Bailey, G., 1999. Source apportionment of PM 2.5 and PM 10 aerosols in Brisbane (Australia) by receptor modelling. Atmospheric Environment 33, 3251-3268.

Choi, J.H., Ryu, J., Jeon, S., Seo, J., Yang, Y.-H., Pack, S.P., Choung, S., Jang, K.-S., 2017. In-depth compositional analysis of water-soluble and-insoluble organic substances in fine (PM 2.5) airborne particles using ultra-high-resolution 15T FT-ICR MS and GC× GC-TOFMS. Environmental Pollution.

Churches, T., Corbett, S., 1991. Asthma and air pollution in Sydney. New South Wales Public Health Bulletin 2, 72-74.

Claeys, M., Szmigielski, R., Kourtchev, I., Van der Veken, P., Vermeylen, R., Maenhaut, W., Jaoui, M., Kleindienst, T.E., Lewandowski, M., Offenberg, J.H., 2007. Hydroxydicarboxylic acids: markers for secondary organic aerosol from the photooxidation of α-pinene. Environ Sci Technol 41, 1628-1634.

Cope, M., Keywood, M., Emmerson, K., Galbally, I., Boast, K., Chambers, S., Cheng, M., Crumeyrolle, S., Dunne, E., Fedele, R., 2013. Sydney Particle Study-Stage-II. Study undertaken by the Centre for Australian Weather and Climate Research (CAWCR) on behalf of the New South Wales Office of Environment and Heritage.

Corsini, E., Vecchi, R., Marabini, L., Fermo, P., Becagli, S., Bernardoni, V., Caruso, D., Corbella, L., Dell'Acqua, M., Galli, C.L., 2017. The chemical composition of ultrafine particles and associated biological effects at an alpine town impacted by wood burning. Sci Total Environ.

Dawson, J.P., Bloomer, B.J., Winner, D.A., Weaver, C.P., 2014. Understanding the meteorological drivers of US particulate matter concentrations in a changing climate. Bulletin of the American Meteorological Society 95, 521-532.

De Vos, A.J., Reisen, F., Cook, A., Devine, B., Weinstein, P., 2009. Respiratory irritants in Australian bushfire smoke: air toxics sampling in a smoke chamber and during prescribed burns. Archives of environmental contamination and toxicology 56, 380-388.

Deshmukh, D.K., Boreddy, S.K., 2016. Dicarboxylic acids, oxoacids, benzoic acid,[alpha]-dicarbonyls, WSOC, OC, and ions in spring aerosols from Okinawa Island in the western North Pacific Rim: size distributions and formation processes. Atmos Chem Phys 16, 5263.

Ding, X., Wang, X.M., Gao, B., Fu, X.X., He, Q.F., Zhao, X.Y., Yu, J.Z., Zheng, M., 2012. Tracer-based estimation of secondary organic carbon in the Pearl River Delta, south China. Journal of Geophysical Research: Atmospheres (1984–2012) 117.

Dusek, U., Hitzenberger, R., Kasper-Giebl, A., Kistler, M., Meijer, H.A., Szidat, S., Wacker, L., Holzinger, R., Röckmann, T., 2017. Sources and formation mechanisms of carbonaceous aerosol at a regional background site in the Netherlands: insights from a year-long radiocarbon study. Atmos Chem Phys 17, 3233-3251.

Engling, G., Carrico, C.M., Kreidenweis, S.M., Collett, J.L., Day, D.E., Malm, W.C., Lincoln, E., Hao, W.M., Iinuma, Y., Herrmann, H., 2006. Determination of levoglucosan in biomass combustion aerosol by high-performance anion-exchange chromatography with pulsed amperometric detection. Atmospheric Environment 40, 299-311.

Engling, G., ZHANG, Y.N., CHAN, C.Y., SANG, X.F., Lin, M., HO, K.F., LI, Y.S., LIN, C.Y., Lee, J.J., 2011. Characterization and sources of aerosol particles over the southeastern Tibetan Plateau during the Southeast Asia biomass-burning season. Tellus B 63, 117-128.

Eveleigh, A., Ladommatos, N., Hellier, P., Jourdan, A.-L., 2015. An investigation into the conversion of specific carbon atoms in oleic acid and methyl oleate to particulate matter in a diesel engine and tube reactor. Fuel 153, 604-611.

Feng, J., Li, M., Zhang, P., Gong, S., Zhong, M., Wu, M., Zheng, M., Chen, C., Wang, H., Lou, S., 2013. Investigation of the sources and seasonal variations of secondary organic aerosols in PM 2.5 in Shanghai with organic tracers. Atmospheric environment 79, 614-622.

Fine, P.M., Cass, G.R., Simoneit, B.R., 2002. Chemical characterization of fine particle emissions from the fireplace combustion of woods grown in the southern United States. Environ Sci Technol 36, 1442-1451.

Finlay, S.E., Moffat, A., Gazzard, R., Baker, D., Murray, V., 2012. Health impacts of wildfires. PLOS Currents Disasters.

Forrester, D.I., Medhurst, J.L., Wood, M., Beadle, C.L., Valencia, J.C., 2010. Growth and physiological responses to silviculture for producing solid-wood products from Eucalyptus plantations: an Australian perspective. Forest Ecology and Management 259, 1819-1835.

Franklin, M., Koutrakis, P., Schwartz, J., 2008. The role of particle composition on the association between PM2. 5 and mortality. Epidemiology (Cambridge, Mass.) 19, 680.

Franklin, M., Zeka, A., Schwartz, J., 2007. Association between PM2. 5 and all-cause and specific-cause mortality in 27 US communities. Journal of Exposure Science and Environmental Epidemiology 17, 279-287.

Fujii, Y., Mahmud, M., Oda, M., Tohno, S., Matsumoto, J., Mizohata, A., 2016. A key indicator of transboundary particulate matter pollution derived from Indonesian peatland fires in Malaysia. Aerosol and Air Quality Research 16, 69-78.

Fuzzi, S., Baltensperger, U., Carslaw, K., Decesari, S., Denier Van Der Gon, H., Facchini, M., Fowler, D., Koren, I., Langford, B., Lohmann, U., 2015. Particulate matter, air quality and climate: lessons learned and future needs. Atmos Chem Phys 15, 8217-8299.

George, I.J., Black, R.R., Geron, C.D., Aurell, J., Hays, M.D., Preston, W.T., Gullett, B.K., 2016. Volatile and semivolatile organic compounds in laboratory peat fire emissions. Atmospheric Environment 132, 163-170.

Grieshop, A., Donahue, N., Robinson, A., 2009. Laboratory investigation of photochemical oxidation of organic aerosol from wood fires 2: analysis of aerosol mass spectrometer data. Atmos Chem Phys 9, 2227-2240.

Guerin, T., 2017. A case study identifying and mitigating the environmental and community impacts from construction of a utility-scale solar photovoltaic power plant in eastern Australia. Solar Energy 146, 94-104.

Guo, H., Zhou, J., Wang, L., Zhou, Y., Yuan, J., Zhao, R., 2015. Seasonal variations and sources of carboxylic acids in PM2. 5 in Wuhan, China. Aerosol Air Qual. Res 15, 517-528.

Harris, S., Mills, G., Brown, T., 2017. Variability and drivers of extreme fire weather in fire-prone areas of south-eastern Australia. International Journal of Wildland Fire 26, 177-190.

Herich, H., Gianini, M., Piot, C., Močnik, G., Jaffrezo, J.-L., Besombes, J.-L., Prévôt, A., Hueglin, C., 2014. Overview of the impact of wood burning emissions on carbonaceous aerosols and PM in large parts of the Alpine region. Atmospheric Environment 89, 64-75.

Ho, K., Ho, S., Lee, S., Kawamura, K., Zou, S., Cao, J., Xu, H., 2011. Summer and winter variations of dicarboxylic acids, fatty acids and benzoic acid in PM 2.5 in Pearl Delta River Region, China. Atmospheric chemistry and physics 11, 2197-2208.

Ho, K., Huang, R.-J., Kawamura, K., Tachibana, E., Lee, S., Ho, S., Zhu, T., Tian, L., 2015. Dicarboxylic acids, ketocarboxylic acids, α-dicarbonyls, fatty acids and benzoic acid in PM 2.5 aerosol collected during CAREBeijing-2007: an effect of traffic restriction on air quality. Atmos Chem Phys 15, 3111-3123.

Ho, K., Lee, S., Ho, S.S.H., Kawamura, K., Tachibana, E., Cheng, Y., Zhu, T., 2010. Dicarboxylic acids, ketocarboxylic acids, α-dicarbonyls, fatty acids, and benzoic acid in urban aerosols collected during the 2006 Campaign of Air Quality Research in Beijing (CAREBeijing-2006). Journal of geophysical research: atmospheres 115.

Hoque, M.M., Kawamura, K., 2016. Longitudinal distributions of dicarboxylic acids, ω-oxoacids, pyruvic acid, α-dicarbonyls, and fatty acids in the marine aerosols from the central Pacific including equatorial upwelling. Global Biogeochemical Cycles 30, 534-548.

Hu, D., Bian, Q., Lau, A.K., Yu, J.Z., 2010. Source apportioning of primary and secondary organic carbon in summer PM2. 5 in Hong Kong using positive matrix factorization of secondary and primary organic tracer data. Journal of Geophysical Research: Atmospheres 115.

Huang, R.-J., Zhang, Y., Bozzetti, C., Ho, K.-F., Cao, J.-J., Han, Y., Daellenbach, K.R., Slowik, J.G., Platt, S.M., Canonaco, F., 2014. High secondary aerosol contribution to particulate pollution during haze events in China. Nature 514, 218-222.

Iinuma, Y., Brüggemann, E., Gnauk, T., Müller, K., Andreae, M., Helas, G., Parmar, R., Herrmann, H., 2007. Source characterization of biomass burning particles: The combustion of selected European conifers, African hardwood, savanna grass, and German and Indonesian peat. Journal of Geophysical Research: Atmospheres 112.

Iinuma, Y., Keywood, M., Gnauk, T., Herrmann, H., 2008. Diaterebic acid acetate and diaterpenylic acid acetate: atmospheric tracers for secondary organic aerosol formation from 1, 8-cineole oxidation. Environmental science & technology 43, 280-285.

Iinuma, Y., Keywood, M., Herrmann, H., 2016. Characterization of primary and secondary organic aerosols in Melbourne airshed: The influence of biogenic emissions, wood smoke and bushfires. Atmospheric Environment 130, 54-63.

Jaeckels, J.M., Bae, M.-S., Schauer, J.J., 2007. Positive matrix factorization (PMF) analysis of molecular marker measurements to quantify the sources of organic aerosols. Environmental Science & Technology 41, 5763-5769.

Jalaludin, B., Morgan, G., Lincoln, D., Sheppeard, V., Simpson, R., Corbett, S., 2006. Associations between ambient air pollution and daily emergency department attendances for cardiovascular disease in the elderly (65+ years), Sydney, Australia. Journal of Exposure Science and Environmental Epidemiology 16, 225-237.

Jordan, T.B., Seen, A.J., Jacobsen, G.E., 2006. Levoglucosan as an atmospheric tracer for woodsmoke. Atmospheric Environment 40, 5316-5321.

Kampa, M., Castanas, E., 2008. Human health effects of air pollution. Environmental pollution 151, 362-367.

Katrib, Y., Biskos, G., Buseck, P., Davidovits, P., Jayne, J., Mochida, M., Wise, M., Worsnop, D., Martin, S., 2005. Ozonolysis of mixed oleic-acid/stearic-acid particles: Reaction kinetics and chemical morphology. The Journal of Physical Chemistry A 109, 10910-10919.

Keywood, M., Guyes, H., Selleck, P., Gillett, R., 2011. Quantification of secondary organic aerosol in an Australian urban location. Environmental Chemistry 8, 115-126.

Keywood, M., Kanakidou, M., Stohl, A., Dentener, F., Grassi, G., Meyer, C., Torseth, K., Edwards, D., Thompson, A.M., Lohmann, U., 2013. Fire in the air: Biomass burning impacts in a changing climate. Critical Reviews in Environmental Science and Technology 43, 40-83.

Khan, M.B., Masiol, M., Formenton, G., Di Gilio, A., de Gennaro, G., Agostinelli, C., Pavoni, B., 2016. Carbonaceous PM 2.5 and secondary organic aerosol across the Veneto region (NE Italy). Sci Total Environ 542, 172-181.

Kourtchev, I., Warnke, J., Maenhaut, W., Hoffmann, T., Claeys, M., 2008. Polar organic marker compounds in PM2. 5 aerosol from a mixed forest site in western Germany. Chemosphere 73, 1308-1314.

Krivácsy, Z., Blazsó, M., Shooter, D., 2006. Primary organic pollutants in New Zealand urban aerosol in winter during high PM 10 episodes. Environmental Pollution 139, 195-205.

Leithead, A., Li, S.-M., Hoff, R., Cheng, Y., Brook, J., 2006. Levoglucosan and dehydroabietic acid: evidence of biomass burning impact on aerosols in the Lower Fraser Valley. Atmospheric Environment 40, 2721-2734.

Lewandowski, M., Jaoui, M., Offenberg, J.H., Kleindienst, T.E., Edney, E.O., Sheesley, R.J., Schauer, J.J., 2008. Primary and secondary contributions to ambient PM in the midwestern United States. Environ Sci Technol 42, 3303-3309.

Li, X.-d., Yang, Z., Fu, P., Yu, J., Lang, Y.-c., Liu, D., Ono, K., Kawamura, K., 2015. High abundances of dicarboxylic acids, oxocarboxylic acids, and α-dicarbonyls in fine aerosols (PM2. 5) in Chengdu, China during wintertime haze pollution. Environmental science and pollution research 22, 12902-12918.

Li, X., Wang, Y., Guo, X., Wang, Y., 2013. Seasonal variation and source apportionment of organic and inorganic compounds in PM2. 5 and PM10 particulates in Beijing, China. Journal of Environmental Sciences 25, 741-750.

Lin, L., Lee, M.L., Eatough, D.J., 2010. Review of recent advances in detection of organic markers in fine particulate matter and their use for source apportionment. Journal of the Air & Waste Management Association 60, 3-25.

Maleknia, S.D., Bell, T.L., Adams, M.A., 2009. Eucalypt smoke and wildfires: Temperature dependent emissions of biogenic volatile organic compounds. International Journal of Mass Spectrometry 279, 126-133.

Mar, T.F., Ito, K., Koenig, J.Q., Larson, T.V., Eatough, D.J., Henry, R.C., Kim, E., Laden, F., Lall, R., Neas, L., 2006. PM source apportionment and health effects. 3. Investigation of inter-method variations in associations between estimated source contributions of PM2. 5 and daily mortality in Phoenix, AZ. Journal of Exposure Science and Environmental Epidemiology 16, 311-320.

Masalaite, A., Holzinger, R., Remeikis, V., Röckmann, T., Dusek, U., 2017. Characteristics, sources and evolution of fine aerosol (PM 1) at urban, coastal and forest background sites in Lithuania. Atmospheric Environment 148, 62-76.

Medeiros, P.M., Simoneit, B.R., 2008. Source profiles of organic compounds emitted upon combustion of green vegetation from temperate climate forests. Environ Sci Technol 42, 8310-8316.

Meena, R.K., Satsangi, A., Lakhani, A., Kumari, K.M., 2017. Carbonaceous aerosols at an urban residential site in Agra. Indian Journal of Radio & Space Physics (IJRSP) 43, 156-162.

Meng, Q.Y., Turpin, B.J., Korn, L., Weisel, C.P., Morandi, M., Colome, S., Zhang, J., Stock, T., Spektor, D., Winer, A., 2005. Influence of ambient (outdoor) sources on residential indoor

and personal PM2. 5 concentrations: analyses of RIOPA data. Journal of Exposure Science and Environmental Epidemiology 15, 17-28.

Mikuška, P., Kubátková, N., Křůmal, K., Večeřa, Z., 2016. Seasonal variability of monosaccharide anhydrides, resin acids, methoxyphenols and saccharides in PM2. 5 in Brno, the Czech Republic. Atmospheric Pollution Research.

Miranda, A.I., Martins, V., Cascão, P., Amorim, J.H., Valente, J., Borrego, C., Ferreira, A.J., Cordeiro, C.R., Viegas, D.X., Ottmar, R., 2012. Wildland smoke exposure values and exhaled breath indicators in firefighters. Journal of Toxicology and Environmental Health, Part A 75, 831-843.

Moise, T., Rudich, Y., 2002. Reactive uptake of ozone by aerosol-associated unsaturated fatty acids: kinetics, mechanism, and products. The Journal of Physical Chemistry A 106, 6469-6476.

Morawska, L., Zhang, J.J., 2002. Combustion sources of particles. 1. Health relevance and source signatures. Chemosphere 49, 1045-1058.

Muir, C., Gilbert, J., O'Hara, R., Day, L., Newstead, S., 2017. Physical bushfire preparation over time in Victoria, Australia. Disaster Prevention and Management: An International Journal 26.

Ng, N.L., Kroll, J.H., Keywood, M.D., Bahreini, R., Varutbangkul, V., Flagan, R.C., Seinfeld, J.H., Lee, A., Goldstein, A.H., 2006. Contribution of first-versus second-generation products to secondary organic aerosols formed in the oxidation of biogenic hydrocarbons. Environ Sci Technol 40, 2283-2297.

Nirmalkar, J., Deb, M.K., Deshmukh, D.K., Tsai, Y.I., Verma, S.K., 2015. Molecular markers in ambient aerosol in the Mahanadi Riverside Basin of eastern central India during winter. Environmental Science and Pollution Research 22, 1220-1231.

NSW RFS, 2014. NSW Rural Fire Service: More than 100 hazard reduction burns planned for this week, https://www.rfs.nsw.gov.au/news-and-media/media-releases/more-than-100-hazard-reduction-burns-planned-for-this-week.

Oliveira, T.S., Pio, C., Alves, C.A., Silvestre, A.J., Evtyugina, M., Afonso, J., Fialho, P., Legrand, M., Puxbaum, H., Gelencsér, A., 2007. Seasonal variation of particulate lipophilic organic compounds at nonurban sites in Europe. Journal of Geophysical Research: Atmospheres 112.

Pant, P., Shi, Z., Pope, F.D., Harrison, R.M., 2017. Characterization of Traffic-Related Particulate MatterEmissions in a Road Tunnel in Birmingham, UK: Trace Metals and Organic Molecular Markers. Aerosol and Air Quality Research 17, 117-130.

Park, S.S., Son, S.-C., 2017. Relationship between carbonaceous components and aerosol light absorption during winter at an urban site of Gwangju, Korea. Atmos Res 185, 73-83.

Pei, B., Cui, H., Liu, H., Yan, N., 2016. Chemical characteristics of fine particulate matter emitted from commercial cooking. Frontiers of Environmental Science & Engineering 10, 559-568.

Peter F Nelson, A.G., Upma Dutt, Ludovic Bernaudat, Anthony L Morrison and Ian Jamie, 2009. Sources of the Organic Fraction of Atmospheric Fine Particles, Final Report Environmental Research Trust 2005/RD/0042, p. 87.

Popovicheva, O.B., Engling, G., Diapouli, E., Saraga, D., Persiantseva, N.M., Timofeev, M.A., Kireeva, E.D., Shonija, N.K., Chen, S.-H., Nguyen, D.L., 2016. Impact of smoke intensity on size-resolved aerosol composition and microstructure during the biomass burning season in Northwest Vietnam. Aerosol Air Qual. Res 16, 2635-2654.

Rada, E.C., Ragazzi, M., Malloci, E., 2012. Role of levoglucosan as a tracer of wood combustion in an alpine region. Environmental technology 33, 989-994.

Rawluk, A., Ford, R.M., Neolaka, F.L., Williams, K.J., 2017. Public values for integration in natural disaster management and planning: a case study from Victoria, Australia. Journal of environmental management 185, 11-20.

Reisen, F., Meyer, C.M., Keywood, M.D., 2013. Impact of biomass burning sources on seasonal aerosol air quality. Atmospheric Environment 67, 437-447.

Robinson, A.L., Subramanian, R., Donahue, N.M., Bernardo-Bricker, A., Rogge, W.F., 2006. Source apportionment of molecular markers and organic aerosol. 2. Biomass smoke. Environ Sci Technol 40, 7811-7819.

Rotstayn, L.D., Keywood, M.D., Forgan, B.W., Gabric, A.J., Galbally, I.E., Gras, J.L., Luhar, A.K., McTainsh, G.H., Mitchell, R.M., Young, S.A., 2009. Possible impacts of anthropogenic and natural aerosols on Australian climate: a review. International Journal of Climatology 29, 461-479.

Saffari, A., Hasheminassab, S., Shafer, M.M., Schauer, J.J., Chatila, T.A., Sioutas, C., 2016. Nighttime aqueous-phase secondary organic aerosols in Los Angeles and its implication for fine particulate matter composition and oxidative potential. Atmospheric Environment 133, 112-122.

Schauer, J.J., Rogge, W.F., Hildemann, L.M., Mazurek, M.A., Cass, G.R., Simoneit, B.R., 1996. Source apportionment of airborne particulate matter using organic compounds as tracers. Atmospheric Environment 30, 3837-3855.

Schmidl, C., Bauer, H., Dattler, A., Hitzenberger, R., Weissenboeck, G., Marr, I.L., Puxbaum, H., 2008. Chemical characterisation of particle emissions from burning leaves. Atmospheric Environment 42, 9070-9079.

Sevimoglu, O., Rogge, W.F., 2015. Organic compound concentrations of size-segregated PM10 during sugarcane burning and growing seasons at a rural and an urban site in Florida, USA. Aerosol Air Qual. Res 15, 1720-1736.

Simoneit, B.R., 2002. Biomass burning—a review of organic tracers for smoke from incomplete combustion. Applied Geochemistry 17, 129-162.

Simoneit, B.T., 1999. A review of biomarker compounds as source indicators and tracers for air pollution. Environmental Science and Pollution Research 6, 159-169.

Singh, N., Mhawish, A., Deboudt, K., Singh, R., Banerjee, T., 2017. Organic aerosols over Indo-Gangetic Plain: Sources, distributions and climatic implications. Atmospheric Environment.

Stone, E.A., Zhou, J., Snyder, D.C., Rutter, A.P., Mieritz, M., Schauer, J.J., 2009. A comparison of summertime secondary organic aerosol source contributions at contrasting urban locations. Environ Sci Technol 43, 3448-3454.

Streets, D., Yarber, K., Woo, J.H., Carmichael, G., 2003. Biomass burning in Asia: Annual and seasonal estimates and atmospheric emissions. Global Biogeochemical Cycles 17.

Turpin, B.J., Lim, H.-J., 2001. Species contributions to PM2. 5 mass concentrations: Revisiting common assumptions for estimating organic mass. Aerosol Science & Technology 35, 602-610.

U.S.EPA, 1999. Compendium of Methods for the Determination of Toxic Organic Compounds in Ambient Air, in: Agency, U.S.E.P. (Ed.), Second Edition ed.

Urban, R., Alves, C., Allen, A., Cardoso, A., Campos, M., 2016. Organic aerosols in a Brazilian agro-industrial area: Speciation and impact of biomass burning. Atmos Res 169, 271-279.

Van Donkelaar, A., Martin, R.V., Brauer, M., Kahn, R., Levy, R., Verduzco, C., Villeneuve, P.J., 2010. Global estimates of ambient fine particulate matter concentrations from satellite-based aerosol optical depth: development and application. Environmental health perspectives 118, 847.

Wan, X., Kang, S., Li, Q., Rupakheti, D., Zhang, Q., Guo, J., Chen, P., Tripathee, L., Rupakheti, M., Panday, A.K., Organic molecular tracers in the atmospheric aerosols from Lumbini, Nepal, in the northern Indo-Gangetic Plain: Influence of biomass burning.

Wang, Y., Hopke, P.K., Xia, X., Rattigan, O.V., Chalupa, D.C., Utell, M.J., 2012. Source apportionment of airborne particulate matter using inorganic and organic species as tracers. Atmospheric Environment 55, 525-532.

Xiang, P., Zhou, X., Duan, J., Tan, J., He, K., Yuan, C., Ma, Y., Zhang, Y., 2017. Chemical characteristics of water-soluble organic compounds (WSOC) in PM 2.5 in Beijing, China: 2011–2012. Atmos Res 183, 104-112.

Xingru, L., Xueqing, G., Xinran, L., Chenshu, L., Zhang, S., Yuesi, W., 2009. Distribution and sources of solvent extractable organic compounds in PM2. 5 during 2007 Chinese Spring Festival in Beijing. Journal of Environmental Sciences 21, 142-149.

Yang, F., Kawamura, K., Chen, J., Ho, K., Lee, S., Gao, Y., Cui, L., Wang, T., Fu, P., 2016. Anthropogenic and biogenic organic compounds in summertime fine aerosols (PM 2.5) in Beijing, China. Atmospheric Environment 124, 166-175.

Yao, X., Chan, C.K., Fang, M., Cadle, S., Chan, T., Mulawa, P., He, K., Ye, B., 2002. The water-soluble ionic composition of PM2. 5 in Shanghai and Beijing, China. Atmospheric Environment 36, 4223-4234.

Yao, X., Fang, M., Chan, C.K., Ho, K., Lee, S., 2004. Characterization of dicarboxylic acids in PM2. 5 in Hong Kong. Atmospheric Environment 38, 963-970.

Zangrando, R., Barbaro, E., Kirchgeorg, T., Vecchiato, M., Scalabrin, E., Radaelli, M., Đorđević, D., Barbante, C., Gambaro, A., 2016a. Five primary sources of organic aerosols in the urban atmosphere of Belgrade (Serbia). Sci Total Environ 571, 1441-1453.

Zangrando, R., Barbaro, E., Vecchiato, M., Kehrwald, N.M., Barbante, C., Gambaro, A., 2016b. Levoglucosan and phenols in Antarctic marine, coastal and plateau aerosols. Sci Total Environ 544, 606-616.

Zhang, Q., Jimenez, J., Canagaratna, M., Allan, J., Coe, H., Ulbrich, I., Alfarra, M., Takami, A., Middlebrook, A., Sun, Y., 2007. Ubiquity and dominance of oxygenated species in organic aerosols in anthropogenically-influenced Northern Hemisphere midlatitudes. Geophysical Research Letters 34.

Zhang, Y., Müller, L., Winterhalter, R., Moortgat, G., Hoffmann, T., Pöschl, U., 2010. Seasonal cycle and temperature dependence of pinene oxidation products, dicarboxylic acids and nitrophenols in fine and coarse air particulate matter. Atmos Chem Phys 10, 7859-7873.

Zhao, X., Wang, X., Ding, X., He, Q., Zhang, Z., Liu, T., Fu, X., Gao, B., Wang, Y., Zhang, Y., 2014. Compositions and sources of organic acids in fine particles (PM2. 5) over the Pearl River Delta region, south China. Journal of Environmental Sciences 26, 110-121.

Zheng, M., Salmon, L.G., Schauer, J.J., Zeng, L., Kiang, C., Zhang, Y., Cass, G.R., 2005. Seasonal trends in PM2. 5 source contributions in Beijing, China. Atmospheric Environment 39, 3967-3976.

Zhou, S., Collier, S., Jaffe, D.A., Briggs, N.L., Hee, J., Sedlacek III, A.J., Kleinman, L., Onasch, T.B., Zhang, Q., 2017. Regional influence of wildfires on aerosol chemistry in the western US and insights into atmospheric aging of biomass burning organic aerosol. Atmos Chem Phys 17, 2477-2493.

CHAPTER 4

Paper three

Application of radiocarbon analysis to source apportionment of carbonaceous $PM_{2.5}$ in urban Sydney：Insights from different seasonal biomass burning triggered haze events

Meng, C., Nelson, P.F.

Draft for submission to Environmental Science and Technology

This paper fills a gap in our knowledge on the contribution of fossil and non-fossil sources to various carbon fractions in Australian urban ambient $PM_{2.5}$ samples. This study presents bulk carbon data and radiocarbon data on various carbonaceous fractions of contrasting fine particulate samples, which are used to determine the proportions of fossil and non-fossil carbon and their contributions from primary emissions and secondary atmospheric formation processes.

Application of radiocarbon analysis to source apportionment of carbonaceous $PM_{2.5}$ in urban Sydney：Insights from different seasonal biomass burning triggered haze events

Chuanping Meng [a,*], Peter F. Nelson [a, b]

[a] Department of Environmental Sciences, Faculty of Science and Engineering, Macquarie University, North Ryde, Sydney, New South Wales, 2109, Australia
[b] Macquarie University Centre for Energy and Environmental Contaminants, Macquarie University, North Ryde, Sydney, New South Wales, Australia

[*] Corresponding author e-mail: Chuanping.meng@students.mq.edu.au

ABSTRACT

Four sets of $PM_{2.5}$ samples were collected simultaneously during winter and summer seasons at two urban sites in Sydney. The samples were collected during periods of winter and summer haze, and on winter weekends and summer sunny days at sampling sites at Macquarie University (MQ) and Rozelle, a harbor side suburb near the central business district. In the study, radiocarbon (^{14}C) measurements were made in total carbon (TC), water-insoluble total carbon (WINTC) and elemental carbon (EC) fractions of the $PM_{2.5}$ particulates in order to investigate spatial and seasonal variations, and the influence of special events. Bulk carbon concentrations (OC, EC, WINSOC and wEC) were obtained using the IMPROVE-A protocol with a thermal optical (TO) instrument which corrects for charring analysis during analysis. According to the carbon mass and radiocarbon mass balances, all of the contemporary carbon for each sub fraction was quantified. A refined EC tracer method was used to estimate the secondary organic carbon by estimating hourly primary OC/EC ratio ((OC/EC)pri).

The Australian 24h standard for $PM_{2.5}$ of 25 $\mu g \cdot m^{-3}$ was exceeded during the period of winter haze sampling (2015/08/20-2015/08/22) at Rozelle and summer haze sampling (2015/12/19-2015/12/21) at MQ, averaging 28.1 $\mu g \cdot m^{-3}$ and 34.9 $\mu g \cdot m^{-3}$, respectively. The average abundances of secondary organic aerosol (SOA) and primary carbonaceous aerosol (PCA) were 2.3 $\mu g \cdot m^{-3}$ and 8.9 $\mu g \cdot m^{-3}$, respectively for the Rozelle and MQ sites, accounting for 11% and 42% of the $PM_{2.5}$ mass. Higher proportions of POC_{nf} (POC_{nf}: non-fossil sources in primary organic carbon (POC)) and $EC_{biomass}$ ($EC_{biomass}$: biomass burning sources in EC) were determined in winter samples, amounting to 60% and 11% compared with 50% and 4% in the

summer samples. Although firm conclusions are limited by the small number of samples, the results suggest that biofuel combustion mainly wood burning for household heating in the cooler months makes a major contribution to total carbon in the collected particulates.

Keywords: PM$_{2.5}$, polar organic compounds, emission sources, urban area

Introduction

Increasing attention has been placed on population exposure to PM$_{2.5}$ (particulate matter with an aerodynamic diameter < 2.5µm), because of potential effects on human health. Many previous studies have examined the effect of exposure toparticulate matter on the mortality or morbidity of urban populations (Atkinson et al., 2014; Lelieveld et al., 2015; Lippmann et al., 2000; Pozzi et al., 2003; Putaud et al., 2004).

Carbonaceous aerosol is one of the most abundant components (20–80%) of atmospheric fine particulates (PM$_{2.5}$), and it has been suggested that this component is responsible for most of the adverse impacts on human health caused by particles (Carmichael et al., 2009; Highwood and Kinnersley, 2006; Kim et al., 2015; Mauderly and Chow, 2008). Some organic compounds are respiratory irritants (such as carbonyls and acids), others are known carcinogens (such as polycyclic aromatic hydrocarbons), and toxins (such as nicotine) (Bell et al., 2007; Kampa and Castanas, 2008; Nel, 2005). EC is known to induce respiratory and cardiovascular problems and may be coated with these toxic and carcinogenic organic species which may then be absorbed into lung tissue and further increase the potential risk for human health (Hong et al., 2002; Pöschl, 2005; Tie and Cao, 2009).

As well as these health consequences carbonaceous aerosols can substantially influence the environment and climate by the scattering and absorption of solar radiation and indirectly through their role as cloud condensation nuclei (Carmichael et al., 2009; Chung and Seinfeld, 2002; Ramanathan and Carmichael, 2008; Ramanathan et al., 2001; Venkataraman et al., 2005). Conventionally, carbonaceous aerosol is categorized as organic carbon (OC) and elemental carbon (EC). OC and EC are the principal short-lived climate forcers. Optically, OC generally triggers a cooling effect by reflecting incoming sunlight; conversely, EC shows an overall warming effect by either absorbing incoming solar radiation in the atmosphere or by reducing the albedo of the Earth's surface (Kaufman et al., 2002).

Most of the carbonaceous $PM_{2.5}$ is derived from combustion processes from a variety of sources, including transport, electricity generation, domestic wood combustion and also from atmospheric oxidation processes which convert gases (such as SO_2 and NO_x) and VOCs to $PM_{2.5}$. Therefore, in considering OC it is important to understand that it can be separated into primary organic carbon (POC, originated from primary emissions) and secondary organic carbon (SOC, formed from gaseous precursors by atmospheric reaction or oligomerization). EC enters the atmosphere exclusively as a primary emission resulting from pyrolysis during incomplete combustion, e.g. due to traffic, industrial incineration, or biomass burning.

Chemically, OC comprises a large group of individual chemical components from light weight polar compounds to heavy weight refractory condensed non-polar materials. It is therefore possible to separate OC into sub-groupings of water soluble organic carbon (WSOC) and water insoluble organic carbon (WINSOC). EC can also be subdivided into char (non-refractory) and soot (refractory). WINSOC better represents POC, whereas WSOC is a major portion of fresh SOC, resulting from biomass burning OC and/or ageing of OC (Krivacsy et al., 2001; Saarikoski et al., 2008; Wozniak et al., 2012a).

Due to the distinctive differences in radio-isotopic signature between fossil and contemporary carbon (contemporary carbon contains a known ^{14}C content, whereas fossil carbon is ^{14}C-free), radiocarbon (^{14}C) analysis is a powerful technique to unambiguously differentiate fossil and contemporary sources of carbonaceous aerosol. The differences of the ^{14}C content of total C in fossil and contemporary materials is independent of individual emission conditions or subsequent chemical transformations in the atmosphere. As OC and EC typically originate from diverse sources with different fossil/non-fossil fractions, ^{14}C measurements of OC and EC as well as some other sub-fractions such as WSOC and WINSOC provide significant information for the apportionment of their sources beyond the ^{14}C analysis of TC alone.

Previous research using radiocarbon-derived source apportionment of carbonaceous $PM_{2.5}$ for elemental and organic carbon has been carried out in China (Liu et al., 2013; Zhang et al., 2014; Zhang et al., 2010; Zhang et al., 2015b), Europe (Bernardoni et al., 2013; Heal, 2014; Heal et al., 2011; Mouteva et al., 2015; Szidat et al., 2007; Szidat et al., 2009; Zhang et al., 2012; Zotter et al., 2014a), the United States (Piletic et al., 2013; Wozniak et al., 2012b) and South Asia (Kirillova et al., 2013), but no detailed studies have been reported in Australia.

However it appears that to allow the natural/anthropogenic and primary/secondary contributions of particulates to be evaluated, radiocarbon measurements by themselves on OC/EC are insufficient. Further radiocarbon analysis on each sub carbonaceous fractions will provide significant additional information. Kirillova, Zhang and Zotter et al. have implemented ^{14}C analysis on the water soluble and water insoluble fraction of OC (Kirillova et al., 2013; Zhang et al., 2015a; Zotter et al., 2014b); however, studies of the detailed and comprehensive ^{14}C based source apportionment of urban atmospheric carbonaceous aerosols are still scarce.

There are challenges in the determination of OC and EC since currently there is no normalized standard for OC/EC separation. The measurements reported here can enhance our understanding of the sources of this important sub-fraction of particulate matter (PM) in a large urban metropolis.

The formation and increase of carbonaceous aerosols in Sydney can be ascribed to several factors; principally these are primary anthropogenic emissions such as wood burning for domestic heating, hazard reduction burning of biomass, motor vehicle exhaust and pollutants from power stations and industry. Atmospheric oxidation by ozone (O_3) and other oxidants increases SOA concentrations while stable meteorological condition (low wind speed, high relative humidity (70–90%) and the presence of a low atmospheric boundary layer result in increased concentrations of carbonaceous aerosols (Cohen et al., 2011; Cope et al., 2014; Greaves et al., 2008; Gupta et al., 2007; Knibbs and de Dear, 2010).

The objectives of this study were to: (1) directly measure and quantify radiocarbon (^{14}C) content of each carbon fraction; (2) calculate (OC/EC)pri in Sydney to estimate primary and secondary sources using a refined EC tracer method; (3) Quantify contributions of fossil and non-fossil sources to primary and secondary carbon in carbonaceous $PM_{2.5}$ samples to examine and discuss the seasonality and spatial variation of different $PM_{2.5}$ samples (4) reveal how haze events and other conditions (i.e. strong solar radiation circumstances) influence and elevate ambient carbon particulate matter concentrations.

Such investigation adds to a sparse database of ^{14}C measurements of combustion-derived atmospheric particles in the Southern Hemisphere for this region. Some tentative conclusions are also possible for the differences between winter and summer and haze situations, although the small number of samples mean that these concusions should be treated with caution.

Materials and Methods

Aerosol sampling

Concurrent samples were collected at a central urban site (Rozelle EPA site) and a sub-urban site (Automatic Weather Station: Macquarie University) in the Sydney metropolitan area, using two high volume aerosols samplers (Ecotech HiVol 3000, Melbourne) with $PM_{2.5}$ inlets and operated at a flow of 67.3 m^3/h. Eight $PM_{2.5}$ samples were collected in 2015 winter (august) and summer (november and december) months for 48h on "8×10" quartz fibre filters (QM-A, 8×10, Whatman). Fine particle samples were collected during each season in order to investigate seasonal variation.
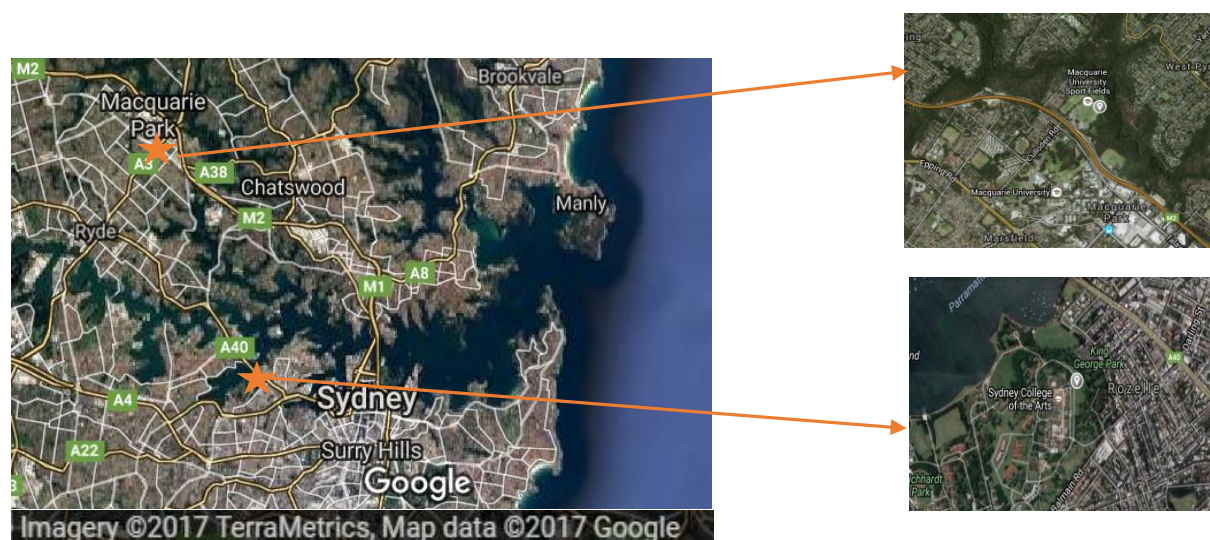
Figure 1. Map of the sampling site locations - automatic weather station at the Macquarie University sports field and Rozelle EPA monitoring site (Map data: Google, DigitalGlobe)

Prior to sampling, quartz filters were pre-baked at 550 ℃ for 20 hours in a muffle furnace to eliminate organic components and were subsequently sealed in cleaned aluminium foil before being used for particulate collections. The filters were conditioned at 20 ℃ and 50% relatively humidity for 24h prior to weighing both before and after exposure. An electronic microbalance (Sartorius, BP 221S MAX 220G D = 0.1 mg) was used to measure mass concentrations of quartz filters gravimetrically. After weighing, the filters were individually wrapped in aluminium foil, packed and sealed in airtight polyethylene bags and stored in a -20 ℃ refrigerator before further chemical analysis. Field blanks were assigned to each sampling season and were treated in the same way as the filters being exposed with regards to preparation, handling, transport and storage with the exception of activating the air pump. To

98

ensure the veracity of the experiments, one field blank was analysed for each seasonal campaign.

Description of sampling sites

The Rozelle site is an Environmental Protection Authority New South Wales (EPANSW) air quality monitoring station, situated inside a park located in the grounds of Rozelle Hospital, off Balmain Road, Rozelle in the central part of the Sydney metropolitan area (33 ° 51' 57" South, 151 ° 09' 45"East and 22 metres above mean sea level).

Macquarie University Automatic Weather Station is operated by the Department of Environmental Sciences, Macquarie University and commissioned as an Environmental Protection Authority New South Wales (EPANSW) air quality monitoring station in 2017, is located within the sports grounds of Macquarie University at North Ryde, Australia (33 °45' 55" South, 151 ° 07' 4.1"East and 49 metres above mean sea level). It is approximately 10 km north-west of the Rozelle EPA monitoring station. Macquarie University Automatic Weather Station is in a residential area, situated to the north of the university and on the northern side of the M2 Hills motorway as shown in Figure 1.

As Rozelle is an EPANSW air quality monitoring station, gas phase pollutants and meteorology are routinely measured at the site. Both gas phase species (ozone: O_3, oxides of nitrogen: NO_x and carbon monoxide: CO) concentrations and meteorological data (Ambient temperature: T, Wind speed: WS, Relative humidity: RH, and Solar radiation: SR) are obtained using air pollution monitoring instruments and meteorological instruments at Rozelle. Measurements of ozone, oxides of nitrogen and regular meteorological variables (Ambient temperature: T, Wind speed: WS, Relative humidity: RH, and Solar radiation: SR) used to interpret the results from the samples collected on the Macquarie University (MQ) campus were taken from a nearby monitoring station (Lindfield: 3.6 km southeast from MQ) operated by EPANSW.

The filter washing procedure

Approximately 12 cm^2 of the filters were water extracted with Milli-Q water for further analysis of water insoluble organic carbon (WINSOC) and ^{14}C analysis in water insoluble total carbon (WINTC) and elemental carbon (EC) before thermal treatment in order to minimize charring. In other words, water-extraction treatment is a prerequisite for EC

isolation. As a result, an approach was developed to obtain minimal removal of EC by water while maintaining high homogeneity on the filter (Zhang et al., 2012).

The water extraction method is described by Bernardoni, Yttri and Zhang et al (Bernardoni et al., 2013; Yttri et al., 2009; Zhang et al., 2012), and is based on gravity feed of water through the exposed filter punch. Briefly, a supporting filter punch was placed on the top and bottom of the exposed punch during extraction. This sandwiched design can prevent loss of water-insoluble carbonaceous material and keeps the EC uniformly distributed. Ultrapure water (100 ml) is then passed through the filter without using a pump. The filter punch then is delicately removed and is placed in the desiccator in a 60 °C oven for drying. Zhang (Zhang et al., 2012) and Bernardoni et al. (Bernardoni et al., 2013) tested this water extraction method and found that there was very little loss (< 3%) of EC using this water extraction procedure.

IMPROVE-A protocol for carbon fractions quantification

$PM_{2.5}$ samples were analysed at CSIRO Ocean and Atmosphere Flagship for carbon fraction concentrations. Details of the methods used to analyze OC, WINSOC and EC can be found in Keywood et al. (Keywood et al., 2015; Keywood et al., 2011). Briefly, small punched areas (0.507 cm^2) of the filter samples were taken for analysis of the operationally defined OC, WINSOC and EC mass concentrations by a thermal-optical carbon analyser (DRI Model 2001A, Desert Research Institute, Reno, NV) following the IMPROVE-A temperature protocol (Chow et al., 2007). The operationally defined OC (OC1-OC4, Table 1) is evolved in an inert 100% He atmosphere and EC fractions (EC1-EC4, Table 1) are prepared by oxidation in a 2% O_2/98% He atmosphere. Liberated carbon compounds are first converted to CO_2 by a manganese oxidizer at 800–900 °C, and then these are reduced to CH_4 by a methanator and quantified using a flame ionization detector (Han et al., 2016). Charring organic carbon (pyrolyzed organic carbon: POC) is generated in a pure He environment. Thermal/optical reflectance (TOR) pyrolysis adjustment is adopted in this study. Therefore, OC equals sum of each OC fractions plus POC; EC is total of each EC fractions minus POC.

$$OC = OC1 + OC2 + OC3 + OC4 - POC$$

$$EC = EC1 + EC2 + EC3 - POC$$

EC also can be divided into char and soot as sub-fractions to further evaluate their climatic influences (Han et al., 2007). Char is quantified as EC1 minus POC; Soot is EC2 plus EC3.

100

Char = EC1 – POC

Soot = EC2 + EC3

Duplicate punches from each filter were analysed to minimise influence from any non-uniform depositions on the filter. Differences between replicate filter samples were within 10% for OC and EC. Field blanks were analysed and subtracted.

Table 1. Parameters (carrier gas, temperature and time) of IMPROVE-A protocol used in this study.

IMPROVE-A	OC1	OC2	OC3	OC4	EC1	EC2	EC3
Gas	pure He	pure He	pure He	pure He	2% O_2/98% He	2% O_2/98% He	2% O_2/98% He
T (°C)	140	280	480	580	580	740	840
t (s)[a]	150-580	150-580	150-580	150-580	150-580	150-580	150-580

[a] The residence time at each temperature depends on when the detector signal returns to the baseline to achieve well-defined carbon fractions.

OC, EC, WINSOC and wEC were measured on each sample using the IMPROVE-A protocol. It should be noted that there was some differences between EC and after water wash EC (wEC) ($p > 0.05$). As the particle loss can be neglected in our study, the smaller wEC values can be ascribed to the combination of artefacts due to pyrolyzed organic carbon, untimely removal of EC and the potential positive artefact leading to co-evolution of EC with residual OC, which overestimated EC values (Zhang et al., 2012). Since water wash pre-treatment can minimise the above artefacts, wEC data should be more reliable and reflect "real" EC. Thus, wEC was estimated using the following calculation. TC, WINTC, WSOC, char and soot were quantified according to the following equations. WINSOC, wEC and WINTC represent water insoluble organic carbon, after water wash elemental carbon and water insoluble total carbon, respectively.

OC + EC = TC

WINSOC + wEC = WINTC

WSOC = TC – WINTC

Char = wEC1 – wPOC

Soot = wEC2 + wEC3

IMPROVE-A protocol is suitable for urban samples, under conditions where extensive traffic emissions and coal combustion exists (Han et al., 2016). However, IMPROVE-A protocol would bias EC fraction for the biomass burning dominated samples. Studies performed near the Alpine region in winter proposed and validated this hypothesis (Bernardoni et al., 2013; Dusek et al., 2014; Zhang et al., 2012). Therefore, some pilot experiments conducted on samples from Australian cities are necessary to determine the optimal split temperature of OC and EC in order to avoid the EC bias.

Radiocarbon analysis (^{14}C) of carbonaceous particle fractions

All radiocarbon measurements were carried out at the ANTARES facility, ANSTO, Sydney using accelerator mass spectrometry (AMS) (Fink et al., 2004) and ^{14}C data were provided by ANSTO and are expressed as percent Modern Carbon (pMC) (Appendix C, Supplementary Table S1-Table S2). Percent Modern Carbon (pMC) converted to fraction of modern (f_M) (division by 100) represents the ratio of ^{14}C/^{12}C content of the sample relative to the isotopic ratio of the reference year 1950 (Stuiver and Polach, 1977). The f_M values were corrected for ^{13}C fractionation and were not corrected for the ^{14}C decay between 1950 and the year of measurement.

$$pMC(sample) = \frac{\frac{^{14}C}{^{12}C}(sample)}{\frac{^{14}C}{^{12}C}(1950)} \times 100$$

Radiocarbon analysis was carried out on the TC, WINTC and wEC, samples and details of the operational procedures to isolate the different carbon fractions are given in the Supplementary Information (Appendix C, Supplementary Information S3).

Radiocarbon data correction

No blank correction was carried out for ^{14}C analysis in each carbon species. The carbon content of field blanks are all less than 5% of those in selected samples and therefore can be neglected.

Theoretically, samples stemmed from fossil fuel sources are depleted of ^{14}C owing to the extinction of ^{14}C with a half-life of 5730 years, and f_M values of contemporary carbon sources should be equal to 1. Thermonuclear weapon tests during the late 1950s and early 1960s increased the ^{14}C content of the atmosphere. Thus, reference values were introduced to correct this bomb peak influence on f_M data. In our study, 1.040 and 1.043 was adapted for f_M corrections on TC and WINTC, respectively, for f_M on EC correction, the value is 1.049. These reference values were determined by chamber experiments conducted in Launceston, Tasmania, Australia (Jordan et al., 2006). Corrected f_M (fraction of contemporary carbon: f_c) is obtained by dividing f_M by the reference values.

Source apportionment methodology

This source apportionment approach is developed according to mass and isotope-mass balance of diverse carbon fraction data and respective ^{14}C data. f_c (TC), f_c (WINTC) and f_c (wEC) were measured and normalized from the corresponding f_M values. All carbonaceous sub-fractions can be split into fossil sources and contemporary sources (non-fossil sources: nf) by ^{14}C analysis. Thus, TC_f (TC_{fossil}: fossil fuel sources in TC), $WINTC_f$ ($WINTC_{fossil}$: fossil fuel sources in WINTC) and EC_f (EC_{fossil}: fossil fuel sources in wEC) are calculated as follows:

$$TC_f = TC \times (1 - f_c (TC))$$

$$WINTC_f = WINTC \times (1 - f_c (WINTC))$$

$$EC_f = wEC \times (1 - f_c (wEC))$$

$WSOC_f$ ($WSOC_{fossil}$: fossil fuel sources in WSOC) and $WINSOC_f$ ($WINSOC_{fossil}$: fossil fuel sources in WINSOC) are calculated from TC_f, $WINTC_f$ and EC_f.

$$WSOC_f = TC_f - WINTC_f$$

$$WINSOC_f = WINTC_f - EC_f$$

WSOC normally contain entire SOC (secondary organic carbon), part of primary organic carbon (~50% $POC_{biomass}$) and $POC_{biogenic}$ (Liu et al., 2014). Consequently, $WSOC_f$ can

103

represent all SOC_f (SOC_{fossil}: fossil fuel sources in SOC). WINSOC has been determined to be entirely derived from primary fossil fuel and biomass burning combustion (Bosch et al., 2014; Budhavant et al., 2015; Kirillova et al., 2013; Kirillova et al., 2014). Hence, $WINSOC_f$ are POC_f.

$$WSOC_f = SOC_f$$

$$WINSOC_f = POC_f$$

In terms of EC, as EC only stems from biomass burning and fossil fuel combustion, therefore, EC_{nf} ($EC_{non-fossil}$: non-fossil fuel sources in wEC) are namely $EC_{biomass}$ ($EC_{biomass}$: biomass burning sources in EC), and are determined as:

$$EC_{biomass} = wEC - EC_f$$

It is difficult to quantify POC and SOC due to the vast number of organic compounds with a variety of chemical and physical properties. However, it is possible to use an indirect method for the quantitative assessment of SOC, (OC/EC)pri has frequently been used to estimate SOA fractions in some research, such as the EC tracer method proposed by Turpin and Huntzicker (Cabada et al., 2004). Total SOC can be estimated by the EC-tracer method using primary OC/EC ratio (OC/EC)pri and taking EC as the primary tracer (Ding et al., 2012). POC is first estimated, and then SOC is calculated by subtracting POC from corrected OC (OC + EC – wEC):

$$POC = (OC/EC)pri \; x \; EC$$

$$SOC = (OC + EC - wEC) - POC$$

The EC-tracer method is a widely applied approach to estimate the bulk SOC. The minimum OC/EC ratio during the sampling periods is often assumed as the primary OC/EC ratio ((OC/EC)pri) when SOC is unlikely to be produced. But, (OC/EC)pri ratio has to be found especially for each season in Australia since biomass burning aerosols have primary OC/EC ratio more than 7 or higher (Fine et al., 2001, 2002; Zhang et al., 2007).

To estimate SOC more precisely, a refined EC tracer method was developed on the basis of the diurnal (OC/EC)pri data from the urban sites research in Melbourne (Keywood and Cope,

2008). In the Melbourne' study, hourly OC and EC were calculated from the concentrations of $PM_{2.5}$, NO_2 and CO. Diurnal (OC/EC)pri data for vehicle, wood heating and bushfires were achieved by using signature gases (O_3, CO and NO) to identify periods dominated by primary emissions for the month of August and the summer months.

We use these diurnal (OC/EC)pri data to obtain the general (OC/EC)pri data on each case selected in our study. (OC/EC)pri data from domestic heating wood smoke (August), bushfires and vehicles are 2.4, 7.6 and 1.7, respectively. Here, in our study, there are four cases: samples influenced by domestic heating + bushfires + vehicles, domestic heating + vehicles, bushfires + vehicles and vehicles only. Bushfires in summer were observed in the period of 10 am–12 pm and 10 am–5 pm on 20/12/2015 at the Rozelle and MQ sampling site, respectively, whereas, winter bushfires plumes occurred in the period 6 am 21/08/2015–4 pm 22/08/2015 and 8 am 21/08/2015–3 pm 22/08/2015 at Rozelle and MQ, respectively. The results for each of these periods are given in Table 2.

Table 2. Calculate Estimated (OC/EC)pri data.

Date	Season	Sources	OC/EC	(OC/EC)pri Rozelle	(OC/EC)pri MQ
2015/08/14–2015/08/16	Winter	Domestic heating Vehicle	2.31EC + 0.16	2.31	2.31
2015/08/20–2015/08/22	Winter	Domestic heating bushfires, vehicle	5.02wEC + 0.16(R); 2.82wEC + 0.16(MQ)	5.02	2.82
2015/11/24–2015/11/26	Summer	vehicle	2.29EC + 0.23	2.29	2.29
2015/12/19–2015/12/21	Summer	Bushfires; vehicle	2.63EC + 0.23(R); 3.19EC + 0.23(MQ)	2.63	3.19

SOC_{nf} ($SOC_{non\text{-}fossil}$: non-fossil fuel sources (biomass burning and biogenic sources) in SOC) is split into $SOC_{biomass}$ and $SOC_{biogenic}$, which is deduced from subtraction of SOC and SOC_f. Analogouly, with regards to POC_{nf} ($POC_{non\text{-}fossil}$: non-fossil fuel sources (biomass burning and biogenic sources) in POC), is defined via POC and POC_f.

$$SOC_{nf} = SOC - SOC_f$$

$$POC_{nf} = POC - POC_f$$

The sub-fractions of $PM_{2.5}$ carbonaceous aerosols including SOC_f, SOC_{nf}, POC_f, POC_{nf}, $EC_{biomass}$ and EC_f are assigned using the above source apportionment approach except $SOC_{biogenic}$, $SOC_{biomass}$, $POC_{biomass}$ and $POC_{biogenic}$. $SOC_{biogenic}$ and $SOC_{biomass}$ can be either

estimated from different SOA tracers such as α-pinene derived biomarkers, isoprene derived biomarkers, β-caryophyllene derived biomarkers and toluene derived biomarkers or from parallel online aerosol mass spectrometer (Ulevicius et al., 2016; Zotter et al., 2014b). As a consequence, $SOC_{biogenic}$ and $SOC_{biomass}$ cannot be estimated in this study due to lack of the concentrations of identified SOA tracers. Likewise, typical $POC_{biomass}$ and $POC_{biogenic}$ biomarkers such as levoglucosan and mannitol need to be quantified, which combined with POC values are the tools to estimate the contribution of different contemporary carbon to primary emissions (Zhang et al., 2015a; Zotter et al., 2014a).

In summary, to implement a comprehensive and elaborate source apportionment of carbonaceous aerosols, not only is there a need for various carbon fractions and ^{14}C data in carbon fractions to be quantified, but also individual source biomarkers and real-time online/offline parallel distinct bulk organic aerosol data need to be included, for example aerosol mass spectrometry data.

Results and Discussion

Meteorological conditions, $PM_{2.5}$ loadings and gas pollutant concentrations

Eight simultaneous $PM_{2.5}$ filter samples were selected and analysed in our study on the basis of the consideration of spatiality, seasonality and haze events for contrasting purpose. Although this is a somewhat low number of samples, the sampling duration of 48 hours result in the inclusion of a range of wind directions, temperatures and other variables, so that some general conclusions are possible. The general descriptions of these eight samples with regards to their meteorological and pollutant characteristics are listed in Table 3 and Table 4. With respect to meteorology, temperature and global solar radiation there are significant differences between winter and summer ($p < 0.05$); as for wind speed and relative humidity, no obvious difference ($p > 0.05$) was apparent using the Student T-test.

Winter haze during the sampling period (20th-22nd August) was caused by the smoke coming from controlled biomass burning of bushland in national parks across the Sydney Metropolitan, Illawarra and Blue Mountains areas. Whereas, extreme summer haze in MQ was the result of the uncontrolled and unexpected bushfires, which caused large-scale air pollution in NSW, lasting almost two days (Lin et al., 2015; NEWS, 2015a, b, c). Apart from bushfires, winter samples will also have a contribution from wood burning for domestic heating purposes, whereas summer samples will not include this source.

106

Table 3. Description of selected samples and meteorological variables: average values of ambient temperature: Temperature: T ($°C$), Wind speed: WS (m/s), Relative humidity: RH (%) and Solar radiation: SR (W/m^2)

Date	Season	Feature	T ($°C$)	WS (m/s)	RH (%)	SR (W/m^2)
2015/08/14–2015/08/16	Winter	Weekend Low wind speed Low atmospheric boundary layer	13.5	1.1	69.3	114.1
2015/08/20–2015/08/22	Winter	Haze (Hazard reduction burns) Hazardous AQI	17.2	1.8	65.9	196.8
2015/11/24–2015/11/26	Summer	Sunny; Fair AQI Max T: 37.8 $°C$	25.5	2.7	56.9	343.4
2015/12/19–2015/12/21	Summer	Haze (wild bushfire triggered) Hazardous AQI	25.8	2.8	63.7	373.9

AQI: Air Quality Index. The specific definition, calculation and interpretation of AQI values can be found in NSW EPA website (Office of Environment & Heritage, 2017).

Unsurprisingly, during periods of winter haze at Rozelle and summer haze at MQ (highlighted in yellow) the Australian a 24h standard of 25 $\mu g·m^{-3}$ for $PM_{2.5}$ fine particles, was exceeded, averaging 28.1 $\mu g·m^{-3}$ and 34.9 $\mu g·m^{-3}$, respectively. No gas phase pollutants exceeded the corresponding Australian standards. Seasonal and spatial variations investigated on $PM_{2.5}$ data via Student T-test show no differences ($p > 0.05$). However, gas phase pollutants (O_3, NO_x and CO) showed significant differences between winter and summer and O_3 concentrations in summer are much higher than those in winter, whereas for NO_x and CO the opposite occurs ($p < 0.05$). Stronger solar radiation in summer ($p < 0.05$) leads to higher ozone concentrations during the summer sampling campaign. However, the higher NO_x and CO levels can be ascribed to lower atmospheric mixing boundary layer in winter, which reduces the mobility and dispersion of gas phase pollutants (Gupta and Christopher, 2009; Gupta et al., 2007; Hart et al., 2006).

Table 4. $PM_{2.5}$ mass concentrations ($\mu g \cdot m^{-3}$) and gas pollutants values including O_3 (ppb), NO_x: $NO + NO_2$ (ppb) and CO (ppm)

Samples	$PM_{2.5}$	O_3	NO	NO_2	CO
R_W_WEEKEND	15.1	12	7	16	0.4
MQ_W_WEEKEND	15.0	11	5	12	na
R_W_HAZE	28.1	17	9	15	0.5
MQ_W_HAZE	24.5	18	4	10	na
R_S_SUNNY	17.3	28	3	9	0.2
MQ_S_SUNNY	12.8	29	2	5	na
R_S_HAZE	22.2	27	2	10	0.2
MQ_S_HAZE	34.9	32	1	6	na

R: Rozelle, MQ: Macquarie University, W: winter, S: summer.
Exceedences are highlighted in yellow

In spite of the fact that both Rozelle and MQ sites are both in the Sydney East Region, small spatial differences can still lead to a distinct distribution and contribution of carbonaceous aerosols. Topograpical differences at Rozelle and MQ may result in different meteorological conditions at the two sites. It should also be noted that the site at Rozelle may be exposed to larger motor vehicle derived compared with those at the MQ site as the Rozelle sampling site is near one of the busiest commuter roads in Sydney. In addition, there might be differences in the types and extent of residential heating between Rozelle and MQ in winter.

General remarks on varieties of carbonaceous aerosol fractions and their contributions

Estimated SOC and POC are scaled to SOA and POA, respectively based on observations in other urban locations. To account for the presence of oxygen and hydrogen in the samples, SOC and POC are multiplied by a conversion factor of 1.6, which provides a reasonable estimate of SOA and POA for urban locations (Turpin and Lim, 2001). The scaling factor has not been determined for urban airsheds in Australia. However, Keywood et al (Keywood et al., 2011) recommended the factor of 1.6 should be adopted in future measurement campaigns in Australia. A factor of 1.1 was applied in this study to convert char and soot to elemental matter (EMchar and EMsoot) (Keywood et al., 2011).

OM (organic matter) = SOA + POA

CM (carbonaceous matter) = OM + EM

NCM (non-carbonaceous matter) = $PM_{2.5}$ − CM

PCA (primary carbonaceous aerosol) = POA + EM

The mass concentration of carbonaceous fraction (CM) in $PM_{2.5}$ ranged from 3.6 µg·m^{-3} to 16.5 µg·m^{-3}, with a median value of 9.3 µg·m^{-3} (Appendix C, Supplementary Table S4), and making up approximately half of the $PM_{2.5}$ mass in the selected samples on average. The average abundances of SOA and POA were 2.3 µg·m^{-3} (ranging from 0.7 µg·m^{-3} to 6.1 µg·m^{-3}) and 8.9 µg·m^{-3} (ranging from 1.8 µg·m^{-3} to 13.1 µg·m^{-3}), respectively, accounting for 11% and 42% in $PM_{2.5}$ mass. EMchar and EMsoot values were approximately one order of magnitude less than the other carbonaceous fractions. The absolute concentrations of distinct carbon fractions are plotted in Figure 2. The lowest concentration of carbonaceous aerosols was observed during the summer sampling campaign at the MQ site, which was reported at 3.6 µg·m^{-3}. This lower PM level can be attributed to the higher wind speed and low emissions.
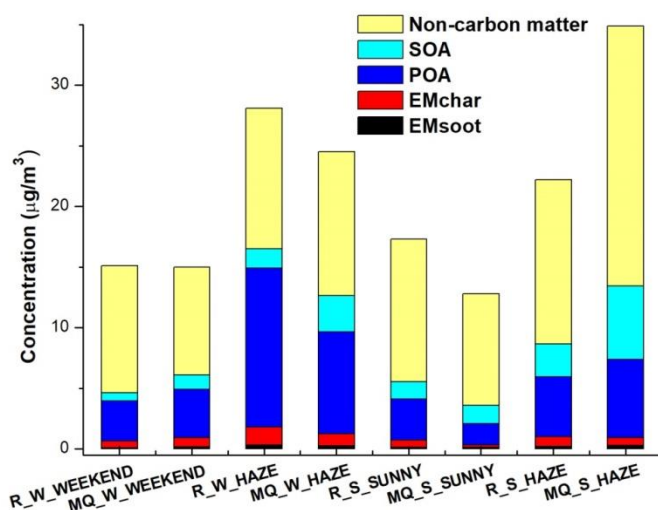
Figure 2. Plot of mass concentrations of Non-carbon matter, SOA, POA, EMchar and EMsoot (µg·m^{-3}) in the selected samples (from winter to summer).

The highest abundances of SOA and POA are all observed in haze events in summer MQ and winter Rozelle, respectively, up to 6.1 µg·m^{-3} and 13.1 µg·m^{-3}, respectively. POA and EMsoot during two haze events were markedly increased compared with those during non-haze events (weekend and sunny) ($p < 0.05$). The incremental increases in SOA and EMchar are in the

range of 0.9 µg·m^{-3} to 4.6 µg·m^{-3} and 0.2 µg·m^{-3} to 0.9 µg·m^{-3}, elevated SOA and EMchar by 87–304% and 30–286%, respectively.

Estimated preliminary source apportionment of carbonaceous aerosols

Various carbonaceous fractions (SOC_{nf}, SOC_f, POC_{nf}, POC_f, $EC_{biomass}$, EC_f, PRI_f and PRI_{nf}) obtained on the basis of the source apportionment approach developed in this study and ratios of primary carbon to secondary carbon are collated in Table 5. The concentrations of PRI_f and PRI_{nf} range from 0.31 µgC·m^{-3} to 0.97 µgC·m^{-3} and from 1.08 µgC·m^{-3} to 8.85 µgC·m^{-3}, with an average of 0.60 µgC·m^{-3} and 3.80 µgC·m^{-3}, respectively.

Table 5. Absolute concentrations (µgC·m^{-3}) of fossil and non-fossil sources on SOC, POC and EC fraction and the relative contribution of secondary and primary sources to total carbon (%).

Samples	SOC_{nf}	SOC_f	POC_{nf}	POC_f	$EC_{biomass}$	EC_f	PRI_f[b]	PRI_{nf}[b]	Sec/pri[a]
R_W_WEEKEND	0.24	0.19	1.85	0.22	0.31	0.27	0.49	2.16	14/86
MQ_W_WEEKEND	0.74	0.03	2.23	0.24	0.45	0.40	0.64	2.68	19/81
R_W_HAZE	1.00	0.00	8.14	0.05	0.70	0.93	0.97	8.85	9/91
MQ_W_HAZE	1.84	0.02	5.21	0.03	0.71	0.43	0.46	5.92	23/77
R_S_SUNNY	0.60	0.29	1.84	0.28	0.10	0.57	0.85	1.93	24/76
MQ_S_SUNNY	0.69	0.25	0.98	0.13	0.10	0.19	0.31	1.08	40/60
R_S_HAZE	1.36	0.32	2.99	0.10	0.42	0.51	0.61	3.41	29/71
MQ_S_HAZE	3.67	0.12	3.87	0.16	0.51	0.32	0.49	4.39	44/46

[a] sec: secondary sources; pri: primary sources
[b] $PRI_f = POC_f + EC_f$; $PRI_{nf} = POC_{nf} + EC_{biomass}$

For all samples, values of non-fossil fraction of primary and secondary carbon were higher ($p < 0.05$) than the corresponding values from fossil carbon sources, indicating that Sydney urban areas are dominated or largely influenced by non-fossil carbon sources as expected on days with major bushfire contributions. Similar observations have been made in some South Asian and central European urban locations (Bosch et al., 2014; Gelencsér et al., 2007; Kirillova et al., 2013; Kirillova et al., 2010; Zotter et al., 2014a).

Among all samples, the percentage of secondary carbon and primary carbon to total carbon vary widely from 9% to 44% and from 46% to 91%, respectively. The higher secondary carbon fractions are observed in MQ summer samples, whereas larger relative primary contribution to total carbon is from Rozelle winter haze samples.

The highest concentrations of SOC_{nf} and SOC_f occurred on summer haze days in MQ and Rozelle (highlighted in yellow in Table 5). The formation or increases in secondary carbon can be attributed to the following factors: enhanced O_3 levels and intensive emissions from respective primary sources. This result implies that in summer intensive non-fossil combustion sources increase SOC_{nf} significantly. As a consequence, it is suggested that controlling the emissions of primary sources could facilitate decreases in particulate levels, by not only lowering the concentrations of primary carbon but also secondary carbon. Given that SOC_f has a lower formation rate than SOC_{nf} as a consequence of its relative stability and refractory properties (Wang et al., 2013), reducing non-fossil combustion will result in greater reductions in PM, and in fact may be more necessary and urgent in Australia.
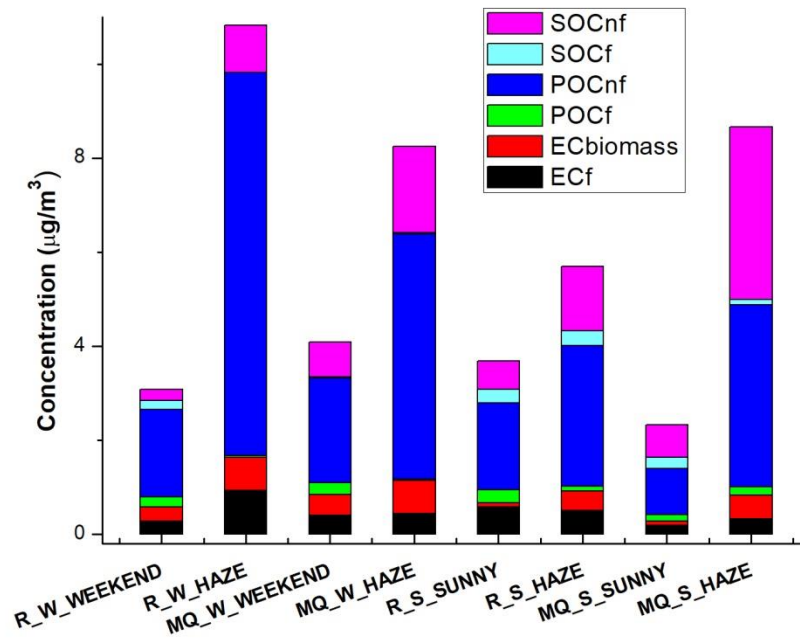
Figure 3. Concentrations ($\mu gC \cdot m^{-3}$) of all carbon sub-fractions in eight samples assigned in this study

Concentrations of each carbon species from the eight samples are shown in Figure 3. To further reveal seasonal variations, spatial distributions and special events vs general circumstances in Sydney urban sites, associated samples were selected for further discussion. Given the low number of samples, only general observations and tentative conclusions are made. In specific terms, seasonality: winter vs summer samples, spatiality: Rozelle vs MQ samples and events: haze vs general samples. Figure 3 stresses the contrast of haze vs general samples.
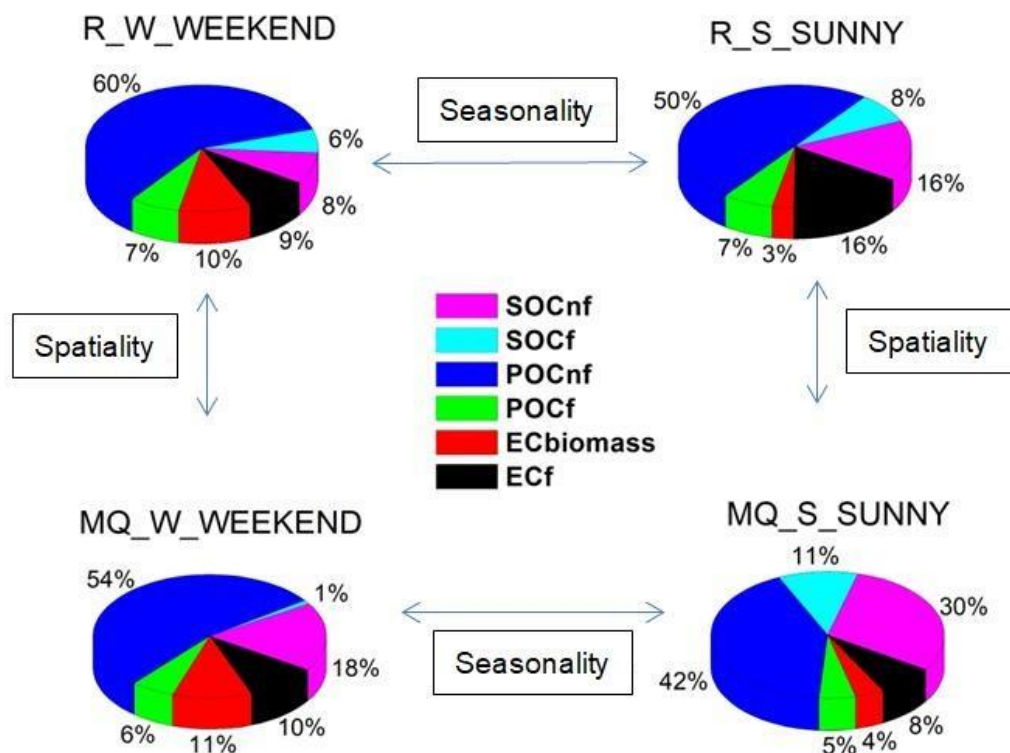
Figure 4. Relative contributions of each carbon fractions on total carbon in general samples.

Relative contributions of each general sample are displayed as pie charts in Figure 4. Regarding POC_{nf} and $EC_{biomass}$, higher contributions are observed in winter samples, amounting to 60% and 11% compared with those percentages (50% and 4%) in summer samples. Similarly, both of secondary sources indicators, SOC_{nf} and SOC_f exhibit seasonal variation, SOC_{nf} makes up nearly 30% of total carbon in the summer MQ sample. SOC_f was estimated at 11% in the summer MQ samples, whereas the value in winter MQ sample was just 1%. In this sampling campaign, no seasonality is observed for primary fossil fraction.

By contrast, POC_f and EC_f have certain spatial variability. POC_f and EC_f in Rozelle have slightly higher values than those at MQ, which may indicate that there is more contribution from traffic exhaust at Rozelle. However, it should be noted that motor vehicle emiisions include a contribution from non fossil carbon as E10 fuel is the dominant gasolione fuel blend and comprises conventional petroleum derived petrol blended with 10% ethanol. As a result a small underestimation of the contribution from motor vehicle exhaust and an overestimation of contribution from non-traffic exhaust to carbonaceous aerosols will be included in the results from this study.

112
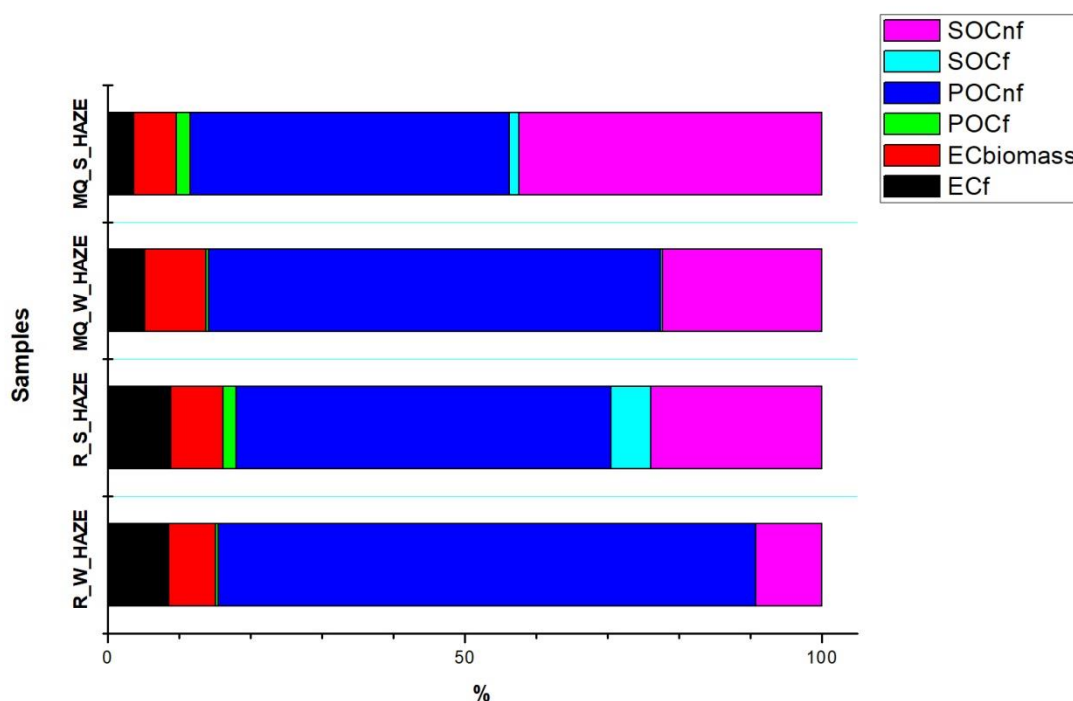
Figure 5. distributions of each carbon species in haze samples.

Relative distributions of carbonaceous fractions are presented in Figure 5. POC_{nf} in winter haze samples makes a larger contribution to those in summer samples, accounting for 75% in Rozelle and 63% in MQ of the total carbon. EC_f constitutes nearly 9% total carbon in Rozelle, whereas the corresponding values in MQ are 4–5%, which may reflect differences at the Rozelle and MQ sites in traffic emission patterns and the relative proportions of diesel and gasoline fueled vehicles.

The SOC fraction shows obvious seasonal variation. Summer haze samples have a greater contribution from the SOC fraction than those of winter haze samples. The proportion (6%) of SOC_f in the Rozelle summer sample also supports this observation. The Rozelle site appears to be more influenced by traffic emissions. In summer SOC_f is easily enhanced and formed due to higher solar radiation.

Conclusions

A subset of eight $PM_{2.5}$ samples was selected for ^{14}C measurements in this study. To facilitate assigning fossil and non-fossil contributions to each carbon species, water insoluble total carbon was quantified and analysed for bulk carbon and ^{14}C analysis. With ^{14}C measurements

in different carbonaceous fractions, the relative contributions of fossil and non-fossil sources to carbonaceous particles are firstly quantified in this study.

The comparison of the concentrations of all variables and the contributions of carbonaceous sub-fractions under different seasonal conditions (winter and summer) suggest that the formation or elevation of carbonaceous matter is attributed to different factors between different seasons. Domestic heating in winter is a major contributor for enhanced ambient carbon material. In summer higher solar radiation increases SOC levels and further enhances the concentration of PM. Higher levels of old carbon in Sydney are principally from mobile combustion sources, whereas, increases in contemporary carbon appear to be mainly due to biomass burning at both the Rozelle and MQ sites.

During haze events, a large increase of the non-fossil contribution of 440–500% was observed during these periods as a result of enhanced open biomass-burning activities. At the same time, SOC_{nf} levels were significantly increased, which suggests that the extensive emissions of primary sources largely elevate the PM concentration not only direcly but also by way of secondary particle formation, particularly SOC_{nf}, which has a faster formation rate than SOC_f.

Consequently, some measures and actions might be considered for mitigating particle air pollution in Sydney. Policy makers may need to consider improving the prediction of the best timing for hazard prevention/reduction burns to avoid meteorological conditions conductive to high pollutant concentrations. However stable conditions with lower wind speeds are usually safer to avoid runaway fires during hazard reduction burns.

114

References

Atkinson, R., Kang, S., Anderson, H., Mills, I., Walton, H., 2014. Epidemiological time series studies of PM2. 5 and daily mortality and hospital admissions: a systematic review and meta-analysis. Thorax, thoraxjnl-2013-204492.

Bell, M.L., Dominici, F., Ebisu, K., Zeger, S.L., Samet, J.M., 2007. Spatial and temporal variation in PM2. 5 chemical composition in the United States for health effects studies. Environmental health perspectives 115, 989.

Bernardoni, V., Calzolai, G., Chiari, M., Fedi, M., Lucarelli, F., Nava, S., Piazzalunga, A., Riccobono, F., Taccetti, F., Valli, G., 2013. Radiocarbon analysis on organic and elemental carbon in aerosol samples and source apportionment at an urban site in Northern Italy. Journal of Aerosol Science 56, 88-99.

Bosch, C., Andersson, A., Kirillova, E.N., Budhavant, K., Tiwari, S., Praveen, P., Russell, L.M., Beres, N.D., Ramanathan, V., Gustafsson, Ö., 2014. Source-diagnostic dual-isotope composition and optical properties of water-soluble organic carbon and elemental carbon in the South Asian outflow intercepted over the Indian Ocean. Journal of Geophysical Research: Atmospheres 119.

Budhavant, K., Andersson, A., Bosch, C., Kruså, M., Kirillova, E., Sheesley, R., Safai, P., Rao, P., Gustafsson, Ö., 2015. Radiocarbon-based source apportionment of elemental carbon aerosols at two South Asian receptor observatories over a full annual cycle. Environmental Research Letters 10, 064004.

Cabada, J.C., Pandis, S.N., Subramanian, R., Robinson, A.L., Polidori, A., Turpin, B., 2004. Estimating the secondary organic aerosol contribution to PM2. 5 using the EC tracer method special issue of aerosol science and technology on findings from the fine particulate matter supersites program. Aerosol Science and Technology 38, 140-155.

Carmichael, G.R., Adhikary, B., Kulkarni, S., D'Allura, A., Tang, Y., Streets, D., Zhang, Q., Bond, T.C., Ramanathan, V., Jamroensan, A., 2009. Asian aerosols: current and year 2030 distributions and implications to human health and regional climate change. Environmental science & technology 43, 5811-5817.

Chow, J.C., Watson, J.G., Chen, L.-W.A., Chang, M.O., Robinson, N.F., Trimble, D., Kohl, S., 2007. The IMPROVE_A temperature protocol for thermal/optical carbon analysis: maintaining consistency with a long-term database. Journal of the Air & Waste Management Association 57, 1014-1023.

Chung, S.H., Seinfeld, J.H., 2002. Global distribution and climate forcing of carbonaceous aerosols. Journal of Geophysical Research: Atmospheres 107.

Cohen, D.D., Stelcer, E., Garton, D., Crawford, J., 2011. Fine particle characterisation, source apportionment and long-range dust transport into the Sydney Basin: a long term study between 1998 and 2009. Atmospheric Pollution Research 2, 182-189.

Cope, M., Keywood, M., Emmerson, K., Galbally, I., Boast, K., Chambers, S., Cheng, M., Crumeyrolle, S., Dunne, E., Fedele, R., 2014. Sydney Particle Study–Stage II. Sydney Particle Study Final Report, CAWCR Publication.

Ding, X., Wang, X.M., Gao, B., Fu, X.X., He, Q.F., Zhao, X.Y., Yu, J.Z., Zheng, M., 2012. Tracer-based estimation of secondary organic carbon in the Pearl River Delta, south China. Journal of Geophysical Research: Atmospheres (1984–2012) 117.

Dusek, U., Monaco, M., Prokopiou, M., Gongriep, F., Hitzenberger, R., Meijer, H., Röckmann, T., 2014. Evaluation of a two-step thermal method for separating organic and elemental carbon for radiocarbon analysis. Atmospheric Measurement Techniques 7, 1943-1955.

Fine, P.M., Cass, G.R., Simoneit, B.R.T., 2001. Chemical characterization of fine particle emissions from fireplace combustion of woods grown in the northeastern United States. Environ Sci Technol 35, 2665-2675.

Fine, P.M., Cass, G.R., Simoneit, B.R.T., 2002. Chemical characterization of fine particle emissions from the fireplace combustion of woods grown in the southern United States. Environ Sci Technol 36, 1442-1451.

Fink, D., Hotchkis, M., Hua, Q., Jacobsen, G., Smith, A.M., Zoppi, U., Child, D., Mifsud, C., van der Gaast, H., Williams, A., 2004. The antares AMS facility at ANSTO. Nuclear Instruments and Methods in Physics Research Section B: Beam Interactions with Materials and Atoms 223, 109-115.

Gelencsér, A., May, B., Simpson, D., Sánchez-Ochoa, A., Kasper-Giebl, A., Puxbaum, H., Caseiro, A., Pio, C., Legrand, M., 2007. Source apportionment of PM2. 5 organic aerosol over Europe: Primary/secondary, natural/anthropogenic, and fossil/biogenic origin. Journal of Geophysical Research: Atmospheres 112.

Greaves, S., Issarayangyun, T., Liu, Q., 2008. Exploring variability in pedestrian exposure to fine particulates (PM2. 5) along a busy road. Atmospheric Environment 42, 1665-1676.

Gupta, P., Christopher, S.A., 2009. Particulate matter air quality assessment using integrated surface, satellite, and meteorological products: Multiple regression approach. Journal of Geophysical Research: Atmospheres 114.

Gupta, P., Christopher, S.A., Box, M.A., Box, G.P., 2007. Multi year satellite remote sensing of particulate matter air quality over Sydney, Australia. International Journal of Remote Sensing 28, 4483-4498.

Han, Y., Cao, J., Chow, J.C., Watson, J.G., An, Z., Jin, Z., Fung, K., Liu, S., 2007. Evaluation of the thermal/optical reflectance method for discrimination between char-and soot-EC. Chemosphere 69, 569-574.

Han, Y., Chen, L.-W., Huang, R.-J., Chow, J., Watson, J., Ni, H., Liu, S., Fung, K., Shen, Z., Wei, C., 2016. Carbonaceous aerosols in megacity Xi'an, China: Implications of thermal/optical protocols comparison. Atmospheric Environment 132, 58-68.

Hart, M., De Dear, R., Hyde, R., 2006. A synoptic climatology of tropospheric ozone episodes in Sydney, Australia. International journal of climatology 26, 1635-1649.

Heal, M.R., 2014. The application of carbon-14 analyses to the source apportionment of atmospheric carbonaceous particulate matter: a review. Analytical and bioanalytical chemistry 406, 81-98.

Heal, M.R., Naysmith, P., Cook, G.T., Xu, S., Duran, T.R., Harrison, R.M., 2011. Application of 14 C analyses to source apportionment of carbonaceous PM 2.5 in the UK. Atmospheric Environment 45, 2341-2348.

Highwood, E.J., Kinnersley, R.P., 2006. When smoke gets in our eyes: The multiple impacts of atmospheric black carbon on climate, air quality and health. Environment International 32, 560-566.

Hong, L., Fangang, Z., Longyi, S., Zongbo, S., 2002. Currenr Status of Study on the Human Health Effects of Inhalable Particulate. Journal of Environment and Health 19, 85-87.

Jordan, T.B., Seen, A.J., Jacobsen, G.E., Gras, J.L., 2006. Radiocarbon determination of woodsmoke contribution to air particulate matter in Launceston, Tasmania. Atmospheric Environment 40, 2575-2582.

Kampa, M., Castanas, E., 2008. Human health effects of air pollution. Environmental pollution 151, 362-367.

Kaufman, Y.J., Tanré, D., Boucher, O., 2002. A satellite view of aerosols in the climate system. Nature 419, 215.

Keywood, M., Cope, M., 2008. Development of Tools for the Identification of Secondary Organic Aerosol in Australian Cities. Department of the Environment and Water Resources.

Keywood, M., Cope, M., Meyer, C.M., Iinuma, Y., Emmerson, K., 2015. When smoke comes to town: The impact of biomass burning smoke on air quality. Atmospheric Environment 121, 13-21.

Keywood, M., Guyes, H., Selleck, P., Gillett, R., 2011. Quantification of secondary organic aerosol in an Australian urban location. Environmental Chemistry 8, 115-126.

Kim, K.-H., Kabir, E., Kabir, S., 2015. A review on the human health impact of airborne particulate matter. Environment international 74, 136-143.

Kirillova, E.N., Andersson, A., Sheesley, R.J., Kruså, M., Praveen, P., Budhavant, K., Safai, P., Rao, P., Gustafsson, Ö., 2013. 13C-and 14C-based study of sources and atmospheric processing of water-soluble organic carbon (WSOC) in South Asian aerosols. Journal of Geophysical Research: Atmospheres 118, 614-626.

Kirillova, E.N., Andersson, A., Tiwari, S., Srivastava, A.K., Bisht, D.S., Gustafsson, Ö., 2014. Water-soluble organic carbon aerosols during a full New Delhi winter: Isotope-based source apportionment and optical properties. Journal of Geophysical Research: Atmospheres 119, 3476-3485.

Kirillova, E.N., Sheesley, R.J., Andersson, A., Gustafsson, O.r., 2010. Natural abundance 13C and 14C analysis of water-soluble organic carbon in atmospheric aerosols. Analytical chemistry 82, 7973-7978.

Knibbs, L.D., de Dear, R.J., 2010. Exposure to ultrafine particles and PM2. 5 in four Sydney transport modes. Atmospheric Environment 44, 3224-3227.

Krivacsy, Z., Hoffer, A., Sarvari, Z., Temesi, D., Baltensperger, U., Nyeki, S., Weingartner, E., Kleefeld, S., Jennings, S., 2001. Role of organic and black carbon in the chemical composition of atmospheric aerosol at European background sites. Atmospheric Environment 35, 6231-6244.

Lelieveld, J., Evans, J.S., Fnais, M., Giannadaki, D., Pozzer, A., 2015. The contribution of outdoor air pollution sources to premature mortality on a global scale. Nature 525, 367.

Lin, Y., Ma, Y., Qiu, X., Li, R., Fang, Y., Wang, J., Zhu, Y., Hu, D., 2015. Sources, transformation, and health implications of PAHs and their nitrated, hydroxylated, and oxygenated derivatives in PM2. 5 in Beijing. Journal of Geophysical Research: Atmospheres 120, 7219-7228.

Lippmann, M., Ito, K., Nadas, A., Burnett, R., 2000. Association of particulate matter components with daily mortality and morbidity in urban populations. Research Report (Health Effects Institute), 5-72, discussion 73-82.

Liu, D., Li, J., Zhang, Y., Xu, Y., Liu, X., Ding, P., Shen, C., Chen, Y., Tian, C., Zhang, G., 2013. The use of levoglucosan and radiocarbon for source apportionment of PM2. 5 carbonaceous aerosols at a background site in East China. Environmental science & technology 47, 10454-10461.

Liu, J., Li, J., Zhang, Y., Liu, D., Ding, P., Shen, C., Shen, K., He, Q., Ding, X., Wang, X., 2014. Source apportionment using radiocarbon and organic tracers for PM2. 5 carbonaceous aerosols in Guangzhou, South China: Contrasting local-and regional-scale haze events. Environmental science & technology 48, 12002-12011.

Mauderly, J.L., Chow, J.C., 2008. Health effects of organic aerosols. Inhalation toxicology 20, 257-288.

Mouteva, G., Fahrni, S., Santos, G., Randerson, J., Zhang, Y., Szidat, S., Czimczik, C., 2015. Accuracy and precision of 14 C-based source apportionment of organic and elemental carbon in aerosols using the Swiss_4S protocol. Atmospheric Measurement Techniques Discussions 8.

Nel, A., 2005. Air pollution-related illness: effects of particles. Science 308, 804-806.

NEWS, A., 2015a. Concerns for volunteer safety in red gum forests during bushfire season ABC.

NEWS, A., 2015b. Emergency crews battle bushfires in Victoria, South Australia endures heatwave, ABC NEWS.

NEWS, A., 2015c. Total fire bans in large area of NSW with extreme heat and strong winds expected, ABC NEWS.

Office of Environment & Heritage, N.G., 2017. About the Air Quality Index

Piletic, I.R., Offenberg, J.H., Olson, D.A., Jaoui, M., Krug, J., Lewandowski, M., Turlington, J.M., Kleindienst, T.E., 2013. Constraining carbonaceous aerosol sources in a receptor model

by including 14 C data with redox species, organic tracers, and elemental/organic carbon measurements. Atmospheric environment 80, 216-225.

Pöschl, U., 2005. Atmospheric aerosols: composition, transformation, climate and health effects. Angewandte Chemie International Edition 44, 7520-7540.

Pozzi, R., De Berardis, B., Paoletti, L., Guastadisegni, C., 2003. Inflammatory mediators induced by coarse (PM2. 5–10) and fine (PM2. 5) urban air particles in RAW 264.7 cells. Toxicology 183, 243-254.

Putaud, J.-P., Raes, F., Van Dingenen, R., Brüggemann, E., Facchini, M.-C., Decesari, S., Fuzzi, S., Gehrig, R., Hüglin, C., Laj, P., 2004. A European aerosol phenomenology—2: chemical characteristics of particulate matter at kerbside, urban, rural and background sites in Europe. Atmospheric environment 38, 2579-2595.

Ramanathan, V., Carmichael, G., 2008. Global and regional climate changes due to black carbon. Nature geoscience 1, 221.

Ramanathan, V., Crutzen, P., Kiehl, J., Rosenfeld, D., 2001. Aerosols, climate, and the hydrological cycle. science 294, 2119-2124.

Saarikoski, S., Timonen, H., Saarnio, K., Aurela, M., Järvi, L., Keronen, P., Kerminen, V.-M., Hillamo, R., 2008. Sources of organic carbon in fine particulate matter in northern European urban air. Atmospheric Chemistry & Physics 8.

Stuiver, M., Polach, H.A., 1977. Discussion reporting of 14 C data. Radiocarbon 19, 355-363.

Szidat, S., Prévôt, A.S., Sandradewi, J., Alfarra, M.R., Synal, H.A., Wacker, L., Baltensperger, U., 2007. Dominant impact of residential wood burning on particulate matter in Alpine valleys during winter. Geophysical Research Letters 34.

Szidat, S., Ruff, M., Perron, N., Wacker, L., Synal, H.-A., Hallquist, M., Shannigrahi, A.S., Yttri, K., Dye, C., Simpson, D., 2009. Fossil and non-fossil sources of organic carbon (OC) and elemental carbon (EC) in Göteborg, Sweden. Atmospheric Chemistry and Physics 9, 1521-1535.

Tie, X., Cao, J., 2009. Aerosol pollution in China: Present and future impact on environment. Particuology 7, 426-431.

Turpin, B.J., Lim, H.-J., 2001. Species contributions to PM2. 5 mass concentrations: Revisiting common assumptions for estimating organic mass. Aerosol Science & Technology 35, 602-610.

Ulevicius, V., Byčenkienė, S., Bozzetti, C., Vlachou, A., Plauškaitė, K., Mordas, G., Dudoitis, V., Abbaszade, G., Remeikis, V., Garbaras, A., 2016. Fossil and non-fossil source contributions to atmospheric carbonaceous aerosols during extreme spring grassland fires in Eastern Europe. Atmospheric chemistry and physics 16, 5513-5529.

Venkataraman, C., Habib, G., Eiguren-Fernandez, A., Miguel, A., Friedlander, S., 2005. Residential biofuels in South Asia: carbonaceous aerosol emissions and climate impacts. Science 307, 1454-1456.

Wang, G.-h., Zeng, Y.-s., Yao, J., Qian, Y., Huang, Y., Liu, K., Liu, W., Li, Y., 2013. Source apportionment of atmospheric carbonaceous particulate matter based on the radiocarbon. Journal of Radioanalytical and Nuclear Chemistry 295, 1545-1552.

Wozniak, A.S., Bauer, J.E., Dickhut, R.M., 2012a. Characteristics of water-soluble organic carbon associated with aerosol particles in the eastern United States. Atmospheric environment 46, 181-188.

Wozniak, A.S., Bauer, J.E., Dickhut, R.M., Xu, L., McNichol, A.P., 2012b. Isotopic characterization of aerosol organic carbon components over the eastern United States. Journal of Geophysical Research: Atmospheres (1984–2012) 117.

Yttri, K.E., Dye, C., Braathen, O.-A., Simpson, D., Steinnes, E., 2009. Carbonaceous aerosols in Norwegian urban areas. Atmospheric Chemistry and Physics 9, 2007-2020.

Zhang, Y.-L., Huang, R.-J., El Haddad, I., Ho, K.-F., Cao, J.-J., Han, Y., Zotter, P., Bozzetti, C., Daellenbach, K., Canonaco, F., 2015a. Fossil vs. non-fossil sources of fine carbonaceous aerosols in four Chinese cities during the extreme winter haze episode of 2013. Atmospheric chemistry and physics 15, 1299-1312.

Zhang, Y.-L., Li, J., Zhang, G., Zotter, P., Huang, R.-J., Tang, J.-H., Wacker, L., Prévôt, A.S., Szidat, S.n., 2014. Radiocarbon-based source apportionment of carbonaceous aerosols at a regional background site on Hainan Island, South China. Environmental science & technology 48, 2651-2659.

Zhang, Y.-x., Min, S., Zhang, Y.-h., Zeng, L.-m., He, L.-y., Bin, Z., Wei, Y.-j., Zhu, X.-l., 2007. Source profiles of particulate organic matters emitted from cereal straw burnings. Journal of Environmental Sciences 19, 167-175.

Zhang, Y., Liu, D., Shen, C., Ding, P., Zhang, G., 2010. Development of a preparation system for the radiocarbon analysis of organic carbon in carbonaceous aerosols in China. Nuclear Instruments and Methods in Physics Research Section B: Beam Interactions with Materials and Atoms 268, 2831-2834.

Zhang, Y., Perron, N., Ciobanu, V., Zotter, P., Minguillón, M., Wacker, L., Prévôt, A., Baltensperger, U., Szidat, S., 2012. On the isolation of OC and EC and the optimal strategy of radiocarbon-based source apportionment of carbonaceous aerosols. Atmospheric Chemistry and Physics 12, 10841-10856.

Zhang, Y., Schnelle-Kreis, J., Abbaszade, G., Zimmermann, R., Zotter, P., Shen, R.-r., Schaefer, K., Shao, L., Prevot, A., Szidat, S., 2015b. Source apportionment of elemental carbon in Beijing, China: insights from radiocarbon and organic marker measurements. Environ Sci Technol.

Zotter, P., Ciobanu, V., Zhang, Y., El-Haddad, I., Macchia, M., Daellenbach, K., Salazar, G., Huang, R.-J., Wacker, L., Hueglin, C., 2014a. Radiocarbon analysis of elemental and organic carbon in Switzerland during winter-smog episodes from 2008 to 2012–Part 1: Source apportionment and spatial variability. Atmospheric chemistry and physics 14, 13551-13570.

Zotter, P., El-Haddad, I., Zhang, Y., Hayes, P.L., Zhang, X., Lin, Y.H., Wacker, L., Schnelle-Kreis, J., Abbaszade, G., Zimmermann, R., 2014b. Diurnal cycle of fossil and nonfossil carbon using radiocarbon analyses during CalNex. Journal of Geophysical Research: Atmospheres 119, 6818-6835.

CHAPTER 5: CONCLUSIONS

In this chapter, the main conclusions regarding the papers previously presented and relevant discussion on the source identification and apportionment of fine carbonaceous aerosols in the Sydney urban region using a radiocarbon technique in combination with measurement of organic biomarkers and statistical analysis.

5.1. Discussion and Conclusions

The aim of this study was to apply organic biomarkers to characterise typical and principal organic constituents in urban Sydney fine particulates. This data was combined with ^{14}C analyses to determine the proportions of the organic constituents arising from fossil and non-fossil carbon sources. The data was also used to estimate contributions from primary emissions and secondary atmospheric formation processes. To address this issue, non-polar organic compounds (PAHs and n-alkanes), twelve polar organic species belonging to six compound classes, and two categories of carbon data (bulk carbon data and radiocarbon data) were measured.

5.1.1 Summary of chemical characterization of selected polar and non-polar organic tracers

Chapters 2 and 3 reveal that during 2014 urban Sydney autumn and winter sampling campaign (17 May to 29 June 2014), several sources of PM$_{2.5}$-biomass burning (indicators: 5-6 rings PAHs (benzo[a]anthracene, chrysene, indeno[1,2,3-c,d]pyrene and benzo[g,h,i]perylene), monosaccharide anhydrides (levoglucosan, mannosan and galactosan), dehydroabietic and syringic acid), referring to domestic wood heating (special indicators: syringic acid) and hazard reduction burning (special indicators: dehydroabietic), traffic exhaust (indicators: fluoranthene, anthracene, pyrene, phenanthrene, benzo[a]pyrene and lower molecular weight n-alkanes (n-C$_{22}$ to n-C$_{24}$)), primary biogenic sources (indicators: higher odd carbon numbered n-alkanes (C$_{27}$, C$_{29}$)), anthropogenic secondary sources (indicators: two dicarboxylic acids (succinic acid C$_4$, and azelaic acid C$_9$) and aromatic derived compounds (terephthalic acid + phthalic acid)) were investigated via several approaches, including diagnostic ratios, correlation analysis, source indices analysis (Cmax, CPI, WNA% and ACL) and a PCA-MLR model.

Table 1 shows the average concentrations and ranges of $PM_{2.5}$, organic fraction and analysed organic species ranked from high average concentrations to low average concentrations. The concentrations of $PM_{2.5}$ and organic fraction were slightly higher in autumn than those in winter. The quantification of solvent-extractable and chromatographically identifiable organic compounds in $PM_{2.5}$ samples demonstrated that biomass burning, represented the chief source of identifiable polar organic aerosol constituents. Palmitic acid and monosaccharide anhydrides were dominant amongst the analysed polar organic compounds during both the autumn and winter sampling campaigns.

Table 1. Concentration ranking (high-low) of quantified organic species (ng·m^{-3}) and the concentration of $PM_{2.5}$ (µg·m^{-3}) and extractable organic fractions (µg·m^{-3}) during the autumn and winter sampling campaigns.

	Autumn			Winter	
Parameter	mean	range	Parameter	mean	range
$PM_{2.5}$ (µg·m^{-3})	9.4	6.5-13.8	$PM_{2.5}$ (µg·m^{-3})	7.1	4.0-12.0
Organic compounds (µg·m^{-3})	4.3	3.1-6.1	Organic compounds (µg·m^{-3})	2.9	0.6-7.4
Palmitic acid (ng m^{-3})	307.7	0.0-655.4	Palmitic acid (ng m^{-3})	287.1	0.0-557.0
monosaccharide anhydrides (ng m^{-3})	303.6	0-578.9	monosaccharide anhydrides (ng m^{-3})	281.9	0.0-593.5
Dehydroabietic acid (ng m^{-3})	50.7	0-96.8	Syringic acid (ng m^{-3})	89.5	0.0-263.4
Syringic acid (ng m^{-3})	32.2	0-133.7	Dehydroabietic acid (ng m^{-3})	29.4	0-100.6
N-alkanes (ng m^{-3})	29.3	14.7-66.4	N-alkanes (ng m^{-3})	23.1	17.4-33.1
Stearic acid (ng m^{-3})	12.3	6.4-21.8	Stearic acid (ng m^{-3})	10.9	4.3-28.2
Phthalic + Terephthalic acid (ng m^{-3})	10.5	0-40.2	Azelaic acid (ng m^{-3})	7.9	0-12.6
Azelaic acid (ng m^{-3})	9.0	0-17.4	Phthalic + Terephthalic acid (ng m^{-3})	3.7	0-20.8
Succinic acid (ng m^{-3})	3.6	0-10.5	Oleic acid (ng m^{-3})	3.6	0-22.6
PAHs (ng m^{-3})	2.9	2-4.8	PAHs (ng m^{-3})	3.3	1.6-10
Oleic acid (ng m^{-3})	1.1	0-6.6	Succinic acid (ng m^{-3})	0.4	0-1.7

Wildfires and prescribed bushfires (hazard reduction burns) are common and frequent throughout Australia, and even in a large urban region such as Greater Sydney contribute a large fraction to fine carbonaceous aerosols and further cause haze days, which deteriorate air quality. For this reason they have the potential to lead to impacts on human health through inhalation exposure (Hyde et al., 2017).

Most of the wildfires belong to natural-scale activities, although the incidence of human lit fires is difficult to estimate accurately. Burnt leaves and wood are part of a healthy natural cycle. Those residues are rich nutrients for soils. However, large areas of intensive uncontrolled wildfires sometimes influence human activities and harm residential properties

and safety. In some cases, anthropogenic activities such as unconsciously tossing cigarettes and human influenced climate change are also an important contributor to some wildfires worldwide (Keeley, 2009).

Prescribed bushfires or hazard reduction burns are an effective approach to reduce and prevent the hazardous disaster incurred by uncontrolled fires. In Australia, prescribed bushfires are usually performed before dry and hot periods to eliminate or lower the risk of possible uncontrolled wildfires and normally occur during appropriate meteorological conditions which assist dispersion and dissipation of the smoke in order to reduce the adverse health impacts of smoke from controlled burning and bushfires (Fernandes and Botelho, 2003; Hyde et al., 2017).

In our study we found that prescribed burnings have different emission patterns when compared with combustion for residential heating. In the latter case hardwood is mostly used, whereas prescribed burnings involve both hardwood and softwood combustion. Thus, in terms of organic molecular biomarkers, levels of typical softwood tracers such as dehydroabietic acid were investigated during prescribed burnings periods. Dehydroabietic acid had nearly opposite distribution during autumn and winter sampling campaigns. Dehydroabietic acid mostly appeared in autumn and was nearly absent in winter. On domestic heating burnings days, the predominant organic compounds were almost all hardwood organic molecular tracers. Syringic acid was detected mostly in winter rather than in autumn.

In addition, ratios of monosaccharide anhydrides reveal different contributions of different wood types during the two sampling seasons; in autumn wood combustion consisted of a major contribution from hardwood burning and a minor contribution from softwood burning. In winter hardwood and grass burning were the major contributors as determined by ratios of monosaccharide anhydrides.

On some occasions, higher concentrations of alkanes were observed in autumn (mean: 29.3 ng/m^3), while lower concentrations were measured in winter (mean: 23.1 ng/m^3). Further source indices analysis (Cmax, CPI, WNA% and ACL) reveal that fossil fuel combustion especially traffic exhaust made a contribution to n-alkanes, particularly in winter, while autumn had a slightly higher contribution from biogenic materials. Correlation analysis was carried out between individual species in n-alkanes homologous series, PAH_S, $PM_{2.5}$, organic matter and meteorological parameters (solar radiation, temperature and wind speed), which confirm the above source identification. Three distinct sources of n-alkanes were identified,

123

and their contributions were estimated using a principal component analysis (PCA) combined with multivariate linear regression (MLR) model; these sources were, fossil fuel combustion (74%), biomass burning + road dust (20%) and biogenic sources (6%).

Dicarboxylic acids (succinic acid, azelaic acid, phthalic acid and terephthalic acid) were formed through photo-chemical processing from anthropogenic precursors. The results of principle component analysis (PCA) elicit four groups, reflecting the contribution of biomass burning, secondary activities and traffic to $PM_{2.5}$.

PAHs had lower concentrations during this sampling campaign. Diagnostic ratios suggest 3-4 ring PAHs (fluoranthene, anthracene, pyrene, phenanthrene and benzo[a]pyrene) may have been contributed from traffic emissions, whereas 5-6 rings PAHs, such as benzo[a]anthracene, chrysene, indeno[1,2,3-c,d]pyrene and benzo[g,h,i]perylene appear to arise at least in part from biomass burning.

5.1.2 Radiocarbon analysis to distinguish fossil/non-fossil and primary/secondary sources of carbonaceous aerosols

Table 2. Concentrations of analysed organic compounds ($\mu g \cdot m^{-3}$), $PM_{2.5}$ ($\mu g \cdot m^{-3}$) and their percentage measured as a proportion of total $PM_{2.5}$ ($\mu g \cdot m^{-3}$) during the 2014 autumn and winter sampling campaigns.

Date	Total analyzed organic compounds	$PM_{2.5}$	Percentage
18/05/2014	0.8	10.4	8%
20/05/2014	1.2	7.4	17%
22/05/2014	1.1	13.8	8%
24/05/2014	0.6	10.7	5%
26/05/2014	0.3	10	3%
28/05/2014	0.0	7.1	1%
30/05/2014	1.0	6.5	16%
01/06/2014	1.0	6.2	16%
03/06/2014	0.6	4.9	13%
05/06/2014	0.8	7.1	11%
12/06/2014	1.0	10.9	9%
14/06/2014	1.3	7.6	17%
16/06/2014	0.5	5.9	9%
18/06/2014	0.7	7.6	9%
20/06/2014	0.9	6	15%
22/06/2014	1.1	12	10%
24/06/2014	0.1	4	1%
26/06/2014	0.2	7.9	2%
28/06/2014	0.3	5.1	6%

Although characterization of polar and non-polar organic compounds is conductive to source assessment of particulate matter, in this study total analyzed organic compounds comprised 1-17% of total $PM_{2.5}$ (Table 2) measured during 2014 autumn and winter sampling campaigns, the sources and proportions of the rest of organic fraction and elemental carbon are still unclear. It is apparent that some common biomarkers, such as PAHs and n-alkanes, unlike specific source biomarkers (i.e. levoglucosan), may have multiple contributors, which creates difficulties and uncertainties when source apportionment is conducted. Specifically, PAHs and n-alkanes can derive both/either from fossil primary sources and/or non-fossil fuel primary sources (traffic and biomass burning) (Chow and Watson, 2002; El Haddad et al., 2009; Heo et al., 2013; Ravindra et al., 2001; Wang et al., 2015). Similarly, some secondary biomarkers, for example, phthalic acid, terephthalic acid and azelaic acid, can originate either or both from fossil derived secondary atmospheric formation processes and/or non-fossil fuel derived secondary atmospheric formation processes. In addition, succinic acid can stem from primary emissions or from secondary sources or from both sources.

Thus, due to the variety and complexities of potential $PM_{2.5}$ sources and compositions, a robust technique (radiocarbon analysis) was performed on various carbon sub-fractions to determine more detailed information about different sources for the materials collected during the sampling campaigns described in Chapter 4.

A subset of eight $PM_{2.5}$ samples from this study was selected for ^{14}C measurements. To facilitate assigning fossil and non-fossil contributions to each carbon species, water insoluble total carbon was quantified and analysed for both bulk carbon and using ^{14}C analysis. Using ^{14}C measurements in different carbonaceous fractions, the relative contributions of fossil and non-fossil sources to carbonaceous particles are firstly quantified in this study.

The comparison of the concentrations of all variables and the contributions of carbonaceous sub-fractions under different seasonal conditions (winter and summer) suggest that the formation and increases in carbonaceous matter can be attributed to different factors at different times of the year. Domestic heating in winter is a major contributor for enhanced ambient carbon material. In summer, higher solar radiation increases SOC levels and enhances the concentration of PM. Higher levels of old carbon in Sydney principally result from mobile combustion sources, whereas, increases in contemporary carbon at both the Rozelle and MQ sites appear to be mainly due to influences from biomass burning.

During atmospheric haze events, a large increase of the non-fossil contribution of 440–500% was observed, as a result of the enhanced open biomass-burning activities. At the same time, SOC$_{nf}$ levels were significantly increased, which suggests that the extensive emissions of primary sources largely elevate the PM concentration not only directly but also by way of secondary particle formation, particularly SOC$_{nf}$, which has a faster formation rate than SOC$_f$ (Wang et al., 2013).

Consequently, some measures and actions might be considered for mitigating particle air pollution in Sydney. Policy makers may need to consider improving the prediction of the best timing for hazard prevention/reduction burns to avoid meteorological conditions conductive to high pollutant concentrations. However stable conditions with lower wind speeds are usually safer to avoid runaway fires during hazard reduction burns.

5.2. Limitations, Improvements and Recommendations for future work

5.2.1 Limitations and Improvements

With respect to characterization of organic biomarkers, more information and convincing conclusions would be revealed if more particulate samples are analyzed and particular secondary organic biomarkers are included, such as secondary biogenic biomarkers listed in Table 1.3 of Chapter 1. On the one hand, more samples (> 20 samples) can enhance the reliability of the results of factor analysis, on the other hand, measurements of secondary biogenic biomarkers (isoprene derived biomarkers, monoterpenes derived biomarkers and cineole derived biomarkers) can specify the biogenic derived secondary sources, which can further reveal the compositions and contributions of summer carbonaceous aerosols. The time requirements of sample collection, sample treatment, quantitative and qualitative analyses, and interpretation of the results obtained precluded the collection of additional samples in the scope of this PhD project.

Regarding the OC/EC protocol, a standardized OC/EC protocol would be preferable for further radiocarbon analyses of various carbon fractions but it is recognized that this has proved to be difficult in many locations. Since there are several OC/EC protocols conducted in different labs worldwide, method-dependent distinction of various carbon fractions would bring large differentiation of radiocarbon levels in various carbon fractions, especially for

refractory part of carbon, which could bring difficulties for further data comparison from different labs (Szidat et al., 2013). A more detailed OC/EC protocol should be considered and established according to different composition/sources of fine carbonaceous aerosols. For example, water soluble organic carbon dominated samples probably need higher OC/EC separation degree, whereas refractory dominated aerosols can be separated in lower temperature.

Furthermore, a refined source apportionment results can be concluded if some specific biomarker and emissions data are involved. Use of models such as Openair (http://www.openair-project.org/Default.aspx) might also reveal more source information from the perspective of geographic distribution.

5.2.2 Recommendations for future work

Apart from the division of fossil/contemporary and primary/secondary sources of carbonaceous aerosols, a division between anthropogenic and natural sources is needed to better constitute and implement relevant regulation policy with respect to climate and human health benefits. Identification and quantification of anthropogenic and natural sources of carbonaceous aerosols can provide policy-maker scientific evidence for mitigating air pollution.

Data from ^{14}C analyses are therefore usefully combined with other information to inform an elaborate source apportionment of carbonaceous aerosols, such as organic biomarker for identifying specific sources (levoglucosan for biomass burning, hopane and sterane for traffic, SOA tracers for SOA, etc)., The modern carbon component for each carbon fraction, organic tracers and gas pollutant data can be incorporated into a PMF analysis for decoupling anthropogenic and biogenic mixed sources. This would significantly aid the confirmation of PMF factor interpretations and help to reveal the relative contributions of sources allocated to mixed or unresolved factors.

The use of HR-ToF-AMS might yield very relevant data on the origin of the OA, especially if combined with speciation of organic aerosol and ^{14}C analysis. Moreover, a synthesis of various techniques and measurements, such as surface online/offline and satellite-based measurements combined with modelling will be a tendency to comprehend air pollution in the future.

References

Chow, J.C., Watson, J.G., 2002. Review of PM2. 5 and PM10 apportionment for fossil fuel combustion and other sources by the chemical mass balance receptor model. Energy & Fuels 16, 222-260.

El Haddad, I., Marchand, N., Dron, J., Temime-Roussel, B., Quivet, E., Wortham, H., Jaffrezo, J.L., Baduel, C., Voisin, D., Besombes, J.L., 2009. Comprehensive primary particulate organic characterization of vehicular exhaust emissions in France. Atmospheric Environment 43, 6190-6198.

Fernandes, P.M., Botelho, H.S., 2003. A review of prescribed burning effectiveness in fire hazard reduction. International Journal of wildland fire 12, 117-128.

Heo, J., Dulger, M., Olson, M.R., McGinnis, J.E., Shelton, B.R., Matsunaga, A., Sioutas, C., Schauer, J.J., 2013. Source apportionments of PM2. 5 organic carbon using molecular marker Positive Matrix Factorization and comparison of results from different receptor models. Atmospheric environment 73, 51-61.

Hyde, J.C., Yedinak, K.M., Talhelm, A.F., Smith, A.M., Bowman, D.M., Johnston, F.H., Lahm, P., Fitch, M., Tinkham, W.T., 2017. Air quality policy and fire management responses addressing smoke from wildland fires in the United States and Australia. International Journal of Wildland Fire 26, 347-363.

Keeley, J.E., 2009. Fire intensity, fire severity and burn severity: a brief review and suggested usage. International Journal of Wildland Fire 18, 116-126.

Ravindra, K., Mittal, A.K., Van Grieken, R., 2001. Health risk assessment of urban suspended particulate matter with special reference to polycyclic aromatic hydrocarbons: a review. Reviews on environmental health.

Szidat, S., Bench, G., Bernardoni, V., Calzolai, G., Czimczik, C.I., Derendorp, L., Dusek, U., Elder, K., Fedi, M., Genberg, J., 2013. Intercomparison of 14 C analysis of carbonaceous aerosols: exercise 2009. Radiocarbon 55, 1496-1509.

Wang, G.-h., Zeng, Y.-s., Yao, J., Qian, Y., Huang, Y., Liu, K., Liu, W., Li, Y., 2013. Source apportionment of atmospheric carbonaceous particulate matter based on the radiocarbon. Journal of Radioanalytical and Nuclear Chemistry 295, 1545-1552.

Wang, J., Ho, S.S.H., Cao, J., Huang, R., Zhou, J., Zhao, Y., Xu, H., Liu, S., Wang, G., Shen, Z., 2015. Characteristics and major sources of carbonaceous aerosols in PM2. 5 from Sanya, China. Science of the Total Environment 530, 110-119.

APPENDICES

Appendix A: Supplementary Information for Chapter Two

Supplementary Table S1

Supplementary Table S2

Supplementary Table S3

Supplementary Table S4

Supplementary Table S5

Supplementary Table S6

Supplementary Table S7

Supplementary Table S8

Supplementary Table S9

Appendix B: Supplementary Information for Chapter Three

Supplementary Table S1

Supplementary Table S2

Supplementary Table S3

Appendix C: Supplementary Information for Chapter Four

Supplementary Table S1

Supplementary Table S2

Supplementary Information S3

Supplementary Table S4

Supplementary References

Appendix A: Supplementary Information for Chapter Two

Supplementary Table S1. Meteorological parameters (temperature ($°C$), wind speed (m/s) and solar radiation (w/m^2)), concentrations of PM$_{2.5}$ (µg·m^{-3}), Organic compounds (µg·m^{-3}), PAHs (ng·m^{-3}) and n-alkanes (ng·m^{-3}) and ratios of PAHs/organic compounds (x10^4) and n-alkanes/organic compounds (x10^4) during autumn sampling campaign

Parameter	Date						
	18/5/2014	20/5/2014	22/5/2014	24/5/2014	26/5/2014	28/5/2014	30/5/2014
Temperature	8.5	9.5	8.9	12.0	10.1	8.2	12.3
Wind speed	0.6	0.9	0.8	1.0	1.0	1.6	1.2
Solar radiation	51.8	40.8	50.6	31.5	41.1	31.2	33.0
PM$_{2.5}$	10.4	7.4	13.8	10.7	10.0	7.1	6.5
Organic compounds	4.3	3.7	6.1	4.6	4.0	3.1	4.0
PAHs	4.3	2.3	2.7	4.8	2.0	2.0	2.0
N-alkanes	66.4	32.2	25.9	22.2	21.9	14.7	22.11
PAHs/organic compounds (x10^4)	10.1	6.3	4.4	10.3	5.0	6.6	5.0
N-alkanes/organic compounds (x10^4)	216.2	124.0	61.4	71.3	77.5	67.9	76.1

Supplementary Table S2. Meteorological parameters (temperature ($°C$), wind speed (m/s) and solar radiation (w/m^2)), concentrations of PM$_{2.5}$ (µg·m^{-3}), Organic compounds (µg·m^{-3}), PAHs (ng·m^{-3}) and n-alkanes (ng·m^{-3}) and ratios of PAHs/organic compounds (x10^4) and n-alkanes/organic compounds (x10^4) during winter sampling campaign.

Parameter	Date											
	1/6/ 2014	3/6/ 2014	5/6/ 2014	12/6/ 2014	14/6/ 2014	16/6/ 2014	18/6/ 2014	20/6/ 2014	22/6/ 2014	24/6/ 2014	26/6/ 2014	28/6/ 2014
Temperature	10.5	5.9	13.0	6.9	7.2	4.9	6.6	5.8	5.2	6.7	4.2	4.5
Wind speed	0.8	0.9	1.0	0.6	1.1	1.2	1.0	0.9	0.9	2.6	1.4	2.7
Solar radiation	47.2	38.7	29.8	37.7	30.1	27.1	41.4	39.2	25.3	12.3	18.1	10.4
PM$_{2.5}$	6.2	4.9	7.1	10.9	7.6	5.9	7.6	6.0	12.0	4.0	7.9	5.1
Organic compounds	2.8	2.2	5.5	3.7	2.8	1.5	4.4	2.2	7.4	0.6	0.9	0.6
PAHs	2.9	2.0	2.8	4.8	3.9	2.3	3.4	2.8	10.0	1.6	1.6	1.6
N-alkanes	23.3	26.3	17.8	17.4	26.4	33.1	19.3	18.0	26.1	23.5	20.8	25.7
PAHs/organic compounds (x10^4)	10.6	9.4	5.1	13.1	14.1	15.0	7.8	12.9	13.5	26.5	17.6	26.7
N-alkanes/ organic compounds (x10^4)	115.2	166.2	43.1	64.1	127.3	294.2	60.9	114.7	50.1	540.0	308.5	588.9

Supplementary Table S3. 16 PAHs concentrations (ng·m^{-3}) during autumn sampling campaign.

PAH	Date						
	18/5/2014	20/5/2014	22/5/2014	24/5/2014	26/5/2014	28/5/2014	30/5/2014
Nap	0.03	0.01	0.02	0.03	0.02	0.02	0.02
Acy	0.04	0.04	0.03	0.04	0.03	0.03	0.03
Ace	0.05	0.03	0.02	0.02	0.03	0.02	0.02
Flo	0.03	0.03	0.03	0.03	0.03	0.03	0.03
Phe	0.07	0.05	0.06	0.08	0.05	0.06	0.06
Ant	0.07	0.07	0.07	0.08	0.07	0.09	0.10
Flu	0.09	0.06	0.07	0.08	0.06	0.06	0.07
Pyr	0.11	0.06	0.07	0.09	0.06	0.07	0.06
BaA	0.20	0.16	0.17	0.19	0.16	0.16	0.17
Chry	0.18	0.15	0.16	0.18	0.15	0.15	0.16
BbF	0.45	0.30	0.35	0.47	0.29	0.29	0.37
BkF	0.42	0.29	0.33	0.43	0.28	0.28	0.34
BaP	0.39	0.33	0.39	0.41	0.00	0.00	0.00
InP	1.36	0.41	0.65	1.72	0.43	0.42	0.57
DbA	0.00	0.00	0.00	0.00	0.00	0.00	0.00
BgP	0.84	0.33	0.31	0.92	0.36	0.34	0.00

Nap: naphthalene, Acy: acenaphthylene, Ace: acenaphthene, Flo: fluorene, Phe: phenanthrene, Ant: anthracene, Flu: fluoranthene, Pyr: pyrene, BaA: bbenzo[a]anthracene, Chry: chrysene, BbF: benzo[b]fluoranthene, BkF: benzo[k]fluoranthene, BaP: benzo[a]pyrene, InP: indeno[1,2,3-c,d]pyrene, DbA: dibenzo[a,h]anthracene, BgP: benzo[g,h,i]perylene.

Supplementary Table S4. 16 PAHs concentrations (ng·m^{-3}) during winter sampling campaign.

PAH	Date											
	1/6/2014	3/6/2014	5/6/2014	12/6/2014	14/6/2014	16/6/2014	18/6/2014	20/6/2014	22/6/2014	24/6/2014	26/6/2014	28/6/2014
Nap	0.01	0.01	0.01	0.02	0.01	0.01	0.01	0.01	0.02	0.01	0.01	0.01
Acy	0.03	0.03	0.03	0.04	0.03	0.03	0.03	0.03	0.04	0.03	0.03	0.03
Ace	0.04	0.02	0.03	0.05	0.02	0.02	0.03	0.02	0.02	0.02	0.02	0.03
Flo	0.03	0.03	0.03	0.03	0.03	0.03	0.03	0.03	0.03	0.03	0.03	0.03
Phe	0.05	0.05	0.05	0.06	0.05	0.04	0.05	0.05	0.06	0.04	0.04	0.04
Ant	0.07	0.07	0.07	0.08	0.07	0.07	0.07	0.07	0.08	0.07	0.07	0.08
Flu	0.07	0.06	0.07	0.08	0.07	0.05	0.06	0.06	0.11	0.05	0.05	0.05
Pyr	0.07	0.06	0.07	0.09	0.07	0.06	0.07	0.07	0.12	0.05	0.05	0.05
BaA	0.17	0.16	0.17	0.21	0.19	0.16	0.18	0.17	0.26	0.16	0.16	0.17
Chry	0.16	0.15	0.16	0.19	0.17	0.14	0.16	0.15	0.24	0.14	0.14	0.14
BbF	0.36	0.30	0.35	0.50	0.43	0.30	0.39	0.34	0.93	0.26	0.26	0.26
BkF	0.34	0.30	0.33	0.48	0.41	0.29	0.38	0.33	0.84	0.25	0.26	0.26
BaP	0.00	0.00	0.39	0.55	0.00	0.29	0.42	0.35	0.99	0.00	0.00	0.00
InP	0.95	0.43	0.60	1.58	1.32	0.44	0.94	0.65	3.96	0.00	0.24	0.23

DbA	0.00	0.00	0.00	0.00	0.34	0.00	0.00	0.00	0.57	0.25	0.00	0.00
BgP	0.57	0.35	0.45	0.85	0.70	0.35	0.55	0.44	1.72	0.27	0.27	0.27

Nap: naphthalene, Acy: acenaphthylene, Ace: acenaphthene, Flo: fluorene, Phe: phenanthrene, Ant: anthracene, Flu: fluoranthene, Pyr: pyrene, BaA: bbenzo[a]anthracene, Chry: chrysene, BbF: benzo[b]fluoranthene, BkF: benzo[k]fluoranthene, BaP: benzo[a]pyrene, InP: indeno[1,2,3-c,d]pyrene, DbA: dibenzo[a,h]anthracene, BgP: benzo[g,h,i]perylene.

Supplementary Table S5. Concentrations (ng·m^{-3}) of n-alkanes during autumn sampling campaign.

N-alkane	Date						
	18/5/2014	20/5/2014	22/5/2014	24/5/2014	26/5/2014	28/5/2014	30/5/2014
C_{17}	0.03	0.03	0.04	0.05	0.04	0.03	0.03
C_{18}	0.07	0.04	0.05	0.05	0.04	0.04	0.03
C_{19}	0.14	0.04	0.07	0.04	0.06	0.04	0.04
C_{20}	0.18	0.08	0.09	0.17	0.10	0.10	0.06
C_{21}	0.22	0.13	0.11	0.14	0.12	0.14	0.06
C_{22}	0.27	0.17	0.13	0.16	0.10	0.19	0.09
C_{17}-C_{22}	0.90	0.48	0.49	0.61	0.45	0.55	0.30
C_{23}	0.55	0.34	0.26	0.00	0.22	0.28	0.21
C_{24}	1.31	0.69	0.53	0.49	0.43	0.40	0.51
C_{25}	2.54	1.34	1.15	0.99	0.97	0.64	1.02
C_{26}	4.16	2.03	1.60	1.40	1.37	0.88	1.61
C_{23}-C_{26}	8.57	4.40	3.53	2.89	2.99	2.21	3.36
C_{27}	7.09	3.54	3.47	2.64	2.70	1.47	2.61
C_{27} fossil	6.74	3.30	2.48	2.18	1.99	1.42	2.40
C_{27} wax	0.35	0.24	1.00	0.46	0.71	0.05	0.21
C_{28}	9.32	4.57	3.36	2.96	2.60	1.95	3.19
C_{29}	19.47	10.12	8.37	7.96	6.46	4.67	5.63
C_{29} fossil	15.19	6.82	5.02	4.06	4.65	2.91	5.11
C_{29} wax	4.29	3.30	3.35	3.90	1.81	1.76	0.52
C_{30}	21.05	9.06	6.68	5.16	6.69	3.87	7.02

Supplementary Table S6. Concentrations (ng·m^{-3}) of n-alkanes during winter sampling campaign.

N-alkane	Date											
	1/6/ 2014	3/6/ 2014	5/6/ 2014	12/6/ 2014	14/6/ 2014	16/6/ 2014	18/6/ 2014	20/6/ 2014	22/6/ 2014	24/6/ 2014	26/6/ 2014	28/6/ 2014
C_{17}	0.03	0.03	0.04	0.06	0.03	0.02	0.03	0.02	0.28	0.02	0.02	0.02
C_{18}	0.03	0.04	0.06	0.05	0.03	0.03	0.04	0.03	0.04	0.02	0.03	0.03
C_{19}	0.03	0.05	0.06	0.07	0.02	0.04	0.03	0.03	0.03	0.03	0.02	0.03
C_{20}	0.08	0.09	0.06	0.12	0.10	0.04	0.06	0.06	0.08	0.04	0.03	0.04
C_{21}	0.08	0.09	0.20	0.13	0.10	0.07	0.10	0.06	0.07	0.06	0.09	0.05
C_{22}	0.12	0.13	0.20	0.15	0.13	0.12	0.13	0.08	0.13	0.08	0.14	0.09
C_{17}-C_{22}	0.37	0.44	0.61	0.58	0.43	0.32	0.39	0.29	0.63	0.24	0.34	0.26
C_{23}	0.26	0.27	0.32	0.23	0.27	0.30	0.00	0.16	0.00	0.18	0.24	0.20
C_{24}	0.51	0.61	0.48	0.46	0.54	0.77	0.49	0.39	0.58	0.45	0.51	0.54
C_{25}	1.09	1.22	0.97	0.93	1.13	1.46	0.80	0.77	1.33	0.91	0.87	1.02
C_{26}	1.66	2.04	1.19	1.24	1.83	2.45	1.29	1.19	1.74	1.45	1.36	1.60
C_{23}-C_{26}	3.52	4.14	2.95	2.86	3.76	4.99	2.58	2.51	3.66	2.98	2.98	3.35
C_{27}	2.53	2.91	1.88	2.09	2.63	3.51	2.13	1.99	2.97	2.49	2.13	2.67
C_{27} fossil	2.49	2.91	1.85	1.86	2.63	3.51	2.07	1.94	2.64	2.37	2.13	2.63
C_{27} wax	0.04	0.00	0.04	0.23	0.00	0.00	0.05	0.05	0.34	0.12	0.00	0.04
C_{28}	3.31	3.96	2.51	2.48	3.61	4.71	2.86	2.68	3.53	3.29	3.01	3.65
C_{29}	6.04	6.51	4.18	4.17	6.20	8.59	5.16	4.67	7.88	7.26	5.54	7.75
C_{29} fossil	5.42	6.17	4.08	3.84	6.20	7.85	4.49	4.29	5.48	5.25	4.89	5.83
C_{29} wax	0.62	0.34	0.09	0.33	0.00	0.74	0.67	0.38	2.40	2.00	0.66	1.91
C_{30}	7.53	8.38	5.66	5.20	9.76	10.99	6.13	5.89	7.42	7.21	6.77	8.01

Supplementary Table S7. Correlation analysis between individual species in n-alkanes homologous series, other related parameters (TAL: total n-alkanes, PM$_{2.5}$ and OM: organic matter) and meteorological parameters (SR: solar radiation, T: temperature and WS: wind speed).

	C_{18}	C_{19}	C_{20}	C_{21}	C_{22}	C_{23}	C_{24}	C_{25}	C_{26}	C_{27}	C_{27} F[a]	C_{27} W[a]	C_{28}	C_{29}	C_{29} F[a]	C_{29} W[a]	C_{30}	TAL	PM$_{2.5}$	OM	SR	T	WS
C_{17}	.1	-.1	.1	-.1	.0	-.4*	.0	.1	.0	.0	.2	.0	.0	-.1	.2	.0	-.1	.0	.5*	.6**	-.1	-.2	-.2
C_{18}		.8**	.7**	.9**	.8**	.4	.5*	.5*	.4	.4	.4	.5*	.4	.4	.5*	.5*	.4	.5*	.6**	.6**	.5**	.4	-.6
C_{19}			.7**	.7**	.7**	.6**	.7**	.7**	.7**	.7**	.4*	.8**	.7**	.7**	.5*	.7**	.7**	.7**	.5*	.4	.6**	.3	-.4
C_{20}				.7**	.6**	.2	.4*	.5*	.4	.4	.4*	.5*	.4	.4	.6**	.5*	.4	.5*	.6**	.5*	.6**	.4	-.5
C_{21}					.9**	.5*	.5*	.4*	.4	.4	.3	.4	.4	.4	.4	.4*	.4	.4	.4	.5*	.5*	.5*	-.5
C_{22}						.6**	.6**	.6**	.5*	.5*	.1	.5*	.6**	.5*	.4	.6**	.5*	.6**	.4	.4	.4	.3	-.4
C_{23}							.6**	.6**	.6**	.6**	.0	.6**	.6**	.6**	.1	.5*	.7**	.6**	-.1	-.2	.3	.1	-.1
C_{24}								1.0**	1.0**	1.0**	.1	1.0**	1.0**	1.0**	.5*	.9**	1.0**	1.0**	.2	.1	.3	.0	-.3
C_{25}									1.0**	1.0**	.2	1.0**	1.0**	1.0**	.5*	.9**	1.0**	1.0**	.3	.2	.4	.0	-.3
C_{26}										1.0**	.1	1.0**	1.0**	1.0**	.4*	.9**	1.0**	1.0**	.1	.0	.3	-.1	-.2
C_{27}											.1	1.0**	1.0**	1.0**	.5*	1.0*	1.0**	1.0**	.1	.0	.3	-.1	-.2

134

	C27 W	C28	C29	C29 F	C29 W	C30	TAL	PM2.5	OM	SR	T	WS
C27 Fa	.3	.1	.1	.6**	.3	.0	.2	.8**	.6**	.5*	.4	-.3
C27 Wa		1.0**	1.0**	.6**	1.0*	.9**	1.0**	.3	.2	.4	.0	-.3
C28			1.0*	.5*	1.0*	1.0**	1.0**	.1	.0	.3	-.1	-.2
C29				.4*	.9**	1.0**	1.0**	.1	.0	.3	-.1	-.2
C29 Fa					.7**	.4	.6**	.5*	.4	.2	.2	.0
C29 Wa						.9**	1.0**	.3	.1	.3	.0	-.1
C30							1.0**	.1	.0	.3	-.1	-.2
TAL								.2	.1	.3	.0	-.2
PM2.5									.8**	.5	.2	-.6
OM										.5*	.5*	-.6
SR											.4	-.8
T												-.3

a F: fossil; W: wax

*. Correlation is significant at the 0.05 level (2-tailed)-highlighted in green.

**. Correlation is significant at the 0.01 level (2-tailed)-highlighted in yellow.

Supplementary Table S8. Correlation analysis between individual species of PAHs congeners, other related parameters (TAL: total n-alkanes, $PM_{2.5}$ and OM: organic matter) and meteorological parameters (SR: solar radiation, T: temperature and WS: wind speed).

	Nap	Acy	Ace	Phe	Ant	Flu	Pyr	BaA	Chry	BbF	BkF	BaP	InP	DbA	BgP	PM2.5	OM	SR	T	WS	TAL
T PAHs	.4	.6**	.1	.5*	.1	.9*	.9*	1.0*	1.0*	1.0**	1.0**	.8**	1.0**	.7**	1.0**	.6**	.7	.1	-.1	-.4	.1
Nap		.6**	.2	.9*	.4	.6*	.6*	.4	.5*	.4	.4	.3	.4	.0	.4	.7**	.5*	.4	.4	-.3	.4
Acy			.4	.6*	.2	.7*	.7*	.6**	.6**	.6**	.6**	.6**	.6**	.2	.6**	.6**	.5*	.2	.2	-.4	.4
Ace				.2	-.1	.3	.4	.2	.2	.1	.1	.2	.1	-.3	.2	.2	.1	.4	.2	-.3	.4
Phe					.4	.7*	.7*	.5*	.6*	.5*	.5*	.4	.5*	.0	.5*	.7**	.7	.5*	.5	-.5	.3
Ant						.2	.1	.2	.2	.2	.2	.0	.1	.0	-.1	.1	.2	-.2	.3	.1	-.2
Flu							.9*	.9**	1.0*	.9**	.9**	.7**	.9**	.5	.8**	.7**	.8	.3	.2	-.5	.3
Pyr								.9**	.9*	.9**	.9**	.8**	.9**	.4	.9**	.7**	.7	.4	.1	-.5	.4
BaA									1.0*	1.0**	1.0**	.8**	1.0**	.7**	.9**	.6**	.6	.0	-.1	-.3	.2
Chry										1.0**	1.0**	.8**	1.0**	.6**	.9**	.6**	.7	.2	.1	-.4*	.1
BbF											1.0**	.8**	1.0**	.7**	.9**	.6**	.7	.1	-.1	-.4	.1
BkF												.8**	1.0**	.7**	.9**	.6**	.7	.1	-.1	-.4	.1
BaP													.8**	.4	.8**	.6**	.7	.2	-.1	-.5	.1
InP														.7**	1.0**	.6**	.7	.1	-.1	-.4	.1
DbA															.7**	.1	.3	-.4	-.3	.1	.0
BgP																.5*	.6	.1	-.1	-.4	.2
PM2.5																	.8	.5	.2	-.6**	.2
OM																		.5	.5	-.6	.1
SR																			.4	-.8**	.3
T																				-.3	.0
WS																					-.2

*. Correlation is significant at the 0.05 level (2-tailed) -highlighted in green.

**. Correlation is significant at the 0.01 level (2-tailed) -highlighted in yellow.

Supplementary Table S9. Correlation analysis between individual species of PAHs congeners and n-alkanes.

	Nap	Acy	Ace	Phe	Ant	Flu	Pyr	BaA	Chry	BbF	BkF	BaP	InP	DbA	BgP
C_{17}	.2	.4	-.1	.3	.2	.8**	.7**	.9**	.9**	.9**	.9**	.7**	.9**	.8**	.8**
C_{18}	.6**	.5*	.5*	.7**	-.1	.5**	.6**	.3	.4	.3	.3	.5*	.3	-.2	.3
C_{19}	.6**	.4	.6**	.5*	-.1	.4	.5*	.2	.2	.1	.1	.2	.1	-.3	.1
C_{20}	.8**	.7**	.4	.9**	.1	.6**	.7**	.4	.5*	.3	.3	.3	.4	-.1	.4*
C_{21}	.5*	.4*	.5*	.5*	-.1	.4	.4	.1	.2	.0	.0	.2	.1	-.3	.2
C_{22}	.5*	.5*	.5*	.5*	-.1	.4	.5*	.2	.3	.2	.1	.3	.2	-.2	.3
C_{23}	.0	.0	.4	-.1	-.2	-.1	-.1	-.3	-.3	-.4	-.4	-.3	-.4	-.4	-.3
C_{24}	.4	.4	.4*	.2	-.2	.3	.4	.2	.2	.1	.1	.2	.1	-.1	.2
C_{25}	.4	.5*	.4*	.3	-.2	.4	.5*	.3	.3	.2	.2	.3	.2	.1	.3
C_{26}	.3	.4	.4	.2	-.2	.3	.4	.2	.1	.1	.1	.1	.1	.0	.2
C_{27} fossil	.3	.4	.4	.2	-.2	.3	.4	.2	.1	.1	.1	.1	.1	.0	.2
C_{27} wax	.6**	.3	.0	.5*	.0	.4	.3	.1	.3	.2	.2	.3	.2	.0	.1
C_{27}	.5*	.5*	.4	.3	-.2	.4	.4	.2	.2	.1	.1	.2	.1	.0	.2
C_{28}	.3	.4	.4	.2	-.2	.3	.4	.2	.1	.1	.1	.1	.1	.0	.2
C_{29} fossil	.3	.3	.4*	.2	-.3	.2	.3	.1	.1	.1	.1	.1	.1	.0	.1
C_{29} wax	.7**	.6**	.1	.6**	.0	.3	.4	.2	.2	.2	.1	.3	.2	.0	.2
C_{29}	.5*	.5*	.4	.3	-.2	.3	.4	.2	.2	.1	.1	.2	.1	.0	.2
C_{30}	.2	.3	.4	.1	-.3	.2	.3	.1	.1	.1	.1	.1	.1	.0	.1

Appendix B: Supplementary Information for Chapter Three

Supplementary Table S1. Concentrations of quantified polar organic compounds during autumn sampling campaign (ng/m^3).

Compound	Date						
	18/5/2014	20/5/2014	22/5/2014	24/5/2014	26/5/2014	28/5/2014	30/5/2014
Levoglucosan	452.5	402.6	233.3	297.7	124.5	0.0	315.8
Mannosan	0.0	0.0	0.0	0.0	4.8	0.0	0.0
Galacotsan	126.4	128.0	0.0	0.0	2.1	0.0	37.5
Dehydroabietic acid	50.8	96.8	66.9	73.1	67.2	0.0	0.0
Syringic acid	92.0	0.0	0.0	133.7	0.0	0.0	0.0
Palmitic acid	n.d.	567.5	655.4	0.0	0.0	0.0	623.5
Stearic acid	21.8	13.8	11.7	9.6	9.3	6.4	13.7
Oleic acid	n.d.	0.0	0.0	0.0	0.0	6.6	0.0
Succinic acid	0.0	0.0	9.7	0.0	10.5	0.0	4.9
Azelaic acid	0.0	0.0	17.4	14.1	13.7	7.5	10.5
Phthalic+Terephthalic acid	0.0	0.0	40.2	14.4	13.4	5.4	0.0

n.d.: not detected.

Supplementary Table S2. Concentrations of quantified polar organic compounds during winter sampling campaign (ng/m^3).

Compound	Date											
	1/6/ 2014	3/6/ 2014	5/6/ 2014	12/6/ 2014	14/6/ 2014	16/6/ 2014	18/6/ 2014	20/6/ 2014	22/6/ 2014	24/6/ 2014	26/6/ 2014	28/6/ 2014
Levoglucosan	269.8	66.5	202.7	262.6	458.4	308.9	498.0	298.7	593.5	0.0	94.7	n.d.
Mannosan	0.0	2.7	2.4	10.6	0.0	7.6	0.0	0.0	0.0	0.0	0.0	n.d.
Galacotsan	0.0	0.9	9.9	9.2	0.0	3.6	0.0	0.0	0.0	0.0	0.0	n.d.
Dehydroabietic acid	69.6	0.0	0.0	75.5	77.4	0.0	0.0	0.0	100.6	0.0	0.0	n.d.
Syringic acid	0.0	0.0	0.0	140.1	148.2	130.9	165.0	137.0	263.4	0.0	0.0	n.d.
Palmitic acid	557.0	510.8	499.5	467.4	538.0	0.0	0.0	433.2	108.2	21.5	25.2	284.0
Stearic acid	7.9	7.8	8.9	8.8	11.4	12.4	13.5	10.4	28.2	4.3	6.4	n.d.
Oleic acid	0.0	0.0	0.0	22.6	0.0	0.0	5.0	9.0	0.0	0.0	3.5	2.8
Succinic acid	0.0	1.5	0.0	0.0	0.0	1.1	0.0	1.7	0.0	0.0	0.0	0.0
Azelaic acid	12.2	8.3	8.1	11.2	9.8	7.9	9.1	8.3	12.6	0.0	7.3	0.0
Phthalic+ Terephthalic acid	20.8	0.0	0.0	0.0	15.0	3.9	5.2	0.0	0.0	0.0	0.0	0.0

n.d.: not detected.

Supplementary Table S3. Correlation analysis results of individual organic species, $PM_{2.5}$ and meteorological parameters.

	Mann	Gala	Dehy	Syringic acid	$C_{16:0}$	$C_{18:0}$	$C_{18:1}$	C_4	C_9	Phthalic+ Terephthalic acid	T	WS	SR	$PM_{2.5}$	OM
Levo	-0.1	0.3	.5*	.7**	0.2	.8**	0	-0.2	0.1	0	0	-.5*	0.3	0.4	.5*
Mann	1	-0.2	0	0.1	-0.1	-0.2	.6*	0.1	0.2	-0.2	-0.2	-0.2	0	0.1	-0.1
Gala		1	0.3	-0.2	0.4	0.4	-0.1	-0.1	-.6**	-0.3	0.2	-0.3	0.4	0.1	0.1
Dehy			1	0.3	0.2	0.4	0	0.1	0.3	0.4	0.2	-.5*	0.3	.7**	.5*
Syringic acid				1	-0.3	.6**	0.3	-0.4	0.2	-0.2	-0.4	-0.3	-0.1	0.3	0.3
$C_{16:0}$					1	0	0	0.2	0.1	0.2	0.3	-0.4	.5*	0	0.2
$C_{18:0}$						1	-0.2	0	0	-0.1	-0.1	-0.4	0.2	.5*	.7**
$C_{18:1}$							1	-0.2	0	-0.3	-0.3	-0.2	0.1	0.1	-0.1
C_4								1	.5*	.6**	0.3	-0.2	0.4	0.4	0.3
C_9									1	.6**	0.3	-.5*	0.4	.6**	.5*
Phthalic+ Terephthalic acid										1	0.3	-0.3	.5*	.5*	0.3
T											1	-0.3	0.4	0.2	.5*
WS												1	-.8**	-.6**	-.6**
SR													1	.5*	.5*
$PM_{2.5}$														1	.8**

*. Correlation is significant at the 0.05 level (2-tailed)-highlighted in green.
**. Correlation is significant at the 0.01 level (2-tailed) highlighted in green.
Only correlations statistically significant (at $p < 0.05$) and correlation coefficients > 0.5 are highlighted in green.
Levo: levoglucosan; Mann: mannosan; Gala: galactosan; Dehy: dehydroabietic acid; $C_{16:0}$: Palmitic acid; $C_{18:0}$: stearic acid; $C_{18:1}$: oleic acid; C_4: succinic acid; C_9: azelaic acid; T: temperature; WS: wind speed; SR: solar radiation; OM: organic matter.

Appendix C: Supplementary Information for Chapter Four

Supplementary Table S1. Radiocarbon results-Report on AMS analysis (AINSE Grant 16/031; RUN 456)

ANSTO code	Sample Type	Submitter ID	$\delta(^{13}C)$ per mil	percent Modern Carbon pMC 1σ error	Conventional Radiocarbon age yrs BP 1σ error
OZU291U1	Quartz filter (field blank)	R_S_FB TC fraction	-25.0*	28.38 +/− 0.27	10,120 +/− 80
OZU292U1	Quartz filter (field blank)	R_W_FB TC fraction	-25.0*	35.59 +/− 0.30	8,300 +/− 70
OZU293U1	Quartz filter (field blank)	MQ_S_FB TC fraction	-25.0*	21.81 +/− 0.17	12,230 +/− 70
OZU293U2	Quartz filter (field blank)	MQ_S_FB WINTC fraction	-25.0*	29.79 +/− 0.30	9,730 +/− 90
OZU294U1	Quartz filter (field blank)	MQ_W_FB TC fraction	-25.0*	42.18 +/− 0.40	6,940 +/− 80
OZU294U2	Quartz filter (field blank)	MQ_W_FB WINTC fraction	-25.0*	59.95 +/− 0.58	4,110 +/− 80
OZU274U1	Quartz filter-U1	MQ_W_HAZE TC fraction	-25.8 +/− 0.2	98.34 +/− 0.31	135 +/− 30
OZU274U2	Quartz filter-U2	MQ_W_HAZE WINTC fraction	-27.3 +/− 0.1	89.79 +/− 0.40	865 +/− 40
OZU275U1	Quartz filter-U1	R_W_HAZE TC fraction	-26.3 +/− 0.1	95.94 +/− 0.41	335 +/− 35
OZU275U2	Quartz filter-U2	R_W_HAZE WINTC fraction	-24.2 +/− 0.3	86.87 +/− 0.36	1,130 +/− 35
OZU276U1	Quartz filter-U1	R_S_HAZE TC fraction	-24.9 +/− 0.3	87.85 +/− 0.33	1,040 +/− 30
OZU276U2‡	Quartz filter-U2	R_S_HAZE WINTC fraction	-25.0*	81.04 +/− 0.49	1,690 +/− 50
OZU277U1	Quartz filter-U1	MQ_S_HAZE TC fraction	-25.0*	97.05 +/− 0.38	240 +/− 35
OZU277U2	Quartz filter-U2	MQ_S_HAZE WINTC fraction	-21.4 +/− 0.1	93.89 +/− 0.41	505 +/− 40
OZU278U1	Quartz filter-U1	MQ_W_WEEKEND TC fraction	-24.6 +/− 0.1	87.90 +/− 0.31	1,035 +/− 30

OZU278U2‡	Quartz filter-U2	MQ_W_WEEKEND WINTC fraction	-25.0 +/− 0.4	72.84 +/− 0.37	2,545 +/− 45
OZU279U1	Quartz filter-U1	R_W_WEEKEND TC fraction	-24.6 +/− 0.1	73.91 +/− 0.31	2,430 +/− 35
OZU279U2‡	Quartz filter-U2	R_W_WEEKEND WINTC fraction	-25.0*	59.47 +/− 0.29	4,175 +/− 40
OZU280U1	Quartz filter-U1	R_S_CLOUDY TC fraction	-24.6 +/− 0.4	73.73 +/− 0.35	2,450 +/− 40
OZU280U2‡	Quartz filter-U2	R_S_CLOUDY WINTC fraction	-25.0*	53.41 +/− 0.28	5,035 +/− 45
OZU281U1‡	Quartz filter-U1	MQ_S_CLOUDY TC fraction	-25.2 +/− 0.1	80.95 +/− 0.42	1,695 +/− 45
OZU281U2‡	Quartz filter-U2	MQ_S_CLOUDY WINTC fraction	-23.6	71.84 +/− 0.47	2,660 +/−60

* = The value of $\delta(^{13}C)$ is assumed. A measured value is not available.

‡ = A small mass correction has been applied to this sample (refer note 3)

Note:

1 $\delta(^{13}C)$ values relate solely to the graphite derived from the fraction that was used for the radiocarbon measurement. It is sometimes the case that the $\delta(^{13}C)$ of this fraction is not the same as that of the bulk material. Measurements are determined using EA-IRMS (except for those, if present, marked with '$' which are accelerator based). Some $\delta(^{13}C)$ values may not have an associated uncertainty due to the limited number of determinations.

2 The ages quoted are radiocarbon ages, not calendar ages.

3 For some samples, the relatively large error is due to the small sample size.

4 The ages have been rounded according to M. Stuiver and A. Polach (Stuiver and Polach, 1977). The definition of percent Modern Carbon and Conventional Radiocarbon age can also be found in this publication.

Issued by Andrew Jenkinson, Email: avj@ansto.gov.au; Tel: +61-2-97173478; Centre for Accelerator Science, ANSTO, Locked Bag 2001 Kirrawee DC NSW 2232 (AUSTRALIA); http://www.ansto.gov.au/ResearchHub/acceleratorsciencecentre/index.htm

Supplementary Table S2. Radiocarbon results-Report on AMS analysis (AINSE Grant 16/031; ANSTO Portal 10171; RUN 458)

ANSTO code	Sample Type	Submitter ID	$\delta(^{13}C)$ per mil	percent Modern Carbon pMC 1σ error	Conventional Radiocarbon age yrs BP 1σ error
		MQ_W_HAZE			
OZU274U3‡	Quartz filter	EC fraction	-25.0*	65.01 +/– 0.93	3,460 +/– 120
		R_W_HAZE			
OZU275U3‡	Quartz filter	EC fraction	-25.0*	45.18 +/– 0.49	6,390 +/– 90
		R_S_HAZE			
OZU276U3‡	Quartz filter	EC fraction	-25.0*	47.32 +/– 0.49	6,020 +/–90
		MQ_S_HAZE			
OZU277U3‡	Quartz filter	EC fraction	-25.0*	64.35 +/– 0.66	3,550 +/–90
		MQ_W_WEEKEND			
OZU278U3‡	Quartz filter	EC fraction	-25.0*	55.52 +/– 0.87	4,730 +/– 130
		R_S_CLOUDY			
OZU280U3‡	Quartz filter	EC fraction	-25.0*	15.03 +/– 0.28	15,230 +/– 160
OZU281U3‡	Quartz filter	MQ_S_CLOUDY EC fraction	-25.0*	35.57 +/– 0.49	8,310 +/– 120

‡ = A small mass correction has been applied to this sample (refer note 3)

* = The value of δ (C) is assumed. A measured value is not available.

Note:

1 The values of δ(^{13}C) values are assumed. Measured values are not available.
2 The ages quoted are radiocarbon ages, not calendar ages.
3   For some samples, the relatively large error is due to the small sample size.
4 The ages have been rounded according to M. Stuiver and A. Polach (Stuiver and Polach, 1977). The definition of percent Modern Carbon and Conventional Radiocarbon age can also be found in this publication.

Issued by Andrew Jenkinson, Email: avj@ansto.gov.au; Tel: +61-2-97173478; Centre for Accelerator Science, ANSTO, Locked Bag 2001 Kirrawee DC NSW 2232 (AUSTRALIA); http://www.ansto.gov.au/ResearchHub/acceleratorsciencecentre/index.htm

Supplementary Information S3

Details of the operational procedures to isolate the different carbon fractions

1. ^{14}C analysis in TC: no extra pre-treatment is applied and the conventional method was performed.

The exposed filter (around 12 cm^2) is cut into strips, loaded into a quartz combustion tube, added pre-cleaned CuO and silver wires. Filled quartz combustion tubes are pumped 1 hour to evacuate the tube, sealed and then combusted at 840 ℃.

2. ^{14}C analysis in WINTC: water-wash procedure is applied before thermal analysis.

The exposed filter is cut into six small rectangles each for around 2 cm^2, each is folded in half (exposed side inside), sandwiched between 2 blank circles of quartz filter material and washed using ultra-pure MilliQ (Millipore, Resistivity > 18 MΩ.cm at 25 ℃). Water quantities at 7 ml/cm^2 (Bernardoni et al., 2013) in a Millipore filter holder similar to the one in Yttri et al. to remove WSOC (Yttri et al., 2009), then filters are dried at 60 ℃.

Dried filter is cut into strips, loaded into a combustion tube. Pre-cleaned CuO and silver wires are added. Filled quartz combustion tubes are pumped 1 hour to evacuate the tube, sealed and then combusted at 840 ℃.

3. ^{14}C analysis in EC: water-wash procedure is applied before thermal analysis and organic carbon is removed to separate EC.

The exposed filter is cut into six small rectangles each for around 2 cm^2, each is folded in half (exposed side in), sandwiched between 2 blank circles of quartz filter material and washed using ultra-pure MilliQ (Millipore, Resistivity > 18 MΩ.cm at 25 ℃). Water quantities at 7

ml/cm^2 (Bernardoni et al., 2013) in a Millipore filter holder similar to the one in Yttri et al. to remove WSOC (Yttri et al., 2009), then filters are dried at 60 ℃.

A simple thermal heating device is built in ANSTO AMS Environment Research Lab, similarly like the THEODORE system in the lab in Europe (Ruff et al., 2010; Szidat et al., 2004; Zhang et al., 2010), to attempt to mimic the IMPROVE-A heating program to isolate various carbon fractions, which is designed based on the IMPROVE-A protocol for the consistency between OC/EC determination and the determination of ^{14}C signatures in these respective carbon fractions.

The water washed filter (around 12 cm^2) is cut into strips, loaded into a quartz combustion tubeand combusted at 375 ℃ for 1 hour under high purity oxygen (99.99%), with the evolved CO_2 removed. Following which the chamber is filled with high purity He (99.99%) and heated at 580 ℃ for 10 minutes to remove all organic carbon material, cooled down, take off and added pre-cleaned CuO and silver wires, pumped 1 hour to evacuate the tube, sealed and then combusted at 840 ℃.

Field blank filters are cut into quarters and process as per procedure 1 to procedure 3, to get a blank for each process to have confidence in the blank C% and pMC values.

All the above pre-treated samples are cut into very thin strips to fit into Vycor combustion tubes that had been pre-cleaned by baking in a stream of oxygen, likewise, CuO and silver wires were pre-cleaned in the same way (Jordan et al., 2006). The resulting CO_2 reduced to graphite CO_2 collection and preparation of graphite targets for AMS analysis is described in detail elsewhere. In brief, the evolved CO_2 was cryogenically separated using ethanol-dry ice and liquid N_2 traps, and quantified by manometry. The CO_2 was reduced to graphite at 600 ℃ using Zn with Fe catalyst in the presence of excess O_2 (Hua et al., 2001; Lawson et al., 2000).

Supplementary Table S4. Mass concentrations of Non-carbon matter, CM, SOA, POA, EMchar and EMsoot ($\mu g \cdot m^{-3}$) in the selected samples

Samples	Non-carbon matter	CM	SOA	POA	EMchar	EMsoot
R_W_WEEKEND	10.5	4.6	0.7	3.3	0.5	0.1
MQ_W_WEEKEND	8.9	6.1	1.2	4.0	0.8	0.2
R_W_HAZE	11.6	16.5	1.6	13.1	1.5	0.3
MQ_W_HAZE	11.9	12.6	3.0	8.4	1.0	0.2
R_S_SUNNY	11.7	5.6	1.4	3.4	0.6	0.1
MQ_S_SUNNY	9.2	3.6	1.5	1.8	0.2	0.1
R_S_HAZE	13.6	8.6	2.7	4.9	0.8	0.2
MQ_S_HAZE	21.5	13.4	6.1	6.5	0.7	0.3

Supplementary References

Bernardoni, V., Calzolai, G., Chiari, M., Fedi, M., Lucarelli, F., Nava, S., Piazzalunga, A., Riccobono, F., Taccetti, F., Valli, G., 2013. Radiocarbon analysis on organic and elemental carbon in aerosol samples and source apportionment at an urban site in Northern Italy. Journal of Aerosol Science 56, 88-99.

Hua, Q., Jacobsen, G.E., Zoppi, U., Lawson, E.M., Williams, A.A., Smith, A.M., McGann, M.J., 2001. Progress in radiocarbon target preparation at the ANTARES AMS Centre. Radiocarbon 43, 275-282.

Jordan, T.B., Seen, A.J., Jacobsen, G.E., Gras, J.L., 2006. Radiocarbon determination of woodsmoke contribution to air particulate matter in Launceston, Tasmania. Atmospheric Environment 40, 2575-2582.

Lawson, E., Elliott, G., Fallon, J., Fink, D., Hotchkis, M., Hua, Q., Jacobsen, G., Lee, P., Smith, A., Tuniz, C., 2000. AMS at ANTARES–the first 10 years. Nuclear Instruments and Methods in Physics Research Section B: Beam Interactions with Materials and Atoms 172, 95-99.

Ruff, M., Szidat, S., Gäggeler, H., Suter, M., Synal, H.-A., Wacker, L., 2010. Gaseous radiocarbon measurements of small samples. Nuclear Instruments and Methods in Physics Research Section B: Beam Interactions with Materials and Atoms 268, 790-794.

Stuiver, M., Polach, H.A., 1977. Discussion reporting of 14 C data. Radiocarbon 19, 355-363.

Szidat, S., Jenk, T., Gäggeler, H., Synal, H.-A., Hajdas, I., Bonani, G., Saurer, M., 2004. THEODORE, a two-step heating system for the EC/OC determination of radiocarbon (14 C) in the environment. Nuclear Instruments and Methods in Physics Research Section B: Beam Interactions with Materials and Atoms 223, 829-836.

Yttri, K.E., Dye, C., Braathen, O.-A., Simpson, D., Steinnes, E., 2009. Carbonaceous aerosols in Norwegian urban areas. Atmos Chem Phys 9, 2007-2020.

Zhang, Y., Liu, D., Shen, C., Ding, P., Zhang, G., 2010. Development of a preparation system for the radiocarbon analysis of organic carbon in carbonaceous aerosols in China. Nuclear Instruments and Methods in Physics Research Section B: Beam Interactions with Materials and Atoms 268, 2831-2834.